Altering the Electron Transfer Mechanism of Cytochrome P450 Reductase Through a Single Point Mutation

A Senior Honors Thesis

Presented in Partial Fulfillment of the Requirements for graduation *with research distinction* in Biochemistry in the undergraduate colleges of The Ohio State University

by

Matthew L. Wohlever

The Ohio State University
May 2008

Project Advisor: Professor Richard P. Swenson, Biochemistry Department

Abstract

Cytochrome P450 reductase (CPR) is an electron transporter enzyme that plays an essential role in xenobiotic transformations, including metabolism of carcinogens, environmental agents, and drugs. CPR, a membrane bound flavoprotein, contains two flavin cofactors--flavin adenine dinucleotide (FAD) and flavin mononucleotide (FMN)--each bound to a separate protein domain. Both flavin cofactors utilize three distinct oxidation states: oxidized (OX), semiquinone (SQ) (one electron reduced), and hydroquinone (HQ) (two electron reduced). The multiple oxidation states of the flavin cofactors allow CPR to catalyze the essential transfer of electrons from the obligate two-electron donor NADPH to the one-electron acceptor heme-iron of cytochrome P450.

A comparison of the FMN-binding domains in various related flavoproteins reveals that the FMN binding loops differ in their size, conformations, and primary structure yet each contains a conserved glycine residue. My research project was designed to evaluate the functional significance of this conserved glycine in rat CPR (Gly-141) through its replacement with threonine using site-directed mutagenesis. This replacement was made in both the intact reductase and the isolated FMN-binding domain (FBD). Based on previous research on the flavodoxin, we hypothesized that the larger, *beta*-branched side chain of threonine would disrupt the hydrogen bond between residue 141's carbonyl group and the N5H of the reduced flavin, which should destabilize the functionally relevant semiquinone state.

Using a standard steady-state turnover activity assay for cytochrome reduction and the physiological reductant NADPH, the G141T mutant was found to exhibit a specific activity that is 30% less than that of the wild type reductase, indicating that the conserved

glycine residue helps modulate electron transfer. A distinctive characteristic of CPR is that the thermodynamically stable neutral FMN SQ serves as the primary electron donor to cytochrome P450. This phenomenon is the direct result of the substantial separation of the midpoint potentials for the OX/SQ and SQ/HQ redox couples (-43 mV and -280 mV, respectively). Reductive titrations of the G141T mutant revealed a significantly lower formation of the FMN SQ at thermodynamic equilibrium in both CPR and the FBD. The direct measurement of the midpoint potentials for this mutant indicated values for the OX/SQ and SQ/HQ couples of -250 mV and -218 mV, respectively. Thus, the midpoint potential for the OX/SQ couple has decreased substantially resulting in a significant loss in stability of the SQ state with the HQ state becoming the most stable thermodynamically. When wild-type CPR is mixed with an equimolar concentration of NADPH in a stopped-flow spectrophotometer, the disemiquinoid species is formed. However, when the experiment is repeated with G141T CPR, the FAD OX, FMN HQ species are preferentially formed. This data suggests that G141T CPR utilizes the FMN HQ as the primary electron donor to the cytochrome rather than the FMN SQ, but apparently in a less efficient manner. Thus the conserved glycine residue plays a critical role in stabilizing the reduced forms of the FMN cofactor, and in determining the mechanism of electron transfer in CPR.

Dedication

I dedicate this thesis to my friends and family who gave me the nurturing environment that allowed me to grow into the person I am today and for putting up with my long hours in the lab.

Acknowledgements

I would like to thank the current and former members of the Swenson lab group, Uday, Huai-Chun, Kun-Yun, Jammi, and Rajitha for their help and guidance during the research process. A special thank you is also is owed to the OSU Biochemistry Department for their support of their strong support of undergraduate research through the H200/H201 Program and the Summer Undergraduate Research Program. Finally, I wish to acknowledge and thank my research advisor, Dr. Richard Swenson for all of his patient support and helpful advice over the past three years. Without his support, this thesis would not be possible.

Table of Contents

List of Abbreviations

CPR	cytochrome P450 reductase
FMN	flavin mononucleotide
FAD	flavin adenine dinucleotide
FBD	FMN-binding domain of CPR
FNR	ferredoxin-$NADP^+$ reductase
BM3	P450BM-3 from *Bacillus megaterium*

Introduction

Physiological role of microsomal cytochrome P450 system: Found predominantly on the endoplasmic reticulum in liver cells, the microsomal cytochrome P450 system consists of two integral membrane proteins, cytochrome P450 reductase (CPR) and cytochrome P450. The role of CPR in the reaction is to couple a two-electron donor (NADPH) with a one-electron acceptor (cytochrome P450) (figure 1). In addition to reducing cytochrome P450, CPR also reduces squalene monooxygenase, heme oxygenase, and cytochrome b_5, however for the purpose of this thesis, the focus will be on the microsomal cytochrome P450 system. The structure of CPR and its mechanism of catalysis will be discussed in more detail later in the thesis. While animals contain only one CPR gene, the human genome project has identified 58 P450 pseudogenes in humans [1, 2]. CPR is capable of supporting catalysis of dozens of different P450s, as is evidenced by a molar ratio of P450 to CPR in microsomes of about 5-10 to 1 [3, 4].

P450s perform a wide variety of reactions throughout nature. Plants use P450s much more extensively than mammals; for example, *Arabidopsis thaliana* has 286 P450s compared to 58 for humans [1, 5]. In plants, many of the P450s are used for the biosynthesis of specific natural products that are used for coloration and defense. While mammals also use P450s for the synthesis of some important steroids and eicosanoids, the majority of P450s in mammals are used for xenobiotic transformations [5]. Xenobiotics are chemical substances that are foreign to a biological system, including environmental agents, carcinogens, insecticides, naturally occurring compounds, and drugs, thus making the cytochrome P450 system of great interest to the pharmaceutical

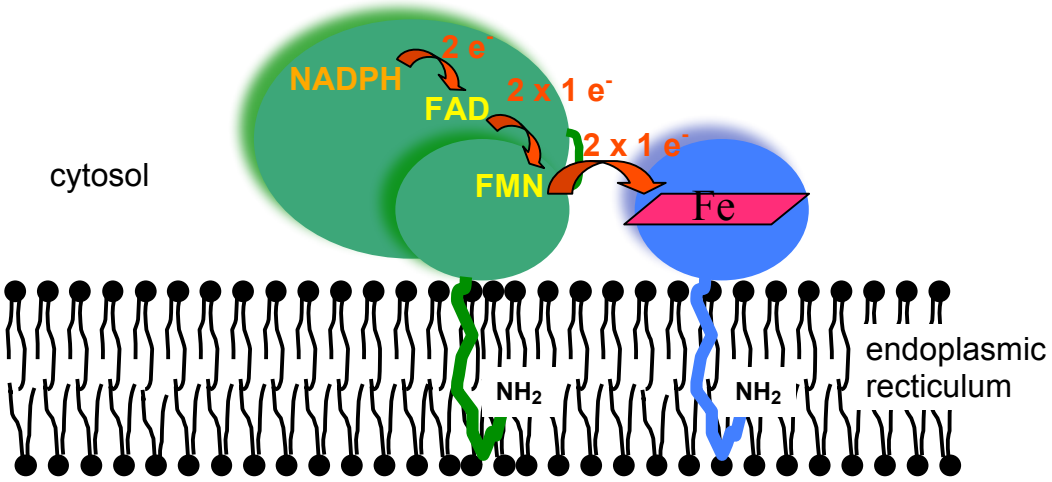

Figure 1: A cartoon showing the flow of electrons in the microsomal cytochrome P450 system. On the left is cytochrome P450 reductase while the heme-iron of cytochrome P450 is on the right.

industry. In fact, most countries now require that all new drug candidates include information about which human P450 enzymes are involved in its metabolism [6, 7]. P450s 1A2, 2C9, 2C19, 2D6, and 3A4 account for the majority of metabolism of drugs in humans [8-10]. It is important for pharmaceutical companies to study the P450s for two reasons. First, P450 catalysis of drugs lowers their bioavailability, thus reducing their effectiveness. Second, if a drug is administer in a pro-drug form, P450 catalyzed oxidation is required for conversion to the active form. Given the role of P450s in drug metabolism and other xenobiotic transformations, a full understanding of the microsomal cytochrome P450 system is needed, including a detailed study of both cytochrome P450s and their primary redox partner, cytochrome P450 reductase.

Cytochrome P450 catalytic cycle: Cytochrome P450s are heme-containing monooxygenases that catalyze a mixed-function oxidation as described in equation 1.

(1) $NADPH + H^+ + O_2 + RH \rightarrow NADP^+ + H_2O + ROH$

The general catalytic cycle of P450s is shown in figure 2 [5]. CPR is responsible for donating a single electron to the heme iron of the P450 in step 2 of the reaction cycle. The only case where CPR is not the donor of the first electron to a microsomal P450 occurs with truncated forms of P450s that are targeted to the mitochondria, in which case the iron-sulfur protein adrenodoxin serves as the electron donor [11]. However, it should be noted that the vast majority of P450s, including those involved in the metabolism of drugs and carcinogens, are located in the endoplasmic reticulum and are thus reduced by CPR [5]. The addition of the first electron reduces the iron from the ferric state to the ferrous state, allowing it to bind to O_2 in step 3. In step 4 of the reaction, a second electron enters the system.

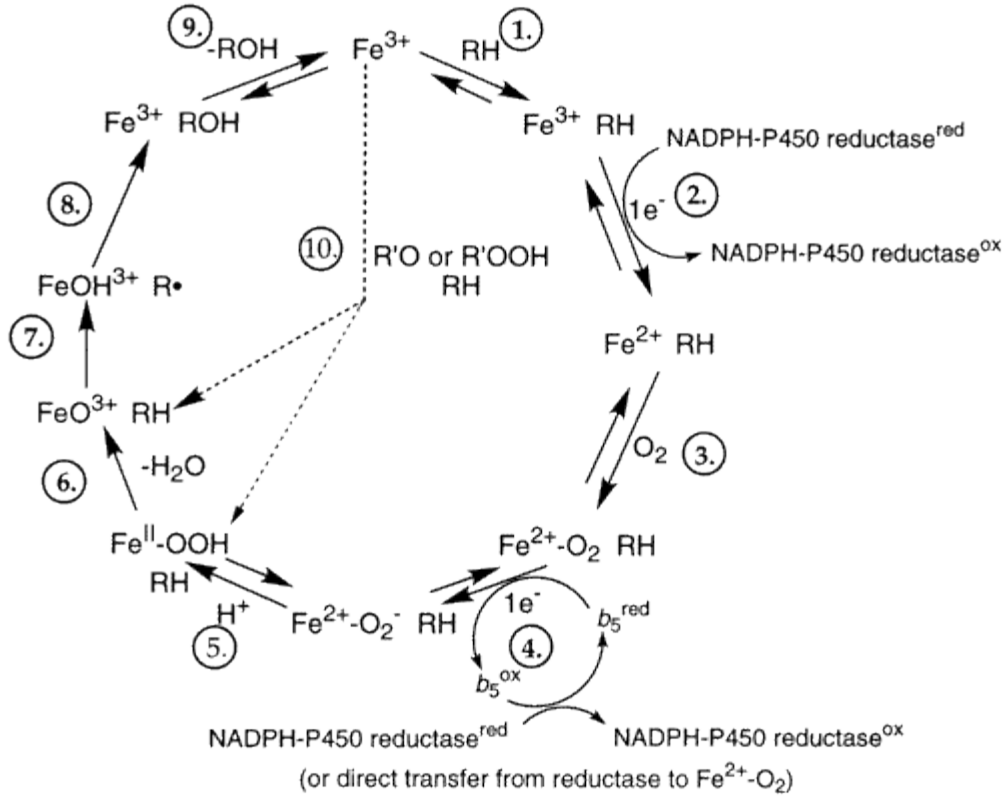

Figure 2: Generalized P450 Catalytic Cycle Fe = iron atom in P450 heme, RH = substrate, ROH = product, NADPH-P450 reductase = cytochrome P450 reductase, ox and red indicate the reduced and (1-electron) oxidized states of the reductase involved in the electron transfers. Reproduced from reference 5.

This second electron may come from CPR or from cytochrome b_5, but as shown in figure 2, CPR reduces cytochrome b_5 [12, 13]. In step 5 a proton is added and in step 6, molecular oxygen is cleaved and water is released. The departure of a water molecule leaves the FeO^{3+} complex wherein it is generally accepted that iron is Fe^{4+} and that the porphyrin ring is one-electron deficient [5]. There is still some debate as to the exact mechanism of steps 7 and 8, but they ultimately result in the release of the oxidized product (ROH) and the regeneration of the heme iron in the ferric state.

Cytochrome P450 reductase and its domains: Cytochrome P450 reductase is a membrane bound electron transfer flavoprotein in the endoplasmic reticulum that utilizes two riboflavin-like cofactors, flavin adenine dinucleotide (FAD) and flavin mononucleotide (FMN). It is one of only four known mammalian enzymes that contain both FAD and FMN, with the others being nitric-oxide synthase, methionine synthase reductase, and protein NR1 [14]. CPR has three domains: the membrane anchor, the FMN-binding domain, and the FAD-binding domain; the two flavin-binding domains are connected by a flexible linker region. A relatively short sequence of hydrophobic residues at the N-terminus form the member anchor. Cleavage of the first 56 residues generates the soluble form of the enzyme, which is capable of passing electrons to the artificial electron receptor cytochrome c, but is incapable of reducing cytochrome P450s [15]. Since the soluble form of CPR was used throughout this study, it shall henceforth be referred to simply as CPR. The crystal structure of rat CPR, lacking the membrane anchor, was determined by Wang et al. (figure 3).

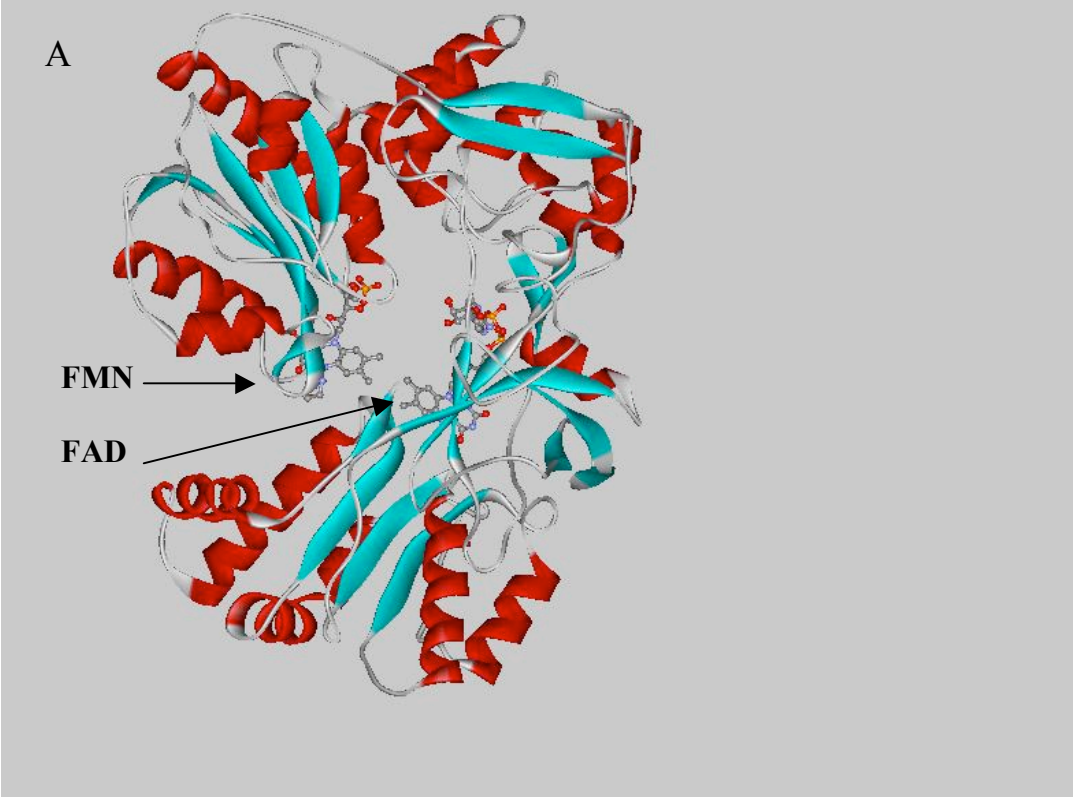

Figure 3: The architecture of cytochrome P450 reductase. **(A)** Crystal structure of the soluble portion of rat cytochrome P450 reductase (PDB = 1AMO) [15]. The flavin cofactors are labeled. **(B)** Gene map of the soluble portion of cytochrome P450 reductase. At the N-terminus is the FMN domain. The flexible linker region, in brown, connects the FMN domain to the FAD domain, which also contains the NADPH binding sub-domain.

Closer investigation of the crystal structure of CPR reveals many important interactions. Both flavin-binding domains display an α/β type structure. The core of the FBD is composed of a five-stranded parallel β-sheet flanked by five α-helices. This is structurally homologous to bacterial flavodoxins (figure 4). A flexible linker connects the FBD to the FAD-binding domain, which also contains the NADPH binding sub-domain. Similar to ferredoxin-$NADP^+$ reductase (FNR), the FAD-binding domain has a flattened, anti-parallel β-barrel while the NADPH binding sub-domain consists of a five-stranded β-sheet sandwiched by α-helices (figure 5) [15]. The structural homology between the FBD and flavodoxins and the FAD-binding domain and FNR led to the conclusion that CPR evolved as a fusion of these two simple flavoproteins [15-19].

P450BM-3 enzyme (BM3) from *Bacillus megaterium* is homologous to the microsomal cytochrome P450 system. This soluble (not membrane anchored) flavocytochrome contains a fatty acid hydroxylase P450 fused to a mammalian-like diflavin NADPH-P450 reductase as a single polypeptide [20-21]. Thus, BM3 is the entire microsomal cytochrome P450 system in a single peptide. Due to its efficient electron transfer from NADPH to the P450 heme, BM3 has the highest catalytic activity yet determined for a P450 monooxygenase (17,000 min^{-1} with arachidonate) [22, 23]. Although there is currently no crystal structure for the full BM3 protein, there is a structure for the heme and FMN domains, and there is a clear homology between the FMN domains of BM3 and CPR (figure 4) [24].

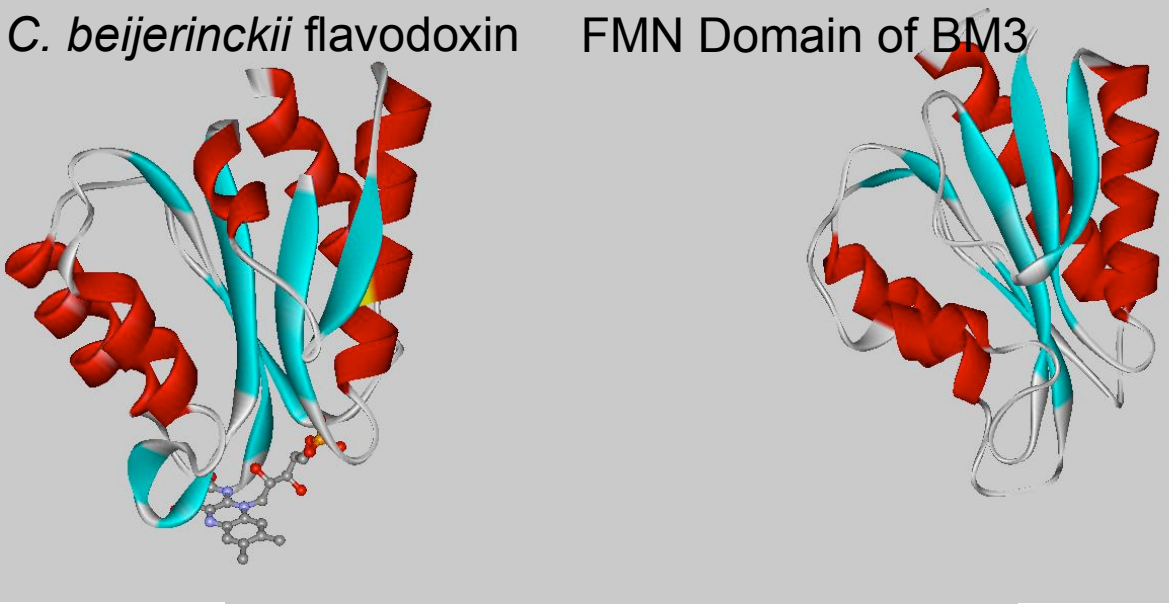

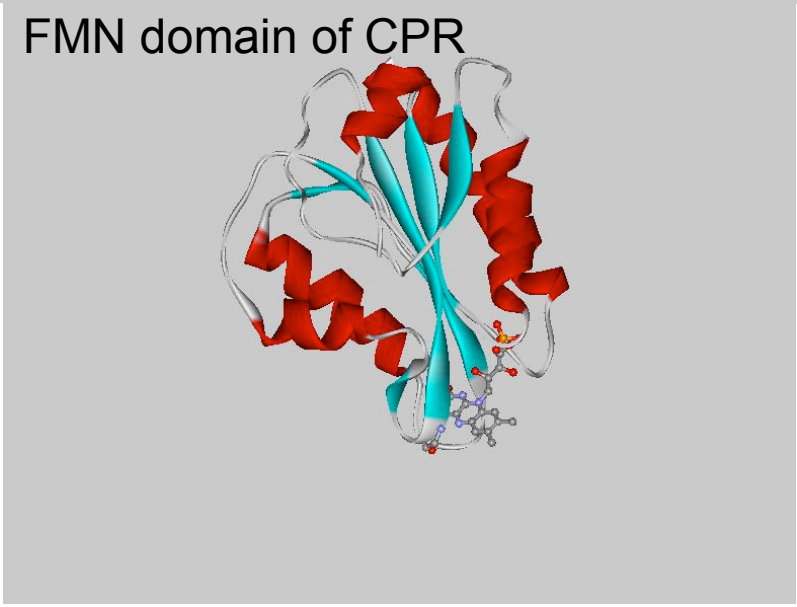

Figure 4: A structural comparison of the *C. beijerinckii* flavodoxin (PDB = 4NUL), the FMN binding domain of BM3 (PDB = 1BVY) (flavin cofactor not shown), and the FMN binding domain of CPR (PDB = 1AMO). The FMN binding domains of CPR and BM3 are thought to have evolved from the bacterial flavodoxin. All three structures share a clear structural homology with a core composed of approximately 5 parallel β-strands flanked by 5 α-helices.

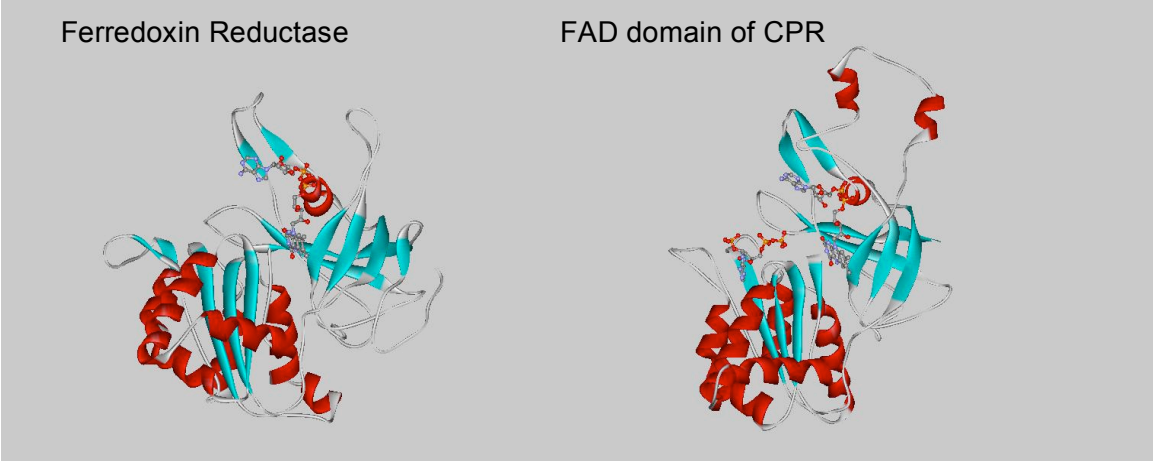

Figure 5: A structural comparison of the *Cyanobacterium anabaena* ferredoxin reductase (PDB = 1QUE) and the FAD binding domain of CPR with the NADPH binding sub-domain (PDB = 1AMO). The FAD cofactor is in the upper right portion of the structure in the sub-domain that has a flattened, anti-parallel β-barrel. The NADPH binding sub-domain is at the bottom left of each structure and consists of a 5-stranded β-sheet sandwiched by α-helices. The FAD binding domain of CPR is thought to have evolved from ferredoxin reductase.

In CPR, the two flavin cofactors do not overlie each other, but rather are end on end with an angle of 150° between the planes of the rings; the closest distance between the rings is 3.5 Å and occurs between the C7M atoms (figure 6). The close arrangement of the flavin cofactors suggests that electron transfer occurs directly between the flavin cofactors and is not mediated by any residue atoms [15]. The initial crystal structure of rat CPR was determined in the presence of $NADP^+$, but the electron density of the nicotinamide cofactor was 30% of the rest of the molecule, indicating that the cofactor adopts multiple conformations. Two $NADP^+$ conformers have been proposed which fit the electron density map. In one case the C4 atom of nicotinamide (the hydride donor) is 9 Å away from the N5 of the FAD cofactor (the hydride acceptor) while in the other it is 14 Å away [15]. These distances were too long for direct hydride transfer. A closer look at the crystal structure revealed that the FAD isoalloxazine ring is shielded by an aromatic amino acid residue (W677), leading to the proposal that for hydride transfer to occur, conformational changes must accompany the binding of the reduced nicotinamide [15, 19, 25-27]. Mutagenesis of W677 in rat CPR revealed a crystal structure where the nicotinamide of $NADP^+$ bound close to the isoalloxazine ring, engaging in π-π stacking interactions, with a distance between the C4 of the nicotinamide ring and the N5 of the FAD isoalloxazine ring of 3.5 Å [28].

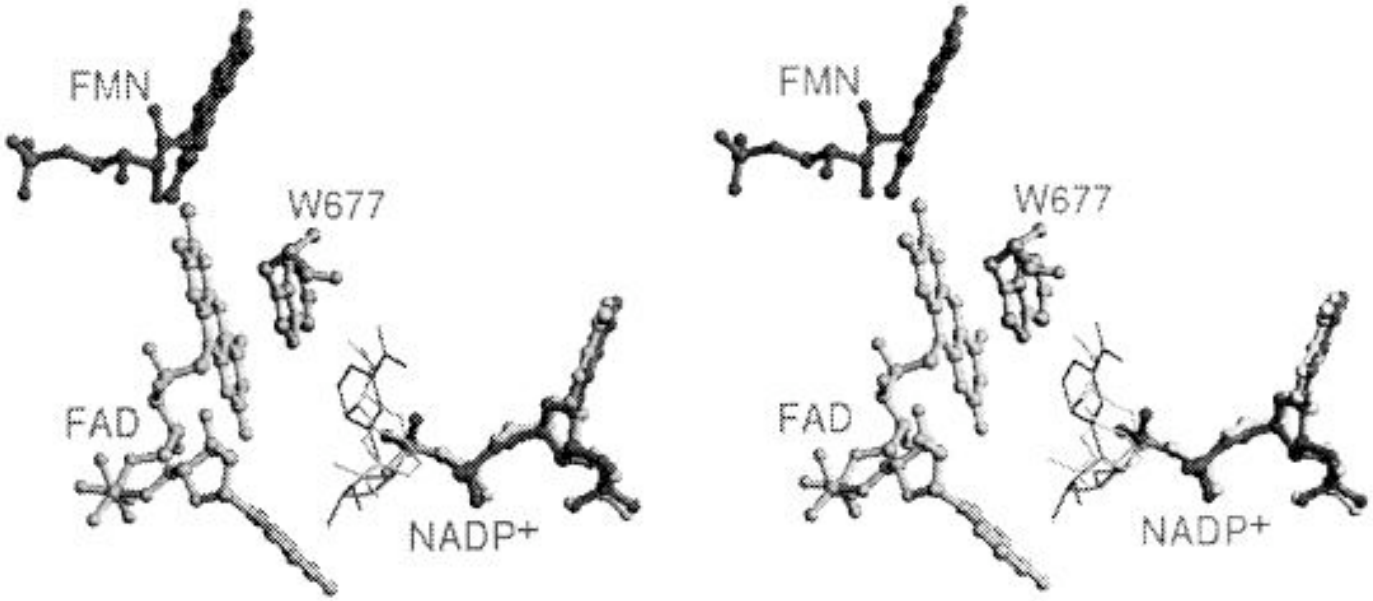

Figure 6: Stereoview of the cofactor arrangement in rat CPR and multiple conformers for the bound $NADP^+$. Electrons flow from NADPH to FAD and then to FMN. The FMN and FAD are represented by ball-and-stick, with the xylene portions of the isoalloxazine rings oriented toward each other. The adenine portion of $NADP^+$ binds in a single conformation (ball-and-stick) while the nicotinamide (stick only) binds in multiple conformations. By rotation about the P_N—O—P_A bond, the nicotinamide ring could displace W677 at the re-side of the FAD ring, placing it in the optimum orientation for hydride transfer from the NADPH to the N5 position of the FAD cofactor. Reproduced from reference 15.

Human [29] and rat [30, Swenson unpublished data] FAD-binding domain and FBD have been separately expressed and purified. The isolated domains are able to fold properly and can bind the appropriate flavin cofactors. The FBD is able to bind the FAD-binding domain and cytochrome c [29]. A reconstituted system consisting of the isolated domains is able reduce cytochrome c, but with only 2% efficiency compared to CPR [29]. Further studies on the isolated domains of human CPR by Munro et al. demonstrated that there is little difference between the midpoint potentials of the flavin cofactors in the isolated domains and in CPR (Table 1) [31].

Although the above data suggests that the flavin binding domains exist in discrete environments, a growing body of evidence argues that the domains interact during the catalytic cycle. Hubbard et al demonstrated that binding of $NADP^+$ in the W677 mutant of rat CPR caused the FBD to shift, increasing the distance between the two flavin cofactors by up to 3 Å [28]. The effect of NADPH binding was further studied by Grunua et al. Through a series of isothermal titration calorimetry studies and pre-steady-state kinetic measurements Grunua et al demonstrated that binding of NADPH caused a conformational change between the flavin domains, making intramolecular (FAD to FMN) and intermolecular (FMN to cytochrome c) electron transfer more favorable [32].

Mechanism of CPR electron transfer: In any given reaction CPR has two substrates, an electron donor (NADPH) and an electron acceptor (cytochrome c). Under physiological conditions, the cytochrome is in the P450 superfamily, but since many *in vitro* studies have been conducted with cytochrome c as the electron acceptor, the mechanism of electron transfer will be outlined with cytochrome c as the electron acceptor. This mechanism should still be physiologically relevant because cytochrome c

and cytochrome P450 have overlapping binding sites on CPR [33-35]. There are two basic kinetic mechanisms for two-substrate enzymes, the Ping-Pong and Bi-Bi mechanism, with the Bi-Bi mechanism further subdivided into ordered and random (figure 7). Studies on a number of diflavins suggest a random Bi-Bi kinetic mechanism for diflavins in general [36]. However, recent investigations show that cytochrome c will not bind to CPR unless the flavoprotein has been reduced by NADPH; leading to the conclusion that CPR may actually utilize an ordered Bi-Bi kinetic mechanism [32].

Flavin cofactors have the unique ability to undergo three different redox states: oxidized, semiquinone (one-electron reduced), and hydroquinone (two-electron reduced) which allows flavoproteins to serve as electron bridges between obligate two-electron donors such as NADPH and obligate one-electron acceptors such as cytochrome P450s (figure 8). In addition to the multiple redox states, the semiquinone form of the flavin cofactor can exist in the cationic, neutral, or anionic forms, but only the neutral and anionic forms are found in flavoproteins [36, 37]. The anionic and neutral semiquinone can easily be distinguished by their spectral properties, and thus are called “red” and “blue” respectively [38, 39]. Rat CPR exclusively utilizes the neutral blue semiquinone. Interestingly, the blue semiquinone is air-stable in CPR and other diflavins, which is in stark contrast to the other reduced states of the flavin cofactors that readily react with oxygen to form superoxide [36, 40].

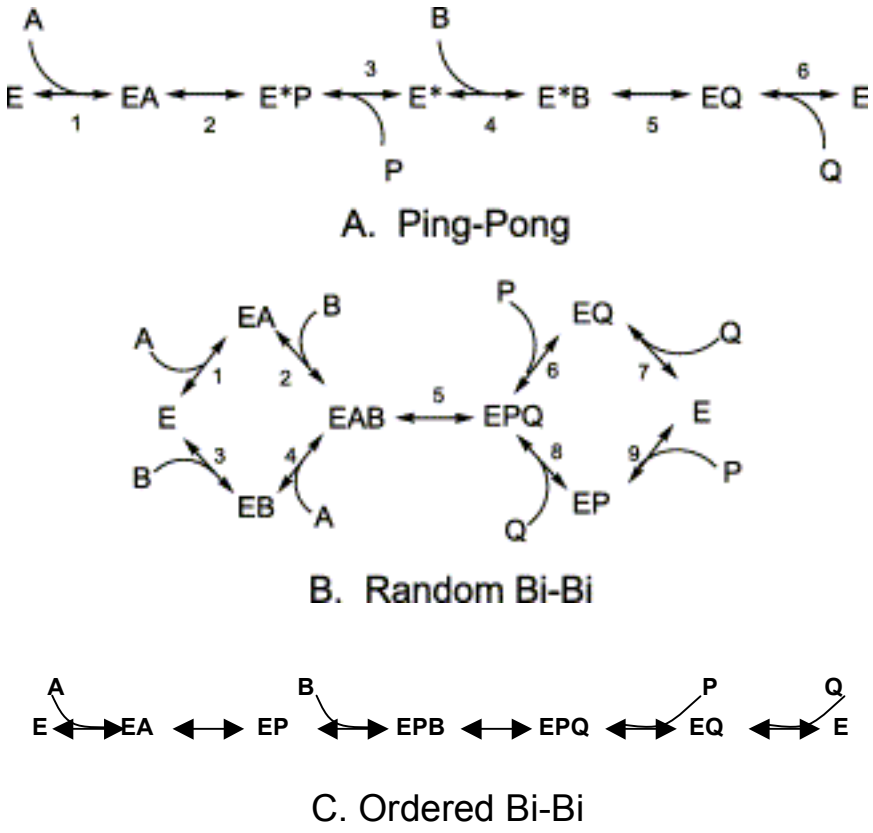

Figure 7: Different proposed mechanisms for CPR and other enzymes with two substrates and two products. **(A)** The ping-pong mechanism has the first product dissociate from the enzyme before the second substrate binds. **(B)** In the random bi-bi mechanism, both substrates bind before product formation. Which substrate binds first or which product is released first is random. **(C)** Like the random bi-bi mechanism, the ordered bi-bi mechanism has both substrates bind before any product is formed. However, in this case, the order of substrate binding and product release occurs in a sequential manner. Based on reference 36.

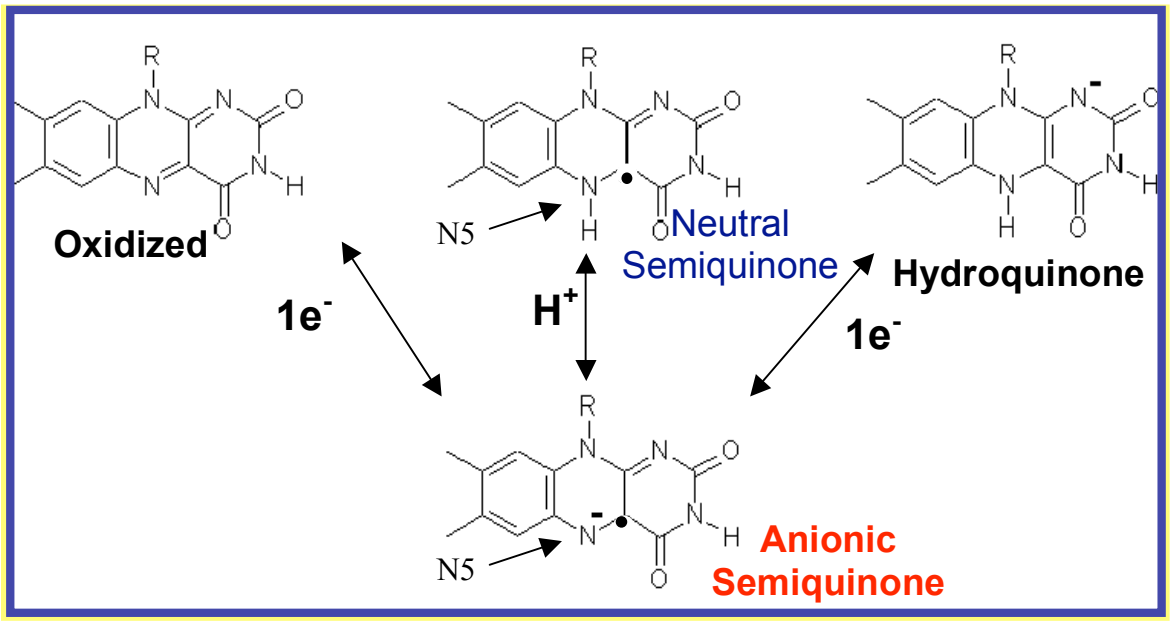

Figure 8: The three redox states of the flavin cofactor. The one electron reduced (semiquinone) state can be either the neutral blue semiquinone or the anionic red semiquinone. CPR exclusively utilizes the neutral blue semiquinone, which means that the N5 position is protonated.

The two flavin cofactors of CPR give rise to nine possible redox state combinations, but since NADPH is an obligate two-electron donor, the number of physiologically relevant states is reduced to five (figure 9). For obvious reasons the fully oxidized reductase is incapable of reducing cytochrome c, leaving only the two and four electron reduced forms as possible electron donors. The four-electron-reduced reductase can be eliminated as the electron donor to cytochrome c because it takes up to 8 hours of incubation under anaerobic conditions in the presence of NADPH and the NADPH regenerating system to form, which clearly is not physiologically relevant [41]. The FAD HQ - FMN OX can also be eliminated as cytochrome c receives electrons from the FMN cofactor. This leaves only two forms of the reductase, the disemiquinoid and the FMN hydroquinone, that can serve as the electron donor. The midpoint potentials of the two states provide the answer. For the FMN cofactor of human CPR, the OX/SQ couple is -66 mV while the SQ/HQ couple is -269 mV; thus it is significantly easier to form the disemiquinoid species than the FAD OX - FMN HQ species [31]. Also, reduction of CPR by a stoichiometric amount of NADPH led to the formation of the disemiquinoid species, not the FAD OX - FMN HQ species [42]. Finally, stopped-flow kinetic studies on human CPR showed that the rate of formation of the FMN HQ is significantly slower than cytochrome c reduction [42].

0 e^-	1 e^-	2 e^-	3 e^-	4 e^-
		FAD HQ FMN OX		
	FAD SQ FMN OX		FAD HQ FMN SQ	
FAD OX FMN OX		FAD SQ FMN SQ		FAD HQ FMN HQ
	FAD OX FMN SQ		FAD SQ FMN HQ	
		FAD OX FMN HQ		

Figure 9: The 9 possible combinations of flavin cofactor redox states in CPR. Since NADPH is an obligate two electron donor, only the two and four electron reduced forms of CPR (in red) are theoretically capable of donating electrons to cytochrome c. Additional evidence, which is expanded upon in the text, suggests that for wild type CPR the disemiquinoid form is the primary electron donor to cytochrome c.

Muratatliev et al combined this data to suggest a general kinetic mechanism of electron transfer (Figure 10) [36]. In the first step of the reaction, NADPH binds to CPR in a bimolecular step with a k_{on} of 1-3 x 10^7 M^{-1} s^{-1} for rat CPR [43, 44]. Hydride transfer occurs in step two while acceptor (cytochrome c) binding is shown in step three. Based on a comparison of the hydride transfer rate to FAD and steady-state catalysis rate, hydride transfer from NADPH is the rate-limiting step [43-45]. In step three, interflavin electron transfer occurs. Based on stopped-flow-kinetic studies, this electron transfer event occurs at least as fast as hydride transfer to FAD. In step four, the acceptor is reduced by the FMN SQ. The reduction of both molecules of cytochrome c can be described in terms of first order Michaelis-Menten kinetics rather than second order kinetics, leading to the conclusion that binding of cytochrome c is not rate limiting [36]. Steps five through seven are not well studied, but must be at least as fast as steady-state catalysis rates.

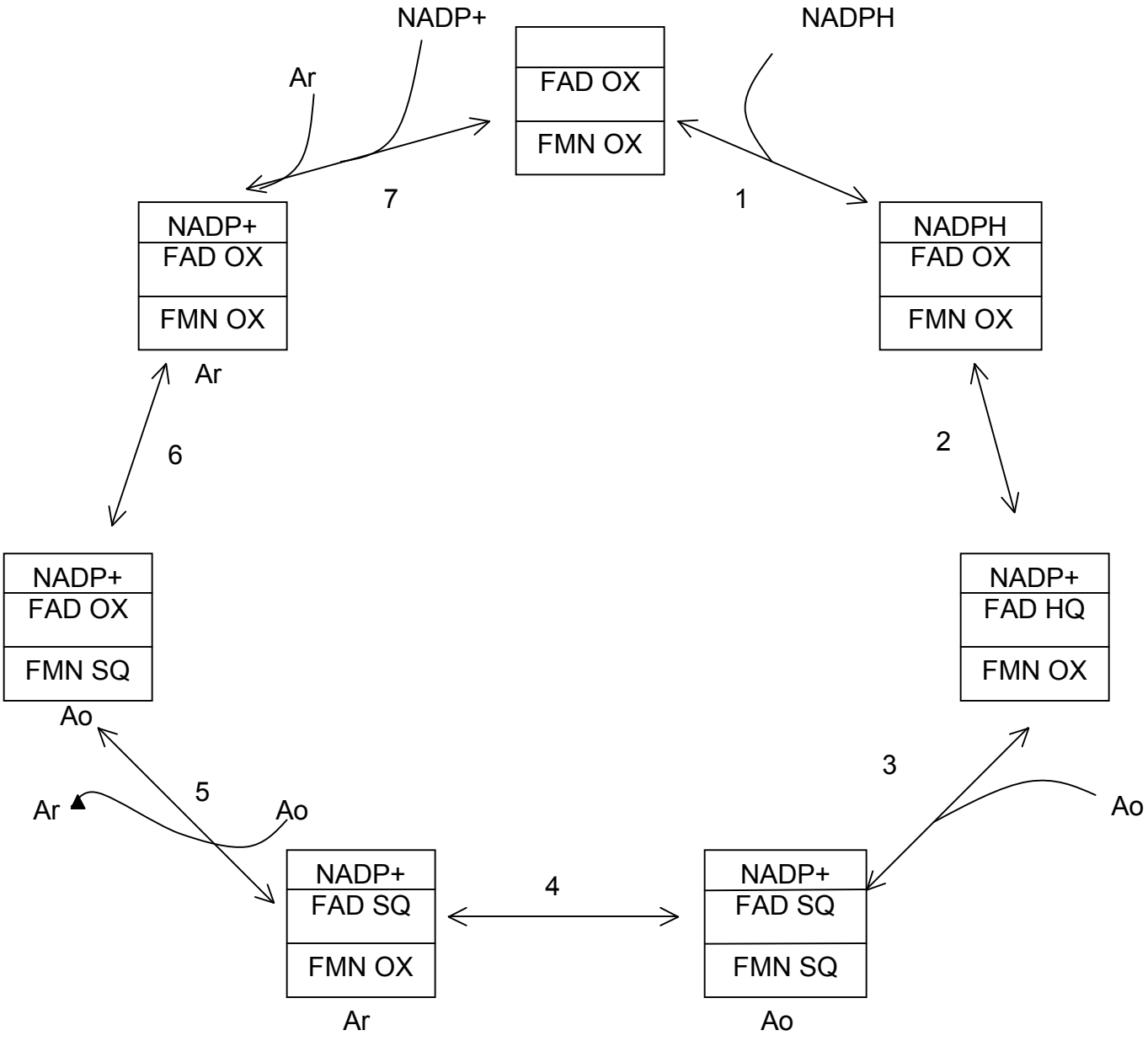

Figure 10: Catalytic cycle of diflavin reductases, including CPR, originally proposed by Murataliev et al. Ao is the oxidized substrate and Ar is the reduced substrate (cytochrome c). Based off of reference 36.

Project history: Given the wide variety of electron transfer mechanisms and redox potentials found in flavoproteins, it is evident that the protein environment plays a substantial role in modulating the redox properties of the flavin cofactor. The goal of this project is to gain a better understanding of how the FMN binding loop in CPR modulates the redox properties of the FMN cofactor. Since CPR is homologous to the reductase domains of BM3, and the FBD of CPR is homologous to bacterial flavodoxins, the FMN binding loops from all these species were compared (Figure 11). Somewhat surprisingly, the FMN binding loops of these homologous domains showed extensive variability in the size, sequence, and conformation. Despite these differences, all of the loops contained a conserved glycine residue. A comparison of the crystal structures of these loops shows that the backbone carbonyl of the conserved glycine residue is positioned to form a hydrogen bond with the N5 position of the isoalloxazine ring (Figure 12). The N5 position is protonated in both the semiquinone and hydroquinone forms (Figure 8), leading to the hypothesis that the hydrogen bond helps to stabilize the reduced states of the flavin cofactor.

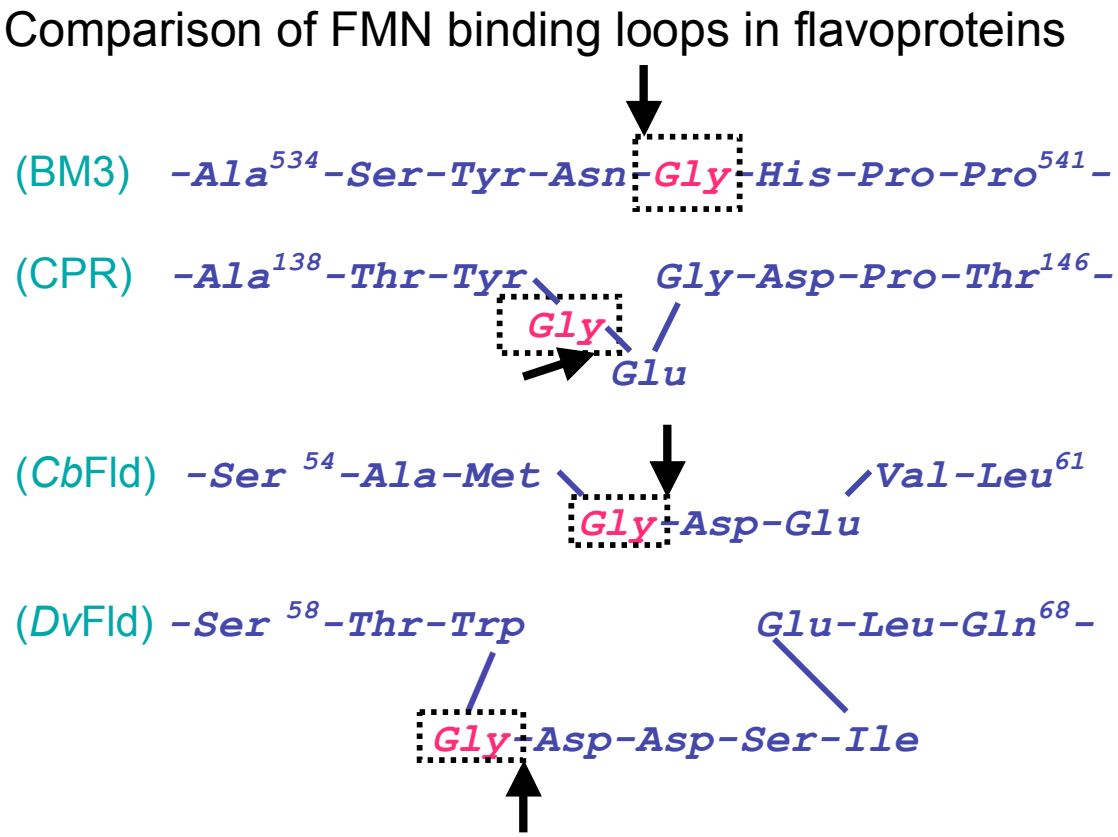

Figure 11: Sequence comparison of the FMN binding loops in BM3, CPR, *C. beijerinckii* flavodoxin, and *D. vulgaris* flavodoxin. The conserved glycine residue is highlighted in pink. The part of the loop that interacts with the N5 position of the isoalloxazine ring is designated with an arrow.

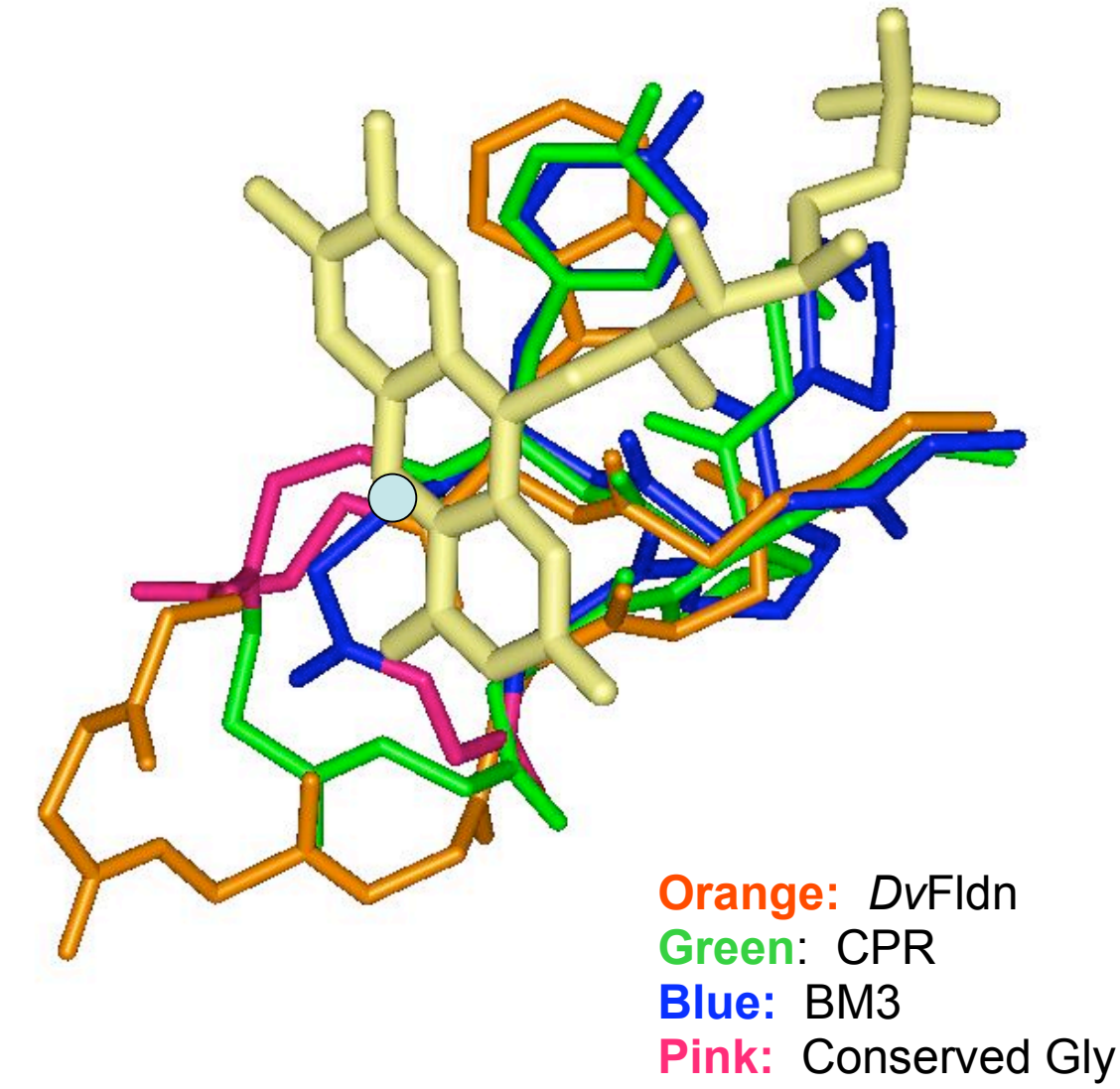

Figure 12: Structural comparison of the FMN binding loops in *D. vulgaris* flavodoxin, CPR, and BM3. The conserved glycine residue is highlighted in pink. The N5 position of the isoalloxazine ring is marked with a blue dot.

The role of the conserved glycine residue has already been rigorously explored in both *Desulfovibrio vulgaris* [46] and *Clostridium beijerinckii* [47]. The FMN binding loop in *D. vulgaris* flavodoxin is approximately four residues longer than the equivalent loop in CPR, which leads to different interactions with isoalloxazine ring. However, crystal structures of the oxidized flavodoxin and its mutants show the backbone carbonyl of the conserved glycine, residue 61, positioned to make a hydrogen bond with the N5H of the reduced flavin cofactors. Mutational analysis of glycine 61 to alanine, valine, leucine, and asparagine showed that all mutations destabilized the semiquinone state and that the extent of destabilization increases with the bulkiness of the side chains, with the β-branched side chain of valine causing the largest change in midpoint potentials [46]. Interestingly, all mutations of glycine 61 increase the OX/SQ midpoint potential and lower the SQ/HQ midpoint potential. This data supports the hypothesis that the hydrogen bond between glycine 61 and the N5H of the semiquinone is important for the regulation of the redox properties of the FMN cofactor [46]. Crystal structures of the mutant flavodoxins show that the steric constraints of the loop are such that insertion of a side chain at position 61, even the methyl group of alanine, will cause a 5 Å shift in the loop, altering the contacts with the flavin cofactor, signifying that a degree of caution is necessary for interpreting the results of this mutational analysis.

The FMN binding loop in *C. beijerinckii* was studied through mutational analysis of the conserved glycine 57 residue by Ludwig and Swenson [47]. The *C. beijerinckii* FMN binding loop is only two residues larger than the FMN binding loop in CPR, rather than four residues, as is the case with *D. vulgaris* flavodoxin. Thus, studies on *C. beijerinckii* should be more relevant for CPR. Ludwig and Swenson rigorously explored

the role of glycine 57 by mutating it to alanine, aspartate, asparagine, and threonine. As with the *D. vulgaris* flavodoxin, the addition of a side chain caused the OX/SQ midpoint potential to decrease and the SQ/HQ midpoint potential to increase, with the larger side chains causing the largest change in midpoint potentials [47]. The introduction of the β-branched side chain of threonine at position 57 caused the OX/SQ midpoint potential to decrease by 178 mV. This decrease is over 100 mV larger than that caused by mutation to alanine, aspartate, or asparagine. The large change in midpoint potentials for the G57T mutant caused all three oxidation states to be present in significant amounts throughout most of the reductive titration, which contrasts with the results for the wild type flavodoxin [47].

Wild type *C. beijerinckii* flavodoxin has three different redox states, *cis* O-down, *trans* O-down, and *trans* O-up, with the fully oxidized flavin existing predominantly in the *cis* O-down conformation (figure 13). In this conformation, the backbone carbonyl is pointed away from the isoalloxazine ring. Upon reduction of the flavin cofactor to either the semiquinone or hydroquinone state, glycine 57 assumes the *trans* O-up conformation with the backbone carbonyl pointed directly at the N5H [47]. This conformational change is linked to the redox state of the FMN cofactor and strongly suggests that residue 57 plays a crucial role in modulating the redox properties of the bound flavin cofactor.

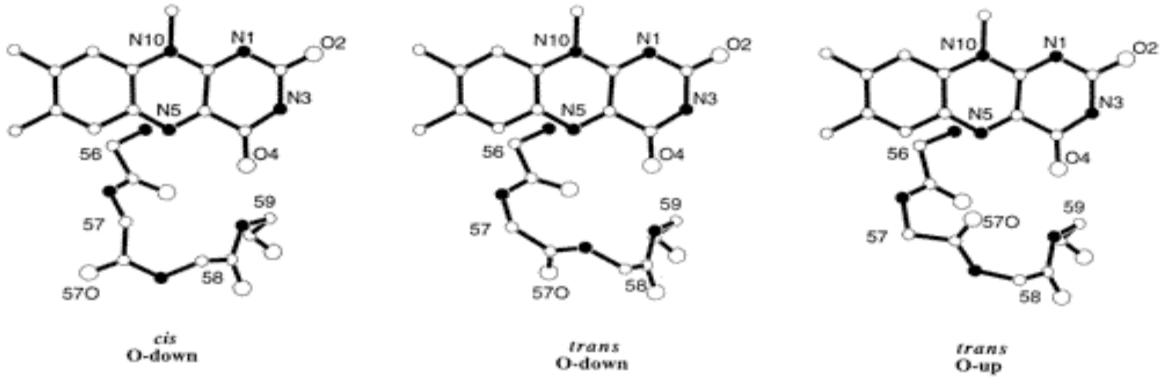

Figure 13: Conformations of the peptide backbone at residues 56-59 in *C. beijerinckii* flavodoxin. The position of O57 and the configuration of the peptide are the features that distinguish the three observed conformers. In the O-up form, the carbonyl oxygen of residue 57 is hydrogen-bonded to the flavin N5H. Side chains have been omitted to simplify the drawings. Nitrogen atoms are filled; C and O atoms are open, with larger radii assigned to the oxygens. Residues are numbered at the Cα atoms. The heteroatoms of the isoalloxazine ring are labeled, and the ribityl side chain has been omitted beyond C1'. Reproduced from reference 47.

Plotting the phi and psi angles of these conformations on a Ramachandran plot provides some insights into the potential cause of the large shift in midpoint potentials for the glycine to threonine mutant. The *cis* O-down conformation (oxidized FMN) has phi-psi angles of -79, 128 while the *trans* O-up conformation (reduced FMN) has phi-psi angles of approximately 50, -130; placing the *trans* O-up conformation in a portion of Ramachandran space that is normally only available to glycine [48, 49] (Figure 14). The G57T mutant in *C. beijerinckii* is capable of achieving these phi-psi angles, but the large, β-branched side chain of threonine should significantly raise the energy necessary for residue 57 to rotate to the *trans* O-up conformation necessary to interact with the N5H of the isoalloxazine ring [47]. Based on the redox potentials, the G57T mutant should have at most 65% SQ during the reductive titration. A crystal structure of the mutant flavodoxin at maximal SQ formation shows electron densities consistent with 60% of residue 57 in the *trans* O-up conformation and 40% in the *trans* O-down conformation, further strengthening the claim that the conserved glycine residue plays a crucial role in modulating the redox properties of the FMN cofactor [47].

Ramachandran Plot for WT and G57T *Clostridium beijerinckii* flavodoxin

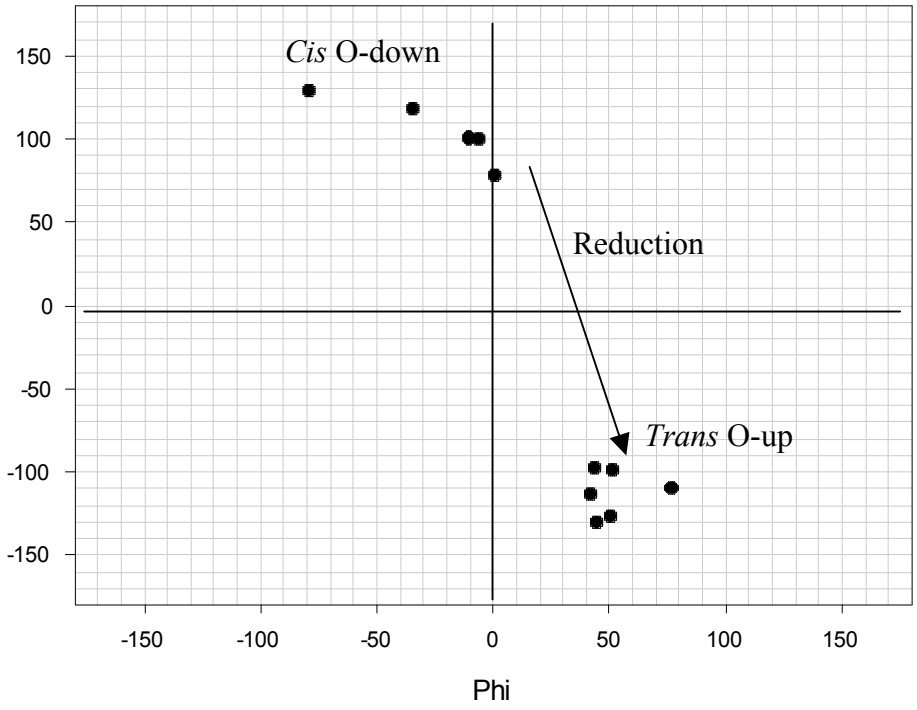

Figure 14: Ramachandran plot of the conserved glycine residue (G57) in the FMN binding loop of wild type and G57T mutant *C. beijerinckii* flavodoxin at various redox states. The position of the conserved glycine residue (G141) in the FMN binding loop of CPR is marked with a star.

Project Objectives: The objective of this project is to extend the studies of the conserved glycine residue in bacterial flavodoxins to the multidomain, mammalian homolog, CPR. We sought to determine if the conserved glycine residue interacts with the N5H of the isoalloxazine ring in the same manner as the flavodoxins. The crystal structure of rat CPR shows the backbone carbonyl of the conserved glycine, residue 141, is already pointed directly at the N5H of oxidized flavodoxin (figure 15). It should be noted that the main chain carbonyl is slightly out of hydrogen bonding range with an inter-atomic distance of 3.66 Å. Previous studies on the role of the conserved glycine residue had focused predominantly on structural effects of the mutation and the midpoint potentials. However, we also wanted to probe the effect of mutation of glycine 141 on the electron transfer mechanism in CPR. Previous studies on *C. beijerinckii* and *D. vulgaris* clearly demonstrated that a large, β-branched side chain such as valine or threonine had the largest effect on the midpoint potentials of the FMN cofactor. Building off of these results, we choose to mutate glycine 141 to threonine in both CPR and the FBD so that we could significantly perturb the interaction between the main chain carbonyl and the N5H.

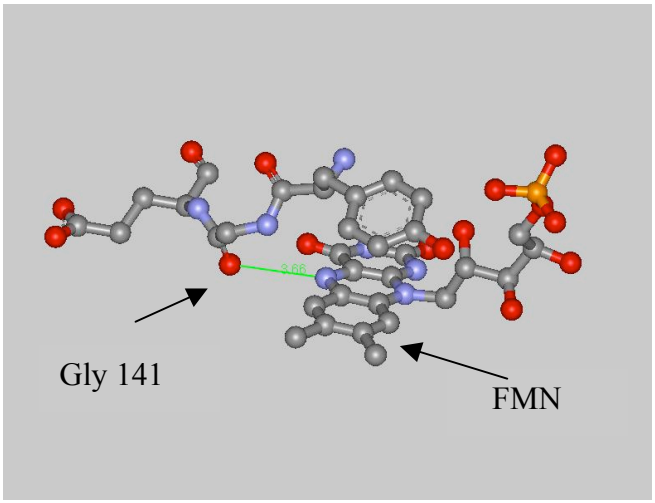

Figure 15: The FMN binding loop of CPR. The backbone carbonyl of glycine 141 is pointed directly at the N5 position in the oxidized isoalloxazine ring.

Materials and Methods

Materials: Mutagenic primers were ordered from Sigma-Genosys. Competent *Escherichia coli* cells (strain DH5α Max Efficiency) were purchased from Invitrogen while the BL21(DE3) Rosetta strain was purchased from Novagen. Horse heart cytochrome c, FMN, NADPH, and $NADP^+$ were all purchased from Sigma. Isopropylthiogalactoside (IPTG) was obtained from Research Products International. Potassium ferricyanide was obtained from Fisher. Sodium dithionite was obtained from JT Baker. Indigo disulfonate, anthraquinone-2,6-disulfonate, and anthraquinone-2-sulfonate were all obtained from Fluka. All other chemicals were analytical grade. The Quikchange® site-directed mutagenesis kit was from Stratagene. The Qiaprep® Spin miniprep kit was from Qiagen.

Site-Directed Mutagenesis: Soluble rat CPR (lacking the N-terminal membrane anchor) and the isolated FMN-binding domain (FBD) were expressed in *E. coli* strain BL21(DE3) Rosetta from the appropriate pT7-7 plasmid constructs [unpublished results]. The G141T mutation was generated in both CPR and the isolated FMN domain using a Quikchange® kit. Mutagenic oligonucleotides for generating the G141T mutation were 5'-GCCACATACA**CA**GAGGGCGACC -3' and 5'-GGTCGCCCTC**TG**TGTATGTGGC-3'. The G141T DNA was transformed into competent *E. coli* strain DH5α Max Efficiency cells as described in the vendor protocol. Plasmid DNA was purified by a Qiaprep® Spin miniprep kit as described by the vendor protocol. Mutations and the sequence integrity of the entire open-reading frame were verified by automated DNA sequencing analyses performed by the Plant Microbe Genomics Facility at the Ohio State

University. Plasmids containing the appropriate mutation were then transformed into competent *E. coli* strain BL21(DE3) Rosetta for over-expression of the holoproteins.

CPR Overexpression and Purification: E. *coli* strain BL21(DE3) Rosetta cells were cultured at 37° C in LB medium containing ampicillin (100 ug/mL) and chloramphenicol (35 ug/mL) until the OD at 600 nm reached approximately 0.8 – 1.0, at which point IPTG was added to a final concentration of 0.4 mM and the temperature was lowered to 25° C for overnight incubation [50]. Cells were harvested by centrifugation, and the cell pellets were suspended in 50 mM Tris, pH 7.7 containing 0.1 mM EDTA, 0.05 mM dithiothreitol and 10% glycerol (Buffer A). Cells were lysed by passage through the French press cell at 12000 psi. The cell lysates from the expression of the WT CPR and the G141T CPR mutant were purified by affinity chromatrography using a resin with immobilized 2', 5'-ADP following the procedure of Rock *et al* followed by ion exchange chromatography. After loading the lysate onto the affinity resin, the column was washed with Buffer A and Buffer A containing 5 mM adenosine; the bound CPR protein was eluted with Buffer A containing 20 mM 2'(3') AMP and 100 mM NaCl [51]. Fractions that were reasonably pure, as determined by SDS PAGE analysis, were concentrated by ultrafiltration using an Amicon stirred cell apparatus with a 10 KDa NMWL filter. The concentrated CPR solution was loaded onto a DEAE Sephacel ion exchange column and washed with Buffer A. CPR was eluted with a linear salt gradient from 0 mM – 400 mM NaCl in Buffer A. The purity of selected fractions was confirmed by SDS PAGE and fractions over 95% pure were pooled and concentrated by ultrafiltration using an Amicon ultracentrifugal filtration device (Centricon-10). The concentrated solution was diluted

with Buffer A and re-concentrated several times so as to remove the NaCl and 2'(3') AMP. The concentrated protein was then stored at -80° C.

FBD Over-expression and Purification: The wild type and G141T FBD were over-expressed in the manner described above, however it was purified by DEAE Sephacel ion exchange and gel permeation chromatography. Cell lysate was loaded onto the ion exchange column and washed with Buffer A and then Buffer A containing 200 mM NaCl. The FBD was eluted with a linear salt gradient from 200 mM to 500 mM NaCl in Buffer A. Fractions that were reasonably pure, as determined by SDS PAGE analysis, were concentrated by ultrafiltration with an Amicon stirred cell apparatus (10 KDa NMWL filter). The concentrated CPR solution was subjected to gel permeation chromatography using a Sephacryl S-200-HR resin. The purity of selected fractions was confirmed by SDS PAGE and fractions over 95% pure were pooled and concentrated by ultrafiltration with an Amicon Centricon device (10 KDa NMWL) [52]. Protein concentrations were determined using the following molar extinction coefficients (M^{-1} cm^{-1}) at 455 nm: CPR 20,357; FBD 10,800 [unpublished data].

Spectral Analyses and Redox Titrations: All ultraviolet—visible absorbance spectra were recorded on an Agilent 8453 photodiode array spectrophotometer at 25° C. Anaerobic titrations of CPR and FBD by sodium dithionite and NADPH were performed in 270 mM potassium phosphate buffer, pH 7.7. NADPH, sodium dithionite, and potassium ferricyanide solutions were made anaerobic by extensive bubbling with argon. Protein samples (1 mL, final concentration 5 uM – 20 uM) were placed in a special sealable titration cuvette and made anaerobic by repeated cycles of partial vacuum evacuation and flushing with argon. Once complete reduction of the flavin cofactors

was achieved through the addition of sodium dithionite, the solution was titrated with potassium ferricyanide to fully re-oxidize the system. After the addition of each aliquot of reductant/oxidant the system was allowed to sit until no more spectral changes were observed, indicating that the system had reached thermodynamic equilibrium.

Steady-State Turnover Kinetic Analyses: Cytochrome c reductase activity was measured under saturating substrate concentrations with NADPH as the reductant. Assay solutions contained 270 mM potassium phosphate buffer, pH 7.7, 100 uM NADPH, 65 uM cytochrome c and CPR concentrations ranging from 1.15 to 15 nM [53, 54]. Reduction of cytochrome c was monitored at 550 nm with $\Delta\varepsilon = 21\ mM^{-1}\ cm^{-1}$ [55]. The ferricyanide reductase activity assay was also performed in 270 mM potassium phosphate buffer, pH 7.7. Reagent concentrations were as follows: 100 uM NADPH, 500 uM potassium ferricyanide, and CPR concentrations ranging from 1.15 to 21 nM. Reduction of ferricyanide was monitored at 420 nm with $\Delta\varepsilon = 1.04\ mM^{-1}\ cm^{-1}$ [56].

Determination of Oxidation—Reduction Potentials: The midpoint potential of the OX/SQ couple of the FMN-binding domain was established spectrophotometrically by equilibration with a standard indicator dye during anaerobic titration with sodium dithionite [31, 47]. Protein samples (1 mL, final concentration 15 uM – 20 uM) were placed in a special sealable titration cuvette along with an indicator dye (final concentration 20 uM) and made anaerobic by repeated cycles of partial vacuum evacuation and flushing with argon. The indicator dye used in the determination of the OX/SQ midpoint potential was anthraquinone-2,6-disulfonate (E_m = -184 mV) or anthraquinone-2-sulfonate (E_m = -225 mV). All measurements were performed in 270 mM potassium phosphate, pH 7.7 at 25° C. The spectrum at each point in the reductive

titration was compared to standard spectra for the redox dyes and each of the three redox states of the flavin cofactors. Multi-component spectral analyses were used to determine the relative concentrations of each of the various redox species of the FMN cofactor and the oxidized and reduced forms of the indicator dyes. The relative concentrations of each redox species at each point of the titration were then inserted into the Nernst equation (Equation 2) to calculate a midpoint potential. Titration points that had significant concentrations of all five redox species were averaged together to determine the midpoint potential of the OX/SQ couple.

(2) $E°_{SQ/OX} = E°_{dye} - ((R*T)/(n*F)) * \ln(([dyeRED]*[OX]) / ([dyeOX]*[SQ]))$

The midpoint potential for the SQ/HQ couple was calculated in the same manner and then verified using equations 3 and 4.

(3) $\Delta E = E_1 - E_2$

(4) $([I]/S)_{max} = (K^{1/2}/(2+K))$

Where $([I]/S)_{max}$ is the maximum concentration of semiquinone formed and S is the total protein concentration [57].

Pre-Steady-State Kinetic Analyses: All pre-steady-state kinetic measurements were performed using a Hi-Tech Scientific Model SF-61 stopped flow spectrophotometer. Reactions were initiated by the rapid mixing of equal volumes of each solution in the combination mixing/flow/observation cell (1-cm pathlength) of the instrument. Absorbance changes were digitally recorded and reaction time courses fit to standard single (5a), double (5b), or triple (5c) exponential equations using the Marquardt Levenberg iterative algorithm.

(5a) $A_\lambda = A_1 * e^{-(k1*t)} + C$

(5b) $A_\lambda = A_1 * e^{-(k1*t)} + A_2 * e^{-(k2*t)} + C$

(5c) $A_\lambda = A_1 * e^{-(k1*t)} + A_2 * e^{-(k2*t)} + A_3 * e^{-(k3*t)} + C$

Unless otherwise stated, measurements were carried out at 25° C under anaerobic conditions. All experiments with FBD, with the exception of single turnover assays, which were performed in 100 mM potassium phosphate, pH 7.0, were performed in 270 mM potassium phosphate, pH 7.7. All experiments with CPR, including single turnover assays, were performed in 100 mM potassium phosphate, pH 7.0. All buffers were made oxygen-free by extensive sparging with argon before use. Reduction of the oxidized flavin cofactors was monitored at 455 nm (Δε OX-HQ per flavin = 9.16 mM^{-1} cm^{-1}), formation and loss of the semiquinone state was monitored at 581 nm (Δε per flavin = 4.21 mM^{-1} cm^{-1})). For experiments involving pre-reduced flavin cofactors, the reducing agent (sodium dithionite or NADPH) was titrated into a sealed cuvette containing the flavoprotein until the desired redox state was achieved as determined by the absorbance spectrum of the solution. The reduced flavoprotein was then transferred anaerobically to the stopped-flow instrument via a gas-tight syringe.

Single Turnover Assay: Single turnover assays were performed using a Hi-Tech Scientific Model SF-61 stopped flow spectrophotometer and all solutions were made anaerobic and/or pre-reduced as described above. One mixing chamber contained 10 uM CPR and the other mixing chamber contained 10 uM NADPH and varying concentrations of cytochrome c (10.5 uM – 311.5 uM). The turnover rate was calculated by monitoring the reduction of cytochrome c at 550 nm (Δε = 21 mM^{-1} cm^{-1}) [55]. Absorbance changes were digitally recorded and reaction time courses fit to a standard single exponential

equation (5a) using the Marquardt Levenberg iterative algorithm. K_{max} and K_d were calculated using equation 6.

(6) $K_i = (K_{max}*[S]) / (K_d + [S])$

Results

FBD Redox Titrations: To determine the effect of the G141T mutation on the FMN cofactor alone, a redox titration was performed on the G141T FBD. Similar to wild type FBD, the oxidized G141T FBD had a characteristic absorbance peak at 455 nm with a slight shoulder at 470 nm. Addition of sodium dithionite reduces the FMN cofactor from the oxidized state to the semiquinone state and then to the hydroquinone state. Reduction of the flavin cofactor decreases the absorbance at 455 nm while formation of the semiquinone causes a band centered at 581 nm to form. As more dithionite is added, the FMN cofactor becomes fully reduced, causing the band at 581 nm to decrease back to the baseline level while the band at 455 nm decreases further. The spectral characteristics of G141T FBD upon reduction with sodium dithionite were quite different than wild type FBD (figures 16). At first glance, G141T FBD exhibits almost no formation of a band centered at 581 nm, suggesting that the majority of the flavin cofactors exist in either the fully oxidized or fully reduced state, even when one electron equivalent has been added to the solution. A more detailed analysis reveals that G141T FBD has a peak absorbance at 581 nm that is less than 30% of the wild type FBD peak absorbance (figure 17).

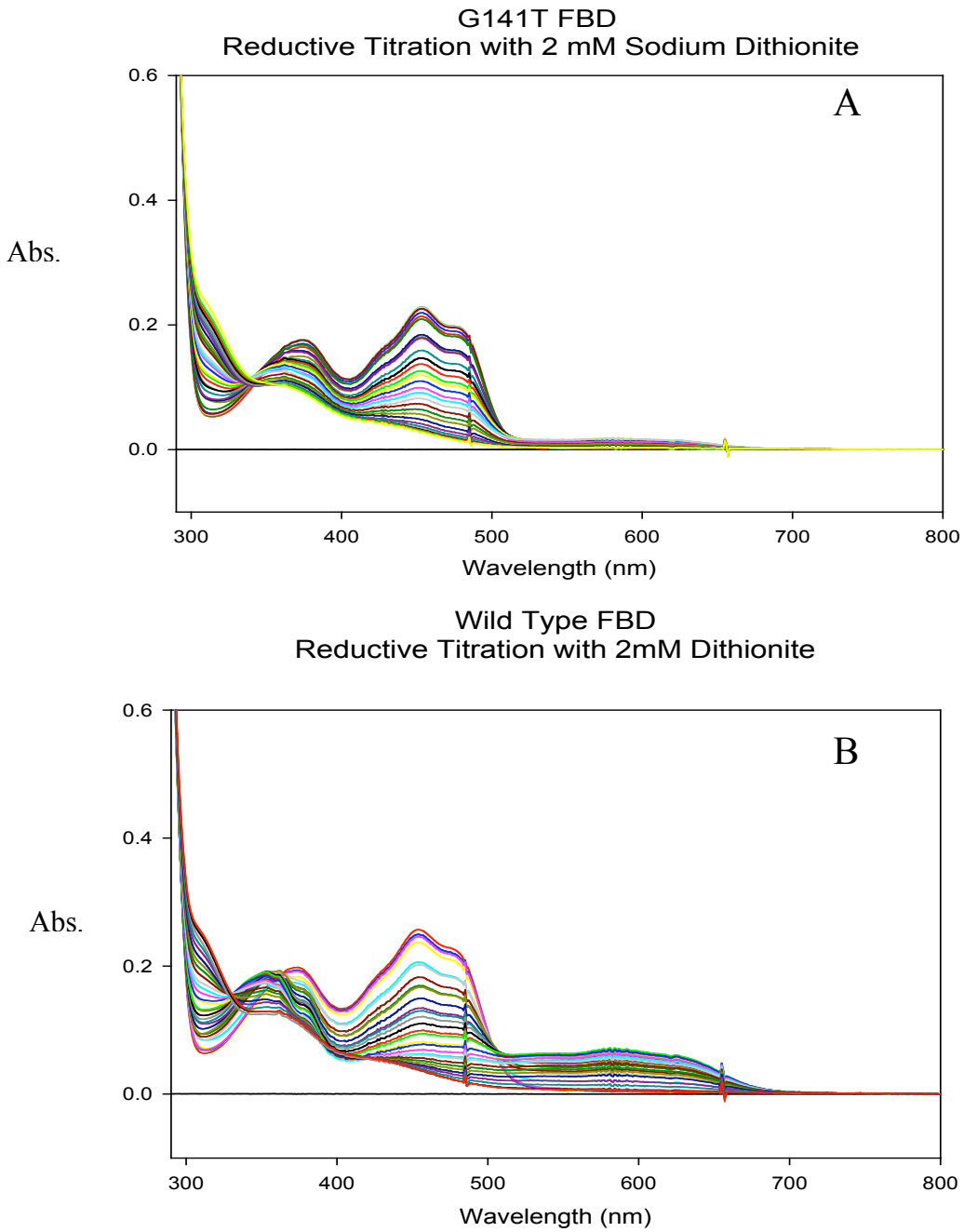

Figure 16: Spectral properties of the FBD during redox titration. (**A)** 20 uM G141T FBD and **(B)** 20 uM wild type FBD were reduced in a stepwise manner by addition of substoichiometric volumes of sodium dithionite (2 mM). After each addition of sodium dithionite, the system was allowed to fully equilibrate before the final spectrum was recorded. Experiments performed at 25° C in 270 mM potassium phosphate, pH 7.7.

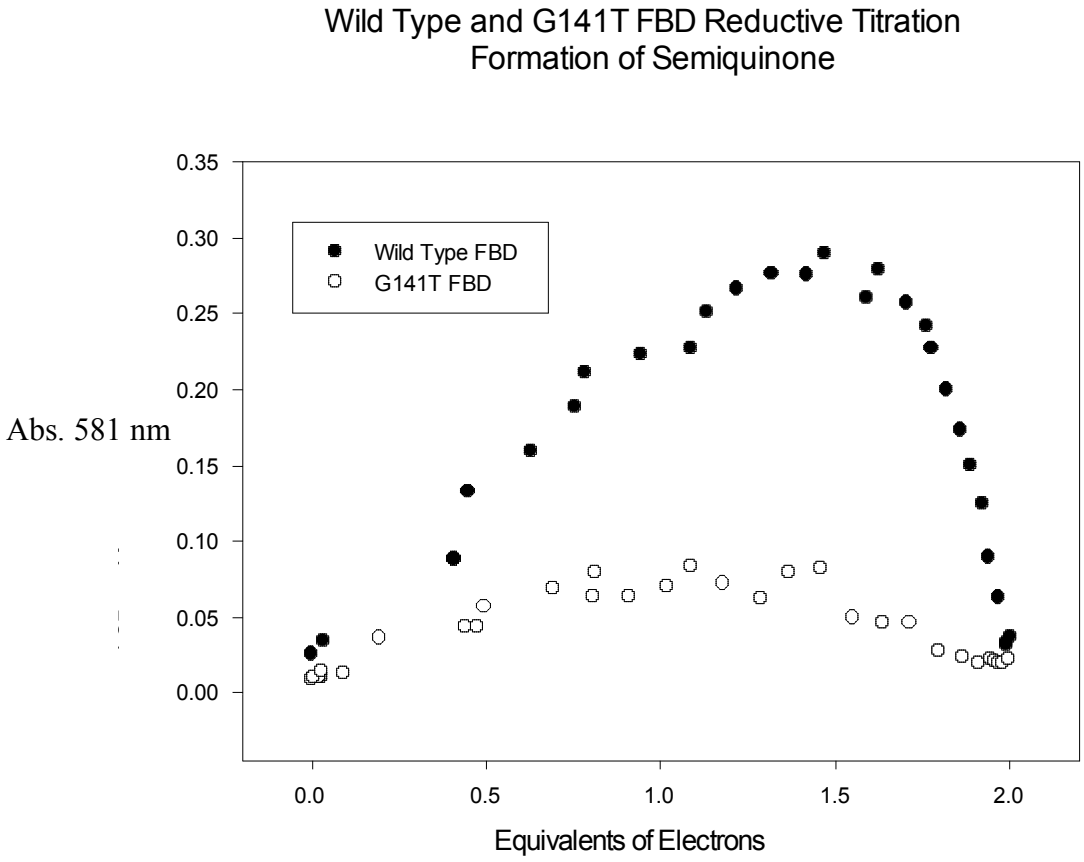

Figure 17: A comparison of the maximal semiquinone formation of wild type and G141T FBD during a redox titration with sodium dithionite. Absorbance at 581 nm is a measure of the amount of flavin cofactor in the semiquinone state. Titrations were performed at 25° C in 270 mM potassium phosphate, pH 7.7.

FBD Midpoint Potential: Given the significant change in the extent of semiquinone formation for the G141T FBD, the one-electron reduction potential of each flavin couple was determined at 25° C and pH 7.7 by equilibration with redox dyes having an established E_m value [47]. The OX/SQ midpoint potential was determined to be -253 mV using anthraquinone-2,6-disulfonate (E_m = -184 mV) as the indicator dye. Since there was a large difference between the OX/SQ midpoint potential and the E_m of the dye, there was little overlap between the five possible redox states in the system, which makes the calculations more difficult and error prone (figure 18a). To correct for this, the OX/SQ midpoint potential measurement was repeated using anthraquinone-2-sulfonate (E_m = -225 mV). This experiment yielded a midpoint potential of -250 mV. The greater overlap of all five redox states (figure 18b) and the reproducibility of the results increased our confidence in the accuracy of our calculation. Using the data from the anthraquinone-2-sulfonate titration, the SQ/HQ midpoint potential for the FMN cofactor of G141T FBD was calculated to be -219 mV. To verify the accuracy of the midpoint potential, it was recalculated using equations 3 and 4, yielding a value of -218 mV.

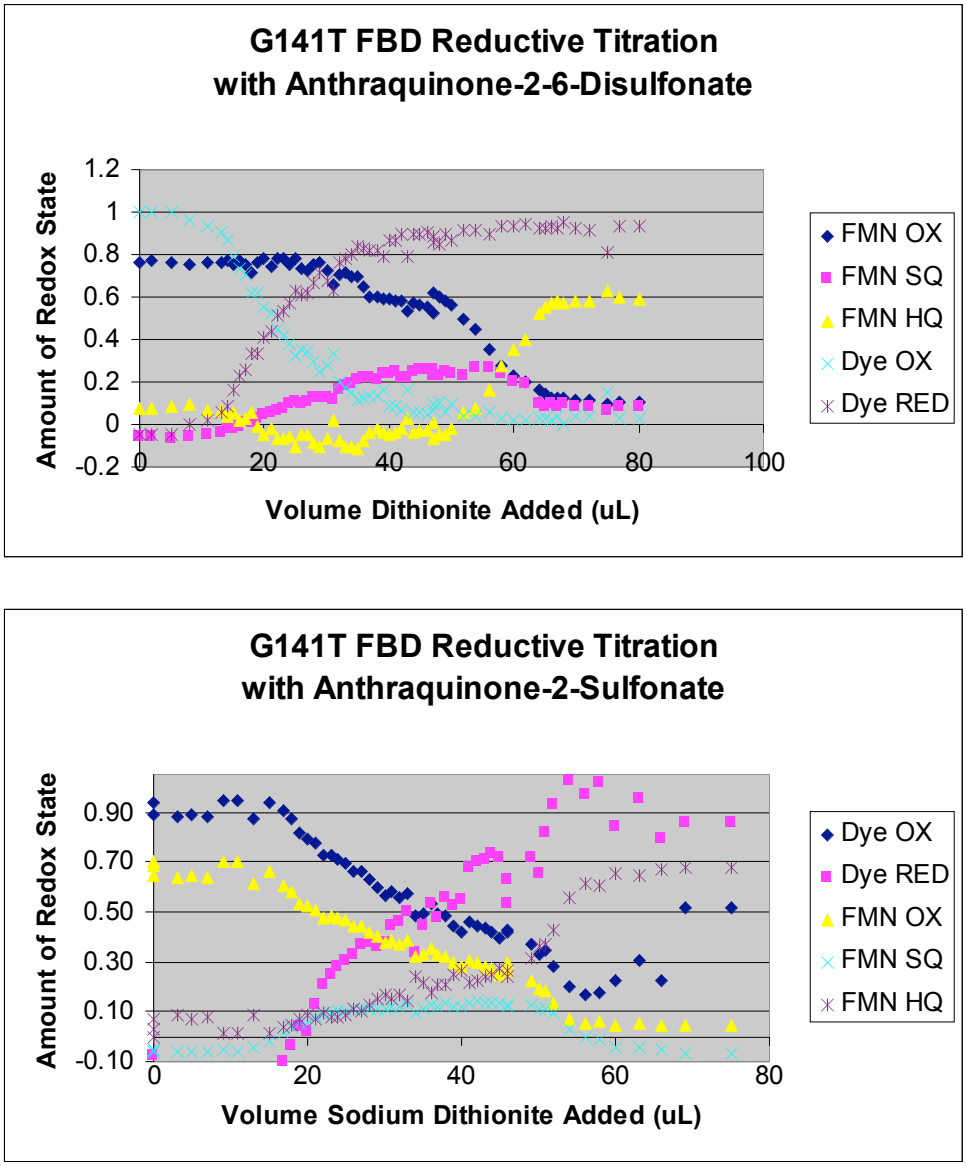

Figure 18: Multi-component analysis of redox titration of G141T FBD with sodium dithionite. **(A)** Indicator dye is anthraquinone-2,6-disulfonate (E_m = -184 mV). Most of the indicator dye is reduced before maximum semiquinone formation occurs. **(B)** Indicator dye is anthraquinone-2-sulfonate (E_m = -225 mV). In this titration, half of the indicator dye is reduced when maximum semiquinone formation occurs. Both titrations were performed in 270 mM potassium phosphate, pH 7.7. Indicator dye was at a concentration of 20 uM, FBD concentrations ranged from 15-20 uM, and titration was performed with 3 mM sodium dithionite.

For the FBD of human CPR, the OX/SQ and SQ/HQ midpoint potentials are -43 mV and -280 mV respectively (table 1) [31]. Although experiments in this lab were conducted on rat CPR, the high level of homology between rat and human CPR, particularly in the FMN binding loop, make comparisons of the midpoint potentials valid (figure 19) [58]. Compared to wild type FBD, the OX/SQ midpoint potential of the FMN cofactor of G141T FBD was decreased by over 200 mV, making it more negative than unbound FMN (-238 mV) [59]. Conversely, the SQ/HQ midpoint potential was increased by 60 mV, so that it is now less negative than the OX/SQ couple (figure 20). The inversion of the relative midpoint potentials makes it thermodynamically more favorable for the FMN cofactor to be in the hydroquinone form rather than the semiquinone form. Since the reductive titration was allowed to reach thermodynamic equilibrium, this offers a viable explanation for the diminished semiquinone formation observed during the dithionite titration of the G141T FBD. Munro et al demonstrated that for human CPR, the midpoint potential of the flavin cofactors in the isolated domains is similar to the midpoint potential in CPR [31]. Given the high homology between human and rat CPR, we assume that the midpoint potentials established in rat G141T FBD are similar to the midpoint potentials of the FMN cofactor in G141T CPR.

Flavin Cofactor Reduction Potential (mV)

	FMN cofactor			FAD cofactor		
Protein	OX/SQ	SQ/HQ	OX/HQ	OX/SQ	SQ/HQ	OX/HQ
rG141T FBD	-250 +/- 6	-219 +/- 5	-235 +/- 6			
hWT FBD	-43 +/- 7	-280 +/- 8	-235 +/- 8			
hWT FAD				-286 +/- 6	-371 +/- 7	-329 +/- 7
hWT CPR	-66 +/- 8	-269 +/- 10	-168 +/- 9	-283 +/- 5	-382 +/- 8	-333 +/- 7

Table 1: Comparison of the midpoint potentials of the flavin cofactors for human wild type and rat G141T CPR and their domains. G141T FBD measurements were made using multi-component analysis of the redox titration with sodium dithionite. The titration was carried out at 25° C in 270 mM potassium phosphate, pH 7.7 with 20 uM anthraquinone-2-sulfonate as the indicator dye. All wild type data comes from reference 31. Wild type experiments were carried out on human CPR, not rat CPR, in 100 mM potassium phosphate, pH 7.0. Midpoint potentials were measured with a Calomel electrode during a redox titration of the protein with sodium dithionite.

```
Identities = 164/170 (96%), Positives = 168/170 (98%), Gaps = 0/170 (0%)

[Rat]     VKESSFVEKMKKTGRNIIVFYGSQTGTAEEFANRLSKDAHRYGMRGMSADPEEYDLADLS  123
          V+ESSFVEKMKKTGRNIIVFYGSQTGTAEEFANRLSKDAHRYGMRGMSADPEEYDLADLS
[Human]   VRESSFVEKMKKTGRNIIVFYGSQTGTAEEFANRLSKDAHRYGMRGMSADPEEYDLADLS  126

[Rat]     SLPEIDKSLVVFCMATYGEGDPTDNAQDFYDWLQETDVDLTGVKFAVFGLGNKTYEHFNA  183
          SLPEID +LVVFCMATYGEGDPTDNAQDFYDWLQETDVDL+GVKFAVFGLGNKTYEHFNA
[Human]   SLPEIDNALVVFCMATYGEGDPTDNAQDFYDWLQETDVDLSGVKFAVFGLGNKTYEHFNA  186

[Rat]     MGKYVDQRLEQLGAQRIFELGLGDDDGNLEEDFITWREQFWPAVCEFFGVEATGEESSIR  243
          MGKYVD+RLEQLGAQRIFELGLGDDDGNLEEDFITWREQFWPAVCE FGVEATGEESSIR
[Human]   MGKYVDKRLEQLGAQRIFELGLGDDDGNLEEDFITWREQFWPAVCEHFGVEATGEESSIR  246
```

Figure 19: Amino acid alignment of *Rattus norvegicus* (rat) and *Homo sapiens* (human) FBD. The two sequences share 96% of amino acids, and 98% of positions are identical or contain a conservative mutation. Glycine 141 is highlighted, notice that it falls within a long stretch of sequence that is identical between rats and humans.

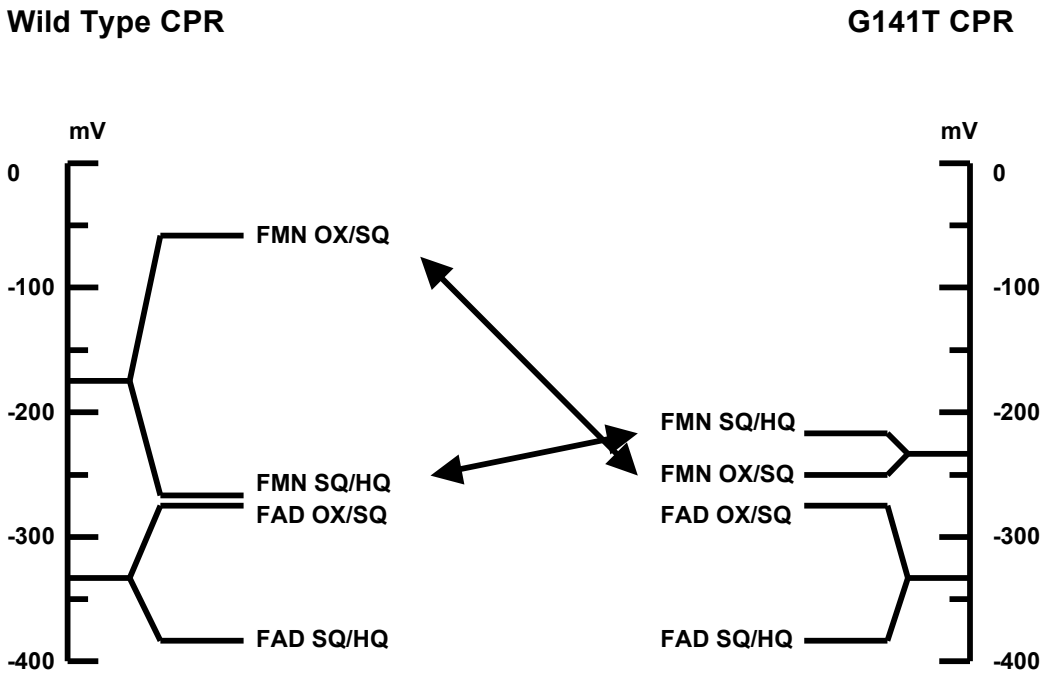

Figure 20: Diagram of the midpoint potentials in wild type and G141T CPR. Notice that the G141T mutation caused a change in the relative stabilities of the two midpoint potentials for the FMN cofactor. Midpoint potentials for FAD cofactor of G141T CPR are assumed to be the same as wild type because Munro et al. [31] demonstrated that the flavin cofactors have the same midpoint potentials in the isolated domains and the intact reductase, suggesting that there is little interaction between domains.

CPR Redox Titrations: The G141T CPR mutant exhibited unique spectral characteristics upon reduction with sodium dithionite (figure 21). Although the locations of the spectral changes upon reduction with sodium dithionite were quite similar to wild type CPR, the magnitude of such changes were different (figure 22). A normalized comparison of the reductive titrations of wild type and G141T CPR shows that G141T CPR has an absorbance maximum at 581 nm that is less than 75% of the wild type value, indicating that less semiquinone is present at thermodynamic equilibrium. The substantial loss of semiquinone state in the reductive titration of G141T FBD confirms that the FBD, not the FAD-binding domain, is responsible for the majority of semiquinone state lost in the reductive titration of G141T CPR. Furthermore, this absorbance maximum at 581 nm for G141T CPR occurs once three equivalents of electrons have been added (full reduction requires four equivalents of electrons) while the absorbance maximum at 581 nm for wild type occurs between one and two electron equivalents.

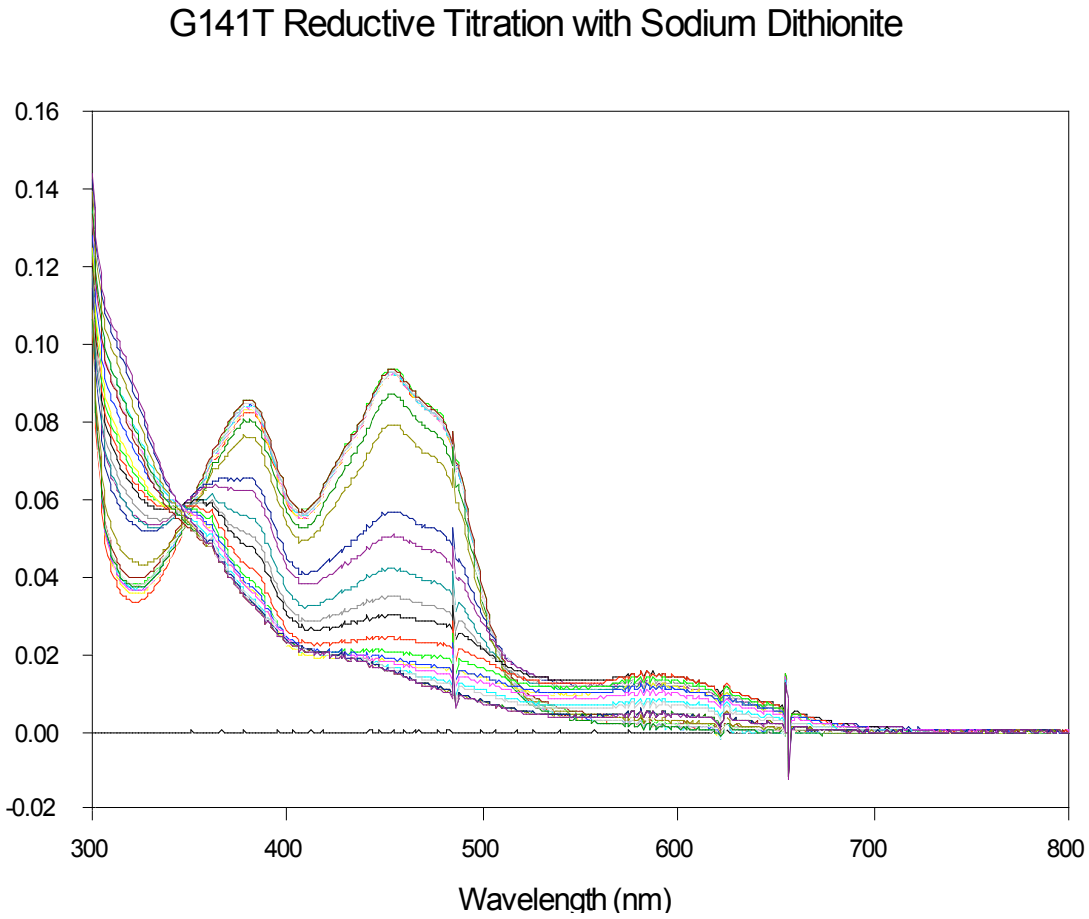

Figure 21: Spectral properties of G141T CPR during redox titration. G141T CPR (5.4 uM) was reduced in a stepwise manner by addition of substoichiometric volumes of sodium dithionite (2 mM). After each addition of sodium dithionite, the system was allowed to fully equilibrate before the final spectrum was recorded. Experiment performed at 25° C in 270 mM potassium phosphate, pH 7.7.

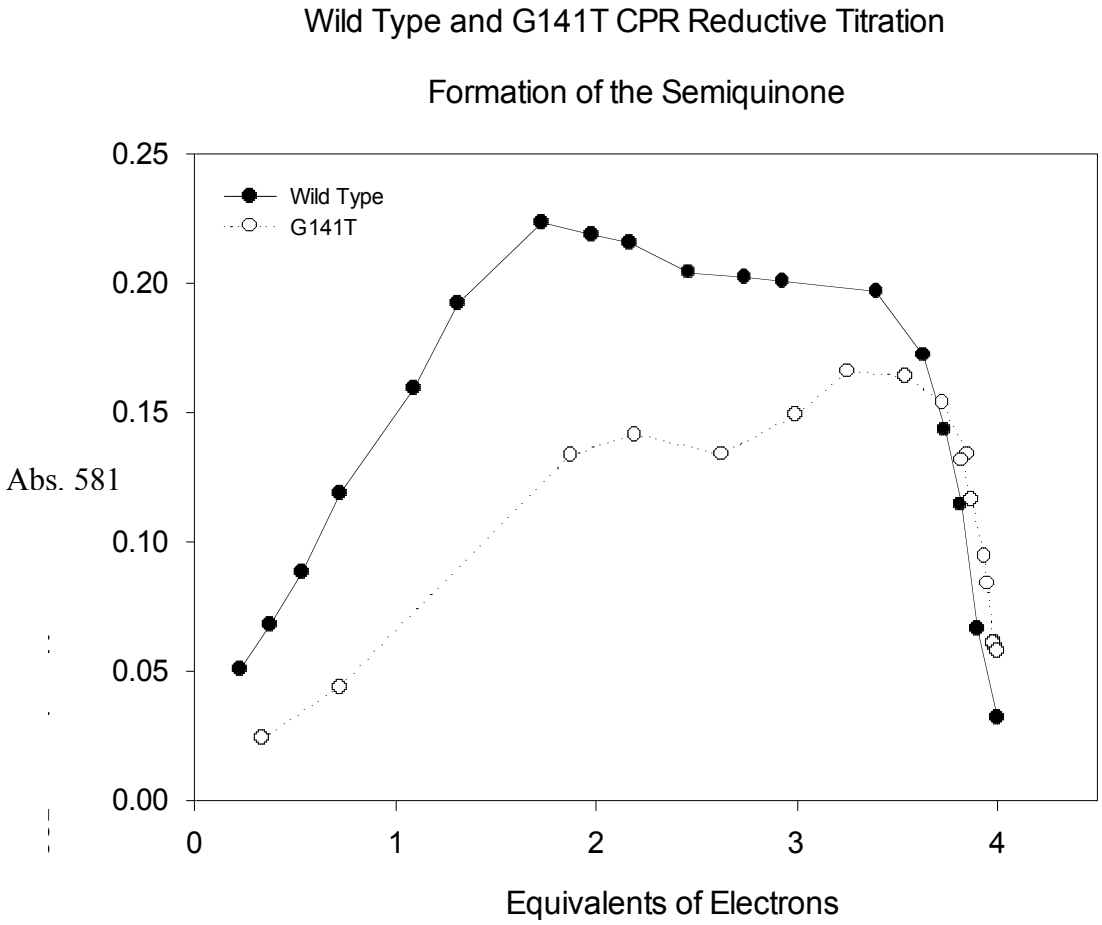

Figure 22: A comparison of the maximal semiquinone formation of human wild type CPR and rat G141T CPR during a redox titration with sodium dithionite. Absorbance at 581 nm is a measure of the amount of flavin cofactor in the semiquinone state. G141T CPR titration was performed at 25° C in 270 mM potassium phosphate, pH 7.7. Wild type data was calculated from reference 31 and was performed at 25° C in 100 mM potassium phosphate.

When the titration is repeated with NADPH, a complex equilibration reaction occurs wherein full reduction of the flavin cofactors is not achieved, even in the presence of excess NADPH (figure 23) [45]. Regardless of the reducing agent used, G141T CPR still forms 25% less semiquinone than wild type CPR. Since G141T FBD has 70% less semiquinone state at thermodynamic equilibrium than wild type FBD, and G141T CPR has only 25% less semiquinone state at thermodynamic equilibrium than wild type CPR, it can be concluded that the vast majority of semiquinone state lost at thermodynamic equilibrium of G141T CPR results from reduced semiquinone formation of the FMN cofactor.

After reduction by sodium dithionite, an oxidative titration was performed on the fully reduced G141T CPR (figure 24). Results indicate that the reduction of CPR by sodium dithionite is completely reversible. Once again, G141T CPR formed 25% less semiquinone than did wild type CPR. Maximal semiquinone formation occurred when three equivalents of electrons had been removed from CPR. Recall that for the reductive titration maximal semiquinone formation occurred when three equivalents of electrons had been added.

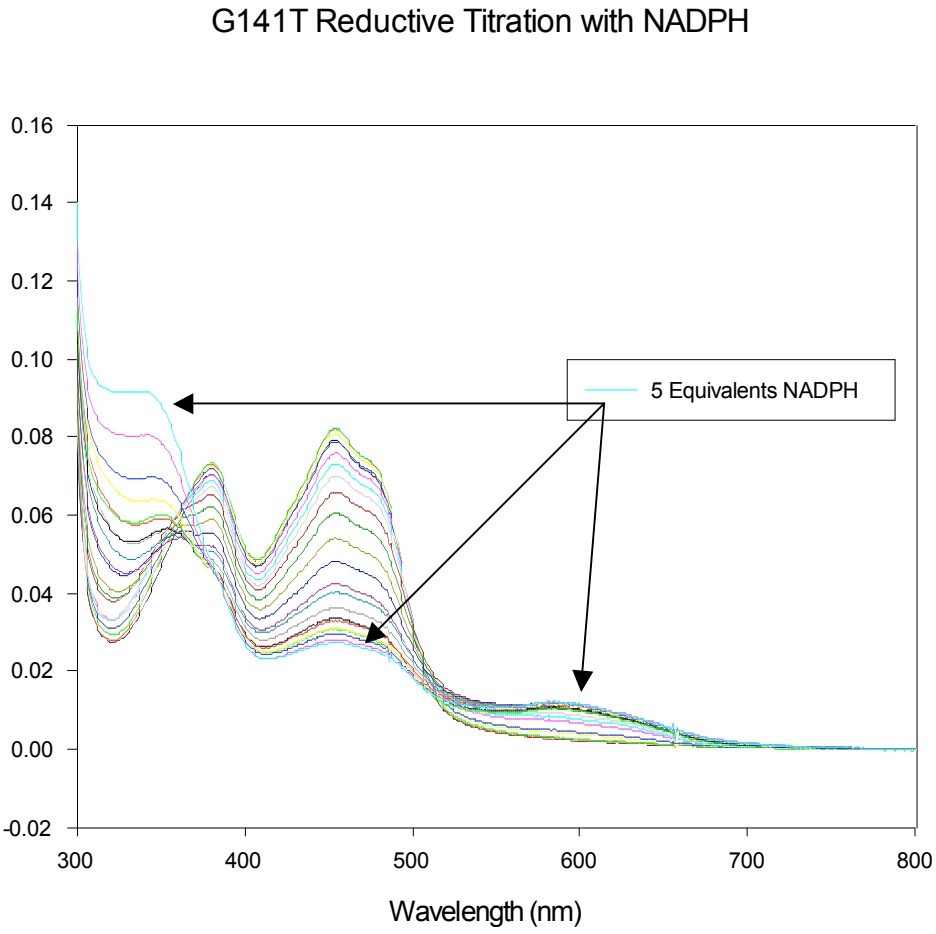

Figure 23: Spectral properties of G141T CPR during redox titration with the physiological reductant NADPH. Arrows point to the spectrum recorded when 5 equivalents of NADPH had been added to the system. Full reduction of CPR should require 2 equivalents of NADPH, however at 5 equivalents the band at 580 nm is still at a maximal level, indicating that a significant fraction of the flavin cofactors are still in the semiquinone state. G141T CPR (5.4 uM) was reduced in a stepwise manner by addition of substoichiometric volumes of NADPH (490 uM). After each addition of NADPH, the system was allowed to fully equilibrate before the final spectrum was recorded. Experiment performed at 25° C in 270 mM potassium phosphate, pH 7.7.

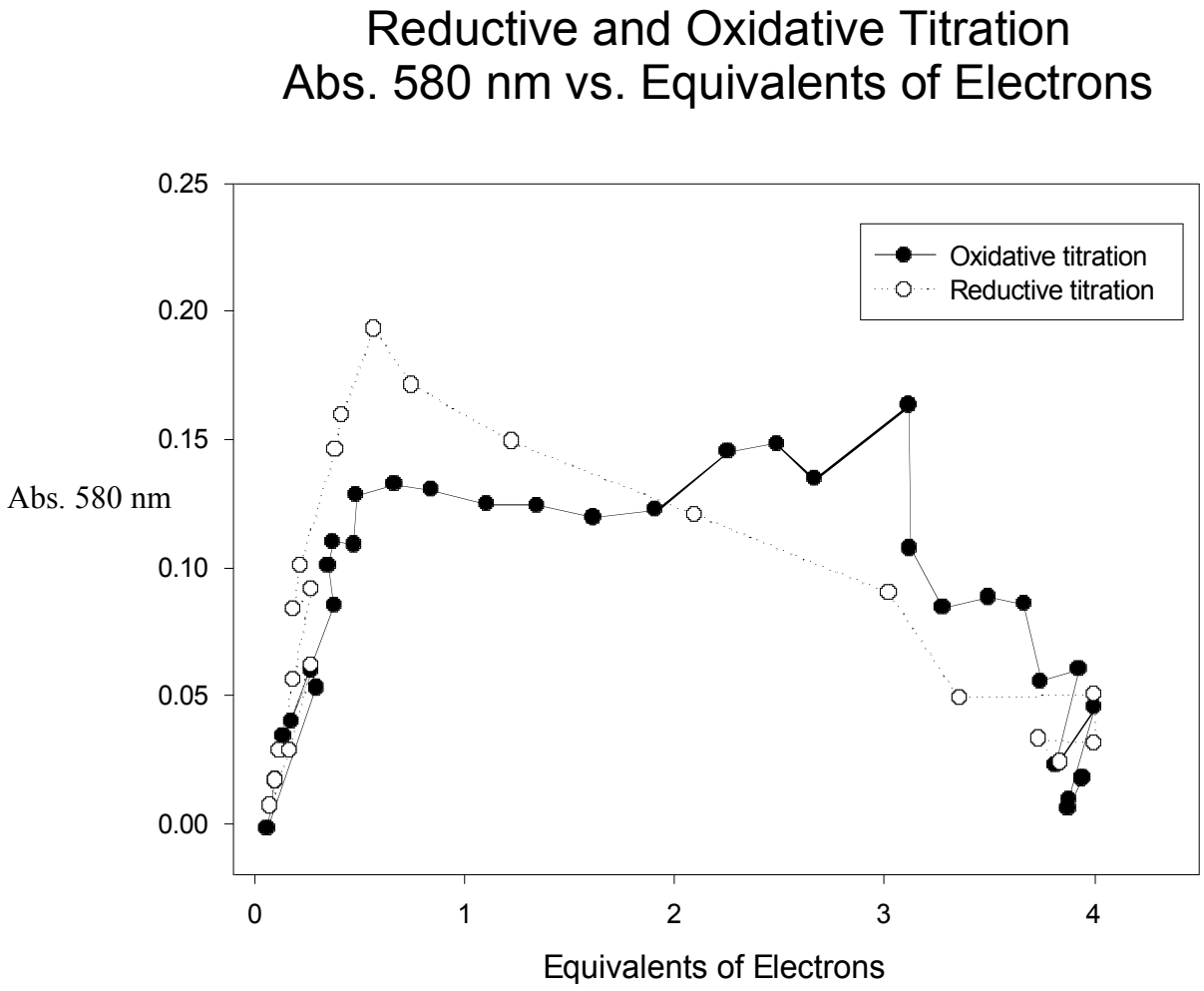

Figure 24: Comparison of maximum semiquinone formation during reductive titration of G141T CPR (5.4 uM) by sodium dithionite (2 mM) and then subsequent oxidative titration by potassium ferricyanide (0.5 mM). Absorbance at 580 nm is a measure of the amount of flavin cofactor in the semiquinone state. Experiment performed at 25° C in 270 mM potassium phosphate, pH 7.7.

CPR Steady-State Kinetics: Given the reduced semiquinone formation and the inversion of the relative midpoint potentials of the FMN cofactor for the G141T mutant, and the fact that wild type CPR utilizes the FMN semiquinone as the primary electron donor to cytochrome c, the effect of the G141T mutation on catalytic activity was probed by steady-state kinetic assays. The cytochrome c reductase assay is a well-established assay to measure the overall electron transfer ability of CPR to the non-physiological receptor cytochrome c [53, 54, 60, 61]. In this assay, the electrons must travel from NADPH to the FAD cofactor and then on to the FMN cofactor before being transferred to cytochrome c. The reduction of cytochrome c is monitored spectrophotometrically at 550 nm. Assays were performed with standard solutions of CPR and then repeated after the CPR solutions had incubated on ice for one to three hours with a 20-fold molar excess of FMN cofactor. The FMN cofactor was added to test for cofactor dissociation caused by the mutation or storage at -80° C.

As shown by the data in table 2, there was a 10% increase in activity for the G141T CPR mutant upon addition of excess FMN cofactor, indicating that there was a small amount of apoprotein present. However, when this assay was performed again at a later date, the addition of excess FMN cofactor caused a 50% drop in activity. We currently have no explanation for this observation. Upon addition of excess FMN cofactor to the wild type stock solution, a 20% increase in activity was observed. Our wild type data without excess FMN cofactor matched well with previously reported data [54]. The activity of G141T CPR without excess FMN is only 70% of the wild type CPR, indicating that the G141T mutation has affected the overall ability of CPR to transfer electrons in a physiological manner.

CPR Steady State Turnover Assays

Sample	Activity	
	TN (min^-1)	%WT
WT CPR to Cytochrome c	3920	100
WT CPR to Cytochrome c (Literature: *ref 53*)	3900	--
G141T CPR to Cytochrome c	2800	71
WT CPR to Cytochrome c + 20x FMN	6600*	(100)
G141T CPR to Cytochrome c + 20x FMN	3100*	(47)
WT CPR to Ferricyanide	6600	100
WT CPR to Ferricyanide (Literature: *ref 53*)	7800	--
G141T CPR to Ferricyanide	4000	61
WT CPR to Ferricyanide + 20x FMN	7000	100
G141T CPR to Ferricyanid + 20x FMN	3600	51

Table 2: Steady state turnover assays with wild type and G141T CPR. Cytochrome c assays were performed with 100 uM NADPH, 65 uM cytochrome c and CPR concentrations ranging from 1.15 to 15 nM. Ferricyanide assays were performed with 100 uM NADPH, 500 uM potassium ferricyanide, and CPR concentrations ranging from 1.15 to 21 nM. Where indicated, samples were incubated on ice for 1 to 3 hours with a 20-fold excess of free FMN. Assays were performed at 25° C in 270 mM potassium phosphate, pH 7.7.

*Note: The activity for wild-type CPR was unusually high in the presence of excess FMN. Excess FMN was added in an effort to insure that the FMN binding domain was saturated with the cofactor. However, highly variable results were obtained when doing so. Attempts to reproduce the result with a different preparation of CPR resulted in substantially lower values both the wild type (2400 to 2800 [+FMN] min^{-1}) and the mutant (~1000 min^{-1}). In contrast, the ferricyanide reductase activities were much less sensitive to added FMN suggesting that FMN may be interfering with the cytochrome c reductase assay. The activities of the mutant were consistently less than wild type under all assay conditions, however. Given the variability in the presence of excess FMN and our inability to adequately establish an explanation for this phenomenon, comparisons to the steady-state turnover activities in the "Results" section will be referenced to the values obtained in the absence of FMN which, for wild type, compare favorably to the established literature values obtained under similar assay conditions.

A ferricyanide reductase activity assay was performed under steady state conditions to probe the electron transfer activity of G141T CPR. Ferricyanide is capable of accepting electrons from the FAD cofactor and thus is best suited for probing the ability of CPR to accept electrons from NADPH [54]. Assays were performed with standard solutions of CPR and then repeated after the CPR solutions had incubated on ice for one to three hours with a 20-fold molar excess of FMN cofactor as described above. There was a 6% increase in activity of the wild type CPR in the presence of a 20-fold excess of FMN cofactor. Our wild type data with excess FMN cofactor matched well with previously reported data [54]. There was a 10% drop in activity of G141T CPR in the presence of FMN. We currently have no viable explanation for this observation. G141T CPR had only 65% of the activity of the wild type CPR. Even though the glycine to threonine mutation is in the FMN binding domain, it has an effect on the ability of the FAD domain to accept electrons from NADPH.

FBD Pre-Steady-State Reduction Kinetics: Since the glycine to threonine mutation affected the steady-state kinetics of CPR, the pre-steady-state reduction kinetics of the FBD were monitored to better understand which step(s) in the catalytic cycle is/are affected by the mutation. The kinetics of electron transfer were measured using a Hi-Tech Scientific Model SF-61 stopped flow spectrophotometer (table 3).

Redox Kinetics for WT and G141T FBD

Sample	Transition	λ	k
WT	OX-HQ	455	0.008 +/- 0.001
G141T	OX-HQ	455	0.010 +/- 0.001
WT	OX-HQ	581	0.004 +/- 0.006
G141T	OX-HQ	581	0.004 +/- 0.004
WT	SQ-HQ	455	0.57 +/- 0.21
G141T	SQ-HQ	455	ND*
WT	SQ-HQ	581	0.55 +/- 0.04
G141T	SQ-HQ	581	6.6 +/- 2.2
WT	HQ-OX	581	8.4 +/- 2.2
G141T	HQ-OX	581	26.8 +/- 3.8

Table 3: Pre-steady state kinetics of redox transitions of wild type and G141T FBD. Formation or loss of the oxidized state was measured at 455 nm while the semiquinone state was monitored at 581 nm. For the OX to HQ transition, FBD with fully oxidized FMN cofactor was mixed against a 20-fold excess of sodium dithionite. For the SQ to HQ transition, the FMN cofactor was pre-reduced with sodium dithionite until maximum semiquinone formation was achieved. The FBD with the pre-reduced FMN cofactor was then mixed against a 20-fold excess of sodium dithionite. For the HQ to OX transition, the FMN cofactor was pre-reduced to the hydroquinone state with sodium dithionite. The FBD with the pre-reduced FMN cofactor was mixed against a 20-fold excess of potassium ferricyanide. All experiments were performed in 270 mM potassium phosphate, pH 7.7.

* Due to the low formation of semiquinone state in the G141T mutant, most of the absorbance change observed at this wavelength is due to the OX – SQ transition rather than the SQ – HQ transition, so an appropriate rate could not be assigned.

In the first set of experiments, FBD was mixed with a 20-fold excess of sodium dithionite to achieve full reduction of the FMN cofactor under pseudo-first order conditions. Absorbance changes were monitored at 455 nm to observe the loss of the oxidized state and also at 581 nm to observe the formation and loss of the semiquinone state. Wild type and G141T FBD both exhibited slow rates of reduction at 455 nm (0.0084 s^{-1} and 0.0095 s^{-1} respectively) (figure 25 a, c). This rate is surprisingly slow considering that steady-state turnover assays with NADPH as the reductant, suggest a rate limiting step of 65 s^{-1} [54]. It is also surprising that there is no difference between wild type and G141T in the rates of reduction of the flavin cofactors.

At 581 nm there is no observable change in absorbance, indicating that there is no buildup of the semiquinone form of the FMN cofactor (figure 25 b, d). Since sodium dithionite is an obligate one-electron donor, the formation and the reduction of the FMN semiquinone must occur as two discrete steps, yet the formation and reduction of the FMN semiquinone are not observable. Furthermore, the data from 455 nm could be fit with a single exponential equation 5a even though both transitions from oxidized to semiquinone and from semiquinone to hydroquinone cause a decrease in absorbance at 455 nm. A viable explanation for these observations is that the two transitions occur at different kinetic rates, with the second step occurring much faster than the first step. Thus, any semiquinone that is formed is quickly converted to hydroquinone, eliminating the absorbance changes at 581 nm. This would make the formation of the semiquinone state rate limiting and could possibly explain the observation of a single phase at 455 nm.

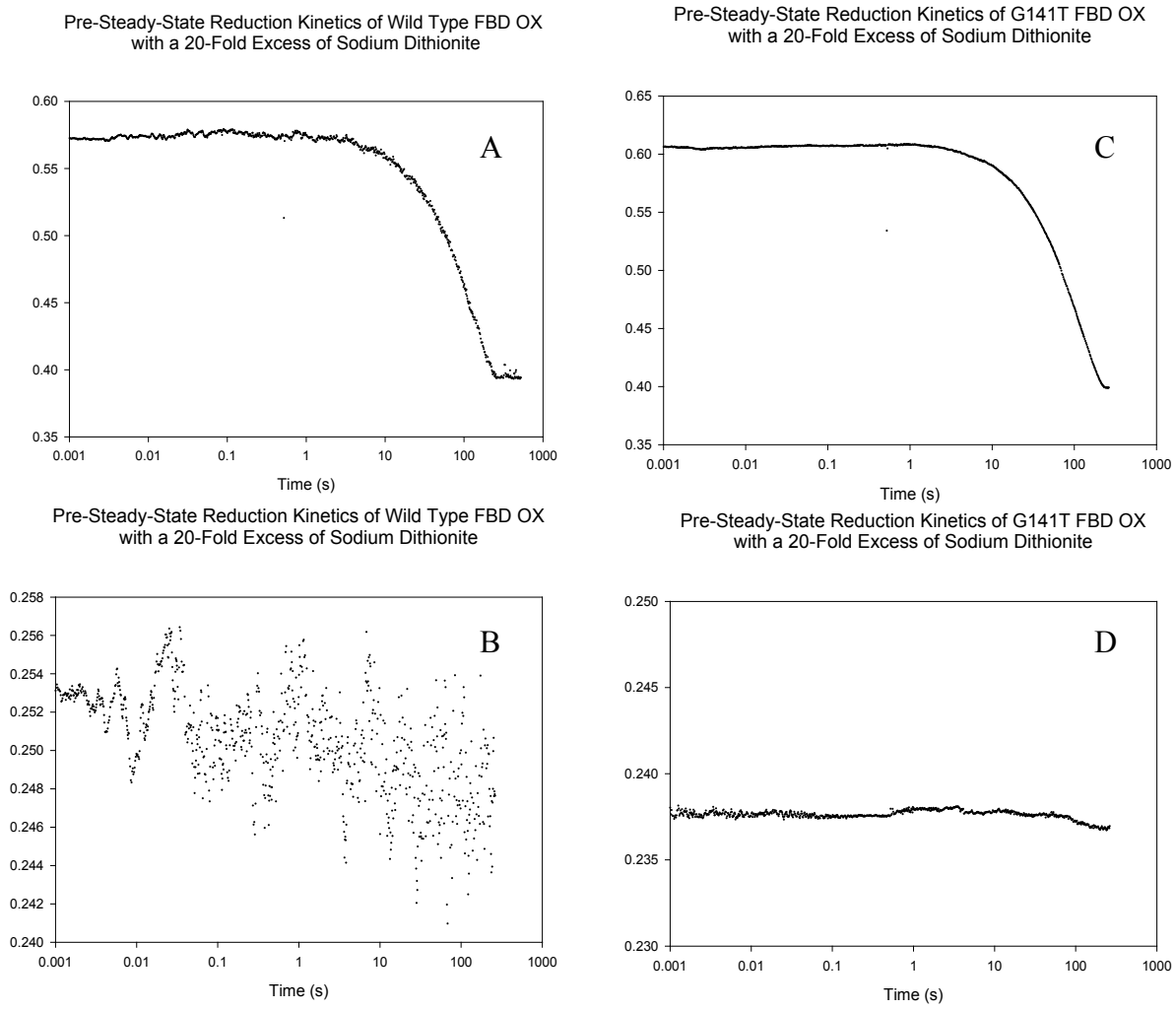

Figure 25: Pre-steady-state reduction kinetics of fully oxidized FMN cofactor in wild type and G141T FBD by a 20-fold excess of sodium dithionite. **(A)** Wild type FBD monitored at 455 nm to observe loss of oxidized state. Data was fit with a single exponential equation with $k_1 = 0.0084\ s^{-1}$. **(B)** Wild type FBD monitored at 581 nm to observe formation and loss of semiquinone state. **(C)** G141T FBD monitored at 455 nm. Data was fit with a single exponential equation with $k_1 = 0.0095\ s^{-1}$. **(D)** G141T FBD monitored at 581 nm. All experiments were performed at 25° C in 270 mM potassium phosphate, pH 7.7.

To test this hypothesis, the FBD was titrated with sodium dithionite until maximum semiquinone formation was achieved, at which point the solution was transferred anaerobically to the stopped flow instrument where it was mixed against a 20-fold excess of sodium dithionite as before. Absorbance changes were again monitored at 455 nm (figure 26 a, c). At 455 nm, the data could be fit to a single exponential equation 5a. The wild type rate was 0.57 s^{-1}, almost two orders of magnitude faster than the oxidized to hydroquinone transition. This confirms the hypothesis of why only one phase was observed at 455 nm for the oxidized to hydroquinone transition. When G141T FBD was pre-reduced with sodium dithionite by one electron equivalent, a rate of 0.018 s^{-1} was observed at 455 nm. This rate is only twice as fast as the oxidized to hydroquinone transition and is more than an order of magnitude slower than the wild type data.

Absorbance changes were also monitored at 581 nm (figure 26 b, d). Since there is only one possible transition (semiquinone to hydroquinone) the absorbance changes from both 455 nm and 581 nm report on the same electron transfer event and thus should give consistent rates. Wild type FBD conformed with this hypothesis with a rate of 0.55 s^{-1} at 581 nm compared to a rate of 0.57 s^{-1} at 455 nm. G141T FBD had different rates at 455 nm (0.018 s^{-1}) and 581 nm (6.6 s^{-1}). What can account for such a difference in rates? Recall that during the reductive titration of G141T FBD that even when one electron equivalent had been added, the majority of the FMN cofactors in solution existed either the oxidized or semiquinone state. Thus, for G141T FBD, even when maximal semiquinone formation is achieved, the majority of the absorbance changes at 455 nm are due to the reduction of the oxidized flavin rather than the semiquinone, thereby accounting for the rate discrepancy between 581 nm and 455 nm.

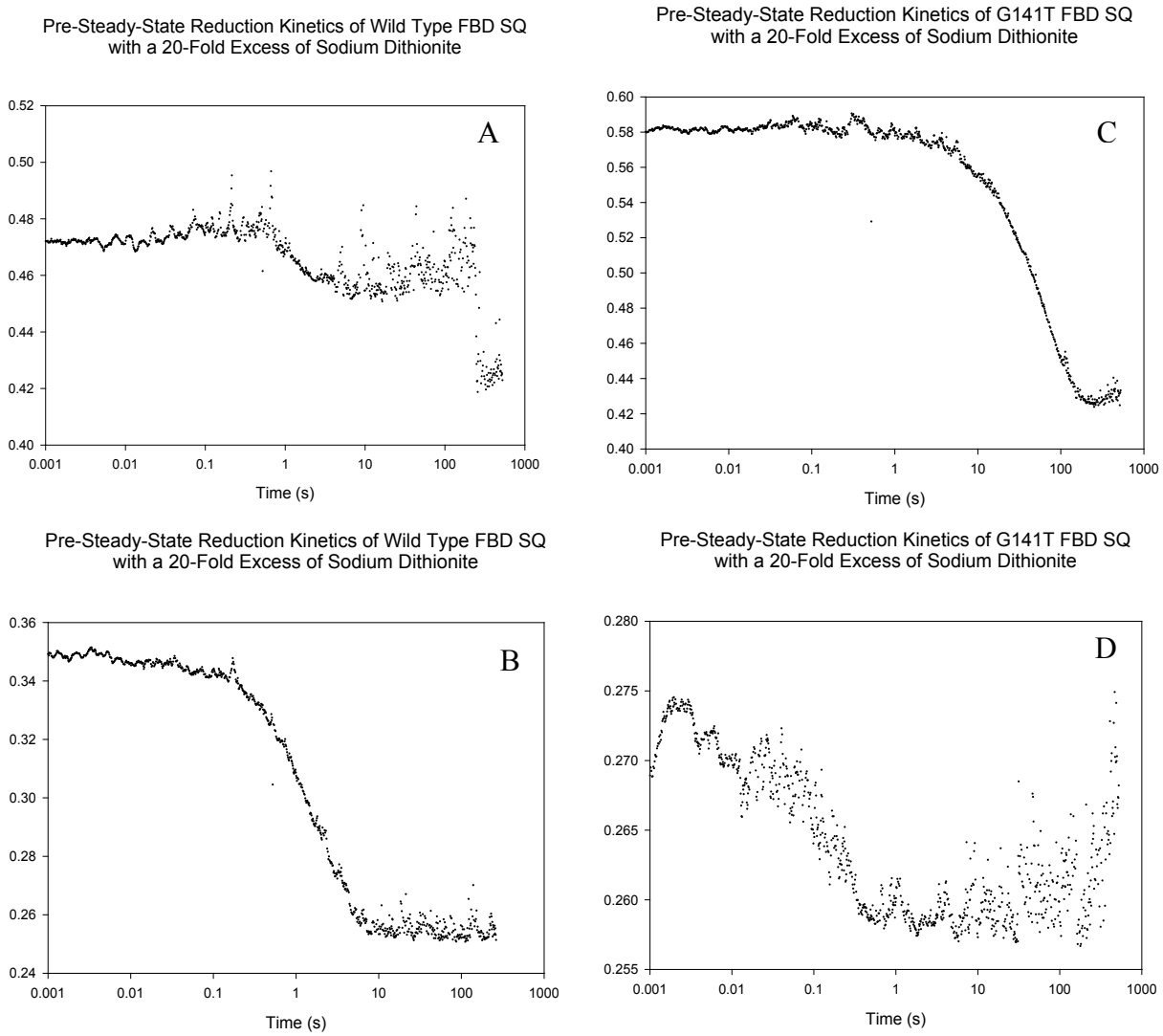

Figure 26: Pre-steady-state reduction kinetics of wild type and G141T FBD by a 20-fold excess of sodium dithionite where the FMN cofactor had been pre-reduced to maximum semiquinone formation by sodium dithionite. **(A)** Wild type FBD monitored at 455 nm to observe loss of oxidized state. Data was fit with a single exponential equation with $k_1 = 0.57\ s^{-1}$. **(B)** Wild type FBD monitored at 581 nm to observe formation and loss of semiquinone state. Data was fit with a single exponential equation with $k_1 = 0.55\ s^{-1}$. **(C)** G141T FBD monitored at 455 nm. Data was fit with a single exponential equation with $k_1 = 0.018\ s^{-1}$. Due to the low formation of semiquinone state in the G141T mutant, most of the absorbance change observed at this wavelength is due to the OX – SQ transition rather than the SQ – HQ transition. **(D)** G141T FBD monitored at 581 nm. Data was fit with a single exponential equation with $k_1 = 6.6\ s^{-1}$. All experiments were performed at 25° C in 270 mM potassium phosphate, pH 7.7.

The observed rate of 6.6 s^{-1} for the semiquinone to hydroquinone transition for G141T FBD is significantly faster than the observed transition from oxidized FMN to hydroquinone FMN (0.0095 s^{-1}), which is consistent with the proposed explanation for the observation of a single phase at 455 nm for the oxidized to hydroquinone transition. The semiquinone to hydroquinone transition observed in G141T FBD is also an order of magnitude faster than the same transition in wild type FBD (0.55 s^{-1}). This difference in rates between wild type and G141T FBD is difficult to explain directly at the molecular level. Many factors control electron transfer rates, especially using non-physiologic reductants such as sodium dithionite as used in these experiments. However the faster reduction rate for the SQ in G141T FBD is consistent with the substantial decrease in the midpoint potentials for the OX/SQ couple reflecting the lower stability of the SQ state in this mutant. Thus, it might be expected that the reduction of the semiquinone to hydroquinone, would occur faster in G141T FBD than wild type FBD (figure 20).

With the rates of reduction of the FMN cofactor of the FBD well characterized, the rates of oxidation were measured. In this experiment, FBD was titrated with sodium dithionite until the FMN cofactor was fully converted to the hydroquinone form. Care was taken so as not to add excess sodium dithionite to the solution. The fully reduced FBD was then transferred anaerobically to the stopped-flow instrument and rapidly mixed with a 20-fold excess of potassium ferricyanide. Absorbance changes were monitored at 455 nm and 581 nm. There is good agreement in the rates of oxidation observed at 455 nm and 581 nm for both wild type (6.7 s^{-1} and 8.4 s^{-1} respectively) and for G141T FBD (26.7 $s^{-1}$and 26.8 s^{-1}) (figure 27). Figures 27b and 27d show the traces taken at 581 nm for wild type and G141T FBD respectively.

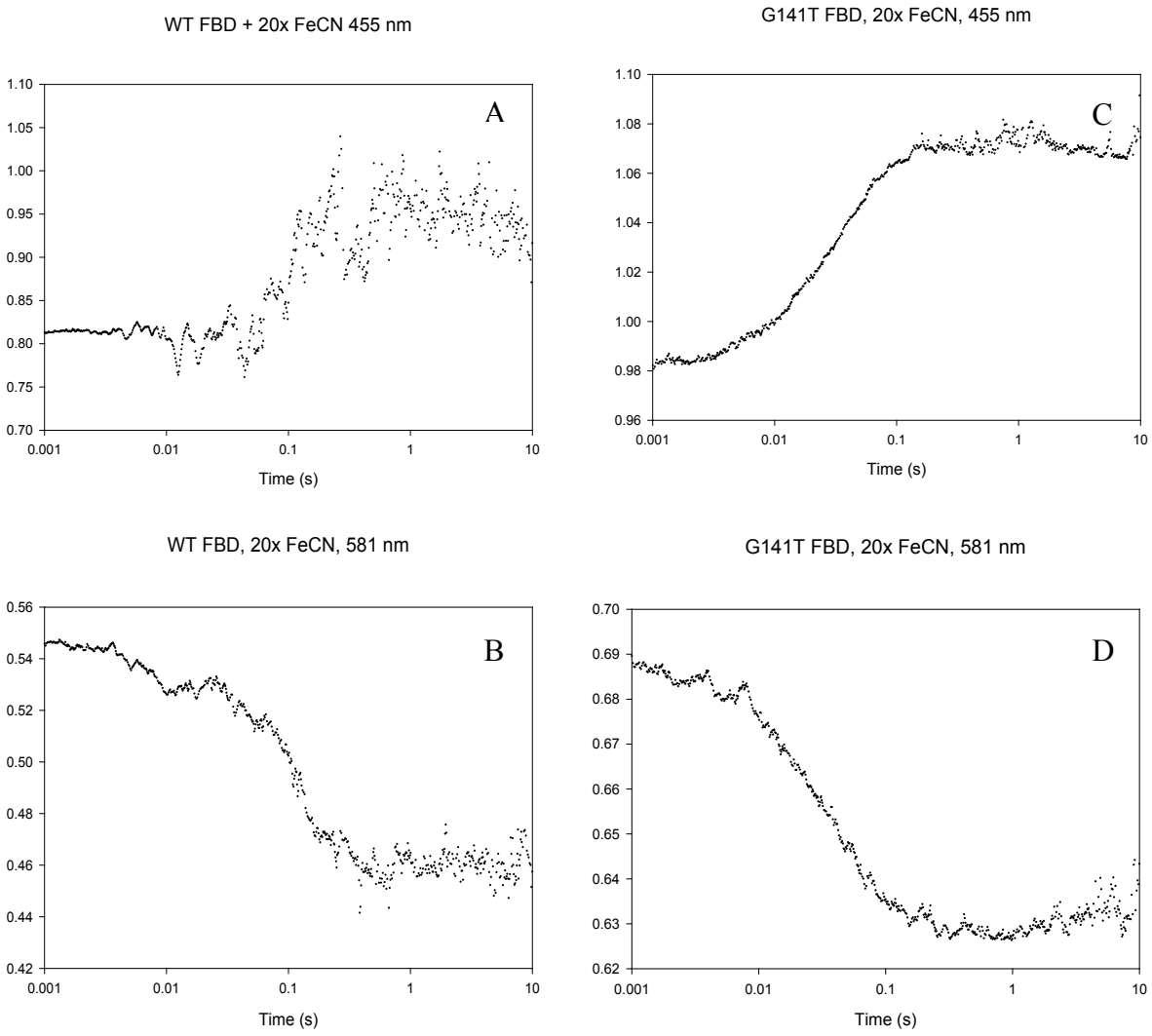

Figure 27: Pre-steady-state oxidation kinetics of wild type and G141T FBD by a 20-fold excess of potassium ferricyanide where the FMN cofactor had been pre-reduced to the hydroquinone state by sodium dithionite. **(A)** Wild type FBD monitored at 455 nm to observe formation of oxidized state. Data was fit with a single exponential equation with $k_1 = 6.7\ s^{-1}$. **(B)** Wild type FBD monitored at 581 nm to observe formation and loss of semiquinone state. Data was fit with a single exponential equation with $k_1 = 8.4\ s^{-1}$. **(C)** G141T FBD monitored at 455 nm. Data was fit with a single exponential equation with $k_1 = 26.7\ s^{-1}$. **(D)** G141T FBD monitored at 581 nm. Data was fit with a single exponential equation with $k_1 = 26.8\ s^{-1}$. For both wild type and G141T FBD at 581 nm, only one phase is observed, corresponding to the loss of semiquinone state. All experiments were performed at 25° C in 270 mM potassium phosphate, pH 7.7.

It is interesting to note that both traces can be fit with a single exponential equation 5a. Potassium ferricyanide can only accept one electron, so two distinct phases are expected, correlating to the formation of the semiquinone and its subsequent oxidation. The only phase that is observed is the oxidation of the semiquinone to the oxidized state, indicating that the oxidation of the hydroquinone to the semiquinone state occurs within the dead time of the instrument (1 ms).

The data shows that G141T FBD donates electrons to potassium ferricyanide three to four times faster than wild type FBD. This is a somewhat unexpected result in light of the steady-state turnover data. Although it should be pointed out that the ferricyanide assay performed on CPR was used to measure the rate of electron transfer from the FAD-binding domain, not the FBD. Additionally, potassium ferricyanide is a chemical oxidant, while cytochrome c is a protein. The interaction between cytochrome c and FBD may be quite different than the interaction between potassium ferricyanide and FBD. Still, these experiments provide insight into the effect of the glycine to threonine mutation. Recall that measurement of the midpoint potentials of the FMN cofactor of the FBD showed that the OX/SQ midpoint potential had been decreased by over 200 mV. With the semiquinone state in G141T FBD significantly destabilized, it is a better reductant and thus it will reduce potassium ferricyanide faster.

CPR Pre-Steady-State Reduction Kinetics: The pre-steady-state reduction kinetics of the FBD showed all measurable transitions to occur faster in the G141T mutant than in wild type. The pre-steady-state reduction kinetics of G141T CPR were determined for all measurable transitions (table 4) to more thoroughly dissect how the mutation affected the mechanism of electron transfer.

Pre-Steady-State Reduction Kinetics of CPR

Sample	Transition	[DT]	λ	k_1	k_2
G141T	OX-HQ	20x	581	0.023 +/- 0.002	0.018 +/- 0.002

Sample	Transition	[NADPH]	λ	k_1	k_2
WT*	OX-HQ	15x	450	20	3.7
G141T	OX-HQ	15x	455	113 +/- 54	12.5 +/- 2.1
WT*	OX-HQ	15x	600	20	3.5
G141T	OX-HQ	15x	581	51 +/- 5	9.5 +/- 0.9
G141T 4°C@	OX-HQ	15x	455	2.7 0.3	0.013
G141T 4°C	OX-HQ	15x	581	3.6 +/- 1.5	0.042 +/- 0.033
WT*	OX-SQ	1 to 1	581	20	0
G141T #	OX-SQ	1 to 1	581	69 +/- 7 2.1 +/- 0.06	0.014
*	Literature Value				

Table 4: Pre-steady-state reduction kinetics of CPR. Absorbance changes were measured at 455 nm to observe reduction of oxidized state and 581 or 600 nm to observe formation and loss of the semiquinone state. G141T data was collected at 25° C in 100 mM potassium phosphate, pH 7.0. Wild type values are from reference 42 and are based on human CPR, rather than rat CPR. Wild type data was collected at 25° C in 50 mM potassium phosphate, pH 7.0.

@ G141T CPR 4° could be fit by a triple exponential equation. The first two phases, $k_1 = 2.7\ s^{-1}$, $k_2 = 0.3\ s^{-1}$, correspond with a decrease in absorbance at 455 nm. The third phase, $k_3 = 0.013\ s^{-1}$, corresponds with an increase in absorbance at 455 nm.

G141T CPR mixed with a 1 to 1 solution of NADPH was fit with a three exponential equation. The first two phases, $k_1 = 69\ s^{-1}$, $k_2 = 2.1\ s^{-1}$, correspond with an increase in absorbance at 581 nm. The third phase, $k_3 = 0.014\ s^{-1}$, corresponds with a decrease in absorbance at 581 nm.

In the first experiment G141T CPR was mixed with a 20-fold molar excess of sodium dithionite to draw comparisons with the pre-steady-state reduction kinetics of the FBD. Two distinct phases were observed at 581 nm, the first correlating with the formation of a flavin semiquinone and the second with the reduction of the semiquinone to a hydroquinone (figure 28). However, both transitions were quite slow ($k_1 = 0.023\ s^{-1}$, $k_2 = 0.018\ s^{-1}$), especially when compared to the SQ to HQ transition for the FBD ($k = 6.6\ s^{-1}$). The rates for the formation and reduction of the semiquinone state were quite similar, so whenever any semiquinone state was formed, it reduced to the hydroquinone state at almost the same speed. This explains why the absorbance change at 581 nm was only 10% of what was expected. Sodium dithionite can reduce both flavin cofactors directly and the two flavin cofactors are essentially indistinguishable in a stopped-flow experiment, so we were unable to determine which flavin was contributing to the absorbance changes at 581 nm. Because of these results, all future experiments were conducted with the physiological reductant NADPH.

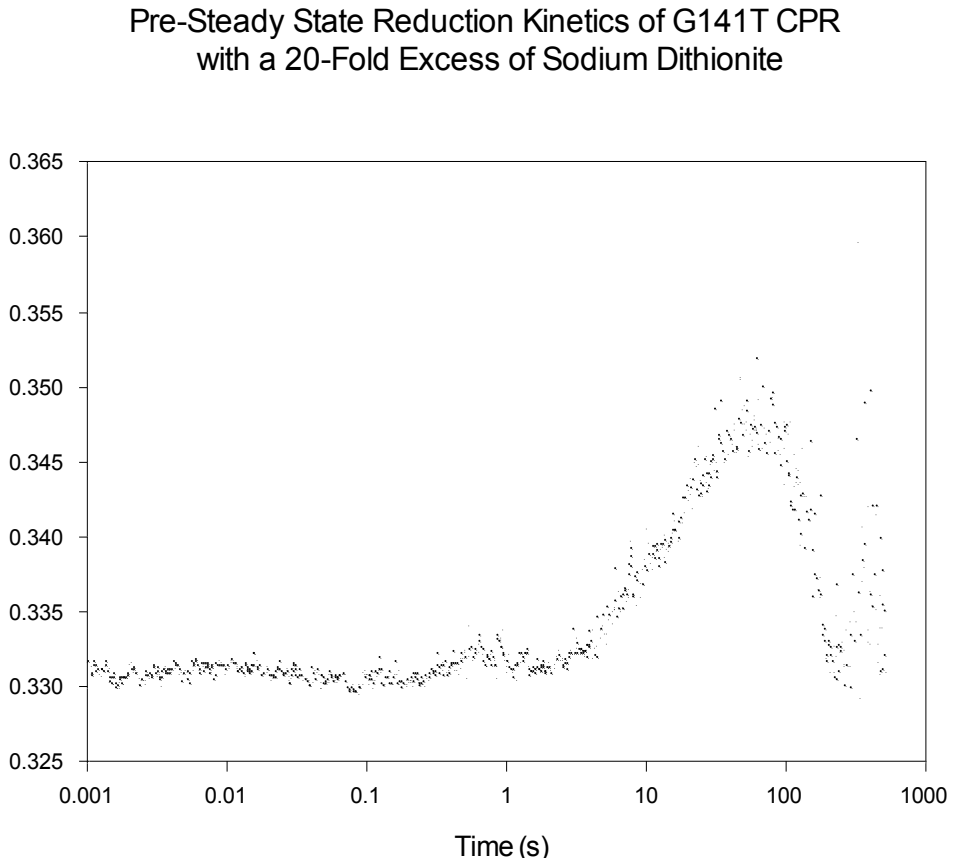

Figure 28: Pre-steady-state reduction of G141T CPR by a 20-fold excess of sodium dithionite, monitored at 581 nm. The trace could be fit by a double exponential equation with k_1= 0.023 s^{-1} and k_2= 0.018 s^{-1} correlating to the formation and then reduction of the semiquinone state of the flavin cofactors. Because the rates for the formation and the reduction of the flavin cofactors are so close together, the absorbance change at 581 nm is only 10% of what was expected. Experiment was performed at 25° C in 100 mM potassium phosphate, pH 7.0.

NADPH is an obligate two-electron donor, so the oxidation of one molecule of NADPH by CPR leads to three possible redox states FAD HQ – FMN OX, FAD SQ – FMN SQ, and FAD OX – FMN HQ (figure 9). The oxidation of a second molecule of NADPH by CPR leads to full reduction of both flavin cofactors. Two distinct phases are observed at 581 nm upon reduction of G141T CPR with a 15-fold molar excess of NADPH (figure 29c). The first phase shows an increase in absorbance, indicating that two electrons had been transferred from NADPH to G141T CPR to form the disemiquinoid species while the second phase shows a drop in absorbance, correlating with the transfer of a second pair of electrons from NADPH to G141T CPR, reducing both flavin cofactors to the hydroquinone. The rates for these two phases are 51 s^{-1} and 9.5 s^{-1} respectively. Previously published results for the reduction of wild type CPR with a 20-fold excess of NADPH also showed two distinct phases. However, the rates for these two phases (20 s^{-1} and 3.5 s^{-1}) were approximately half the rates observed for G141T CPR [42]. It is interesting to note that the rate of reduction of the G141T CPR disemiquinoid state (k_2 = 9.5 s^{-1}) is comparable to the SQ to HQ transition for the G141T FBD (k_1 = 6.6 s^{-1}). Although caution must be used in this comparison due to the multiple flavin cofactors in CPR and the different nature of the reductants used. Upon observation at 581 nm for an extended period of time, one to eight minutes, a third phase is observed with complex kinetics wherein the absorbance at 581 nm increases (figure 29d). This is most likely due to equilibration of the flavin cofactors with NADPH/$NADP^+$ [45]. Due to the extended time scale needed to observe this phase, it is not physiologically relevant and will not be included in further discussion of the reduction kinetics.

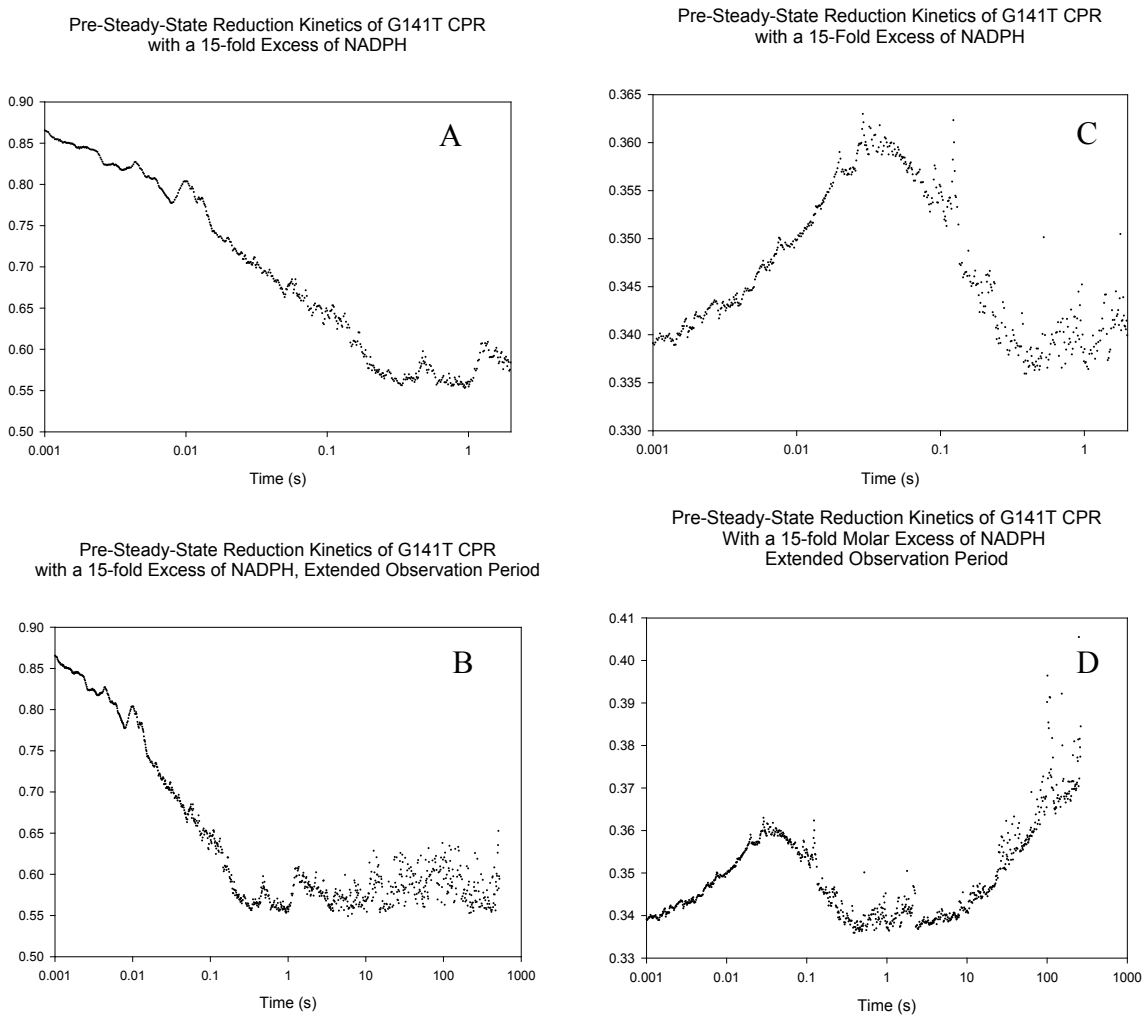

Figure 29: Pre-steady-state reduction of G141T CPR by a 15-fold excess of NADPH. All experiments were performed at 25° C in 100 mM potassium phosphate, pH 7.0. **(A)** Absorbance changes monitored at 455 nm over a physiologically relevant time period of 2 s. The data can be fit by a double exponential equation with $k_1 = 113\ s^{-1}$ and $k_2 = 12.5\ s^{-1}$. **(B)** When the observation period at 455 nm is extended out past 5 minutes, no additional phases were absorbed. **(C)** When absorbance values are monitored at 581 nm over a physiologically relevant time period of 2 s, the data can be fit by a double exponential equation with $k_1 = 51\ s^{-1}$ and $k_2 = 9.5\ s^{-1}$. **(D)** When the observation period at 581 nm is extended out past 5 minutes, a third phase is observed. This increase in absorbance at 581 nm has a rate of $k_3 = 0.027\ s^{-1}$.

Interestingly, the pre-steady-state reduction experiments conducted on human wild type CPR with a 20-fold excess of NADPH by Gutierrez et al. showed two phases with nearly identical rates when the absorbance changes were monitored at 455 nm and 581 nm (20 s^{-1}, 3.7 s^{-1}, and 20 s^{-1}, 3.5 s^{-1} respectively) [42]. However, absorbance changes at 455 nm monitor reduction of the oxidized flavins while changes at 581 nm monitor formation and reduction of the semiquinone state. Transfer of the hydride ion from NADPH to FAD should cause a loss of absorbance at 455 nm but should not affect absorbance at 581 nm. The subsequent transfer of an electron from FAD HQ to the FMN cofactor to the form the disemiquinoid state will cause the absorbance at 581 nm to increase. Finally, the transfer of a second hydride ion from NADPH will form the FAD HQ – FMN HQ and cause a drop in absorbance at both 455 nm and 581 nm. If there are three different transitions, why are only two rates observed, and why does k_1 at 455 nm match k_1 at 581 nm? Figure 30 provides a possible explanation. The transfer of an electron from FAD HQ to the FMN OX to form FAD SQ – FMN SQ occurs significantly faster than transfer of a hydride ion from NADPH to FAD OX, thus causing the first two transitions to appear as one event. When the standard deviations are taken into account for G141T CPR, k_1 at 581 nm and k_1 at 455 nm are very similar, suggesting that the above explanation for the observation of two rates for three different phases still valid.

WT CPR

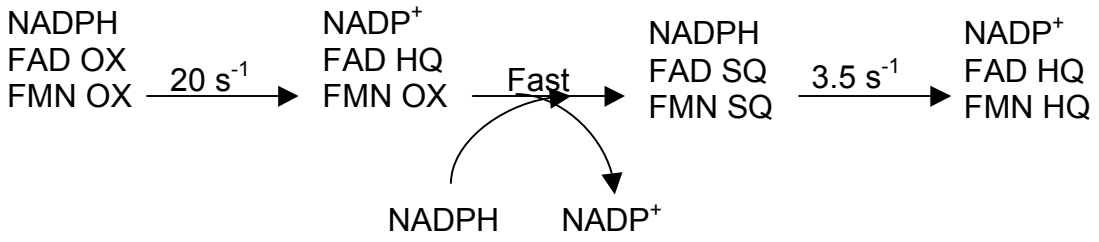

G141T CPR

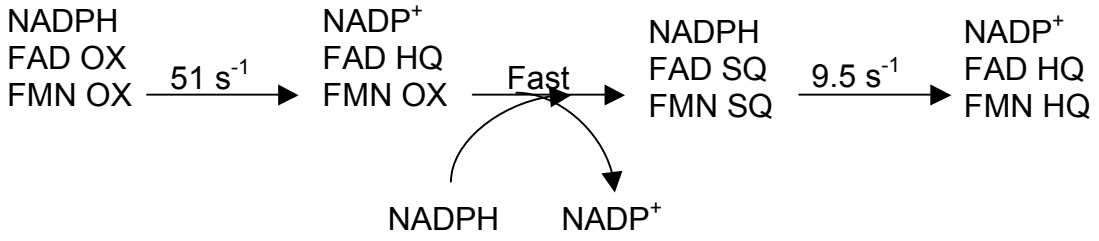

Figure 30: A schematic comparison of the pre-steady-state reduction kinetics of wild type and G141T CPR with a 20-fold and 15-fold excess of NADPH respectively. Wild type data is from reference 42. The increase in absorbance at 581 nm is due to the formation of the disemiquinoid state. Transfer of the hydride ion from NADPH to the FAD cofactor is rate limiting step in the formation of the disemiquinoid species.

The above experiment was then repeated except the temperature was dropped to 4° C with the hypothesis that interflavin electron transfer is more temperature sensitive than reduction by NADPH. Thus, dropping the temperature to 4° C could allow for the observation of CPR going from FAD HQ – FMN OX to FAD SQ – FMN SQ [45, 62]. Lowering the temperature did change the kinetics of the reaction, significantly decreasing all observable rates (table 4) (figure 31). At 581 nm two phases were observed, except this time both phases showed an increase in absorbance at 581 nm. Since NADPH is an obligate two-electron donor to the FAD cofactor, the only way to increase the absorbance at 581 nm is to go from the FAD hydroquinone to the disemiquinoid species. Unless a series of complex inter-protein electron transfers are occurring, we currently have no viable explanation for a biphasic increase in absorbance at 581 nm. Attempts to clarify this issue by monitoring the reduction of G141T CPR with a stoichiometric solution of NADPH at 4° C failed because the lower concentration of NADPH and the lower temperatures combined to make the signal to noise ratio too low. The data at 455 nm was triphasic with the first two rates corresponding to a decrease in absorbance at 455 nm (k_1 = 2.7 s^{-1}, k_2 = 0.3 s^{-1}). The first rate at 455 nm matches the first rate at 581 nm (k_1 = 3.6 s^{-1}), while the third rate at 455 nm (k_3 = 0.013 s^{-1}) corresponds with the second rate observed at 581 nm (k_2 = 0.04 s^{-1}).

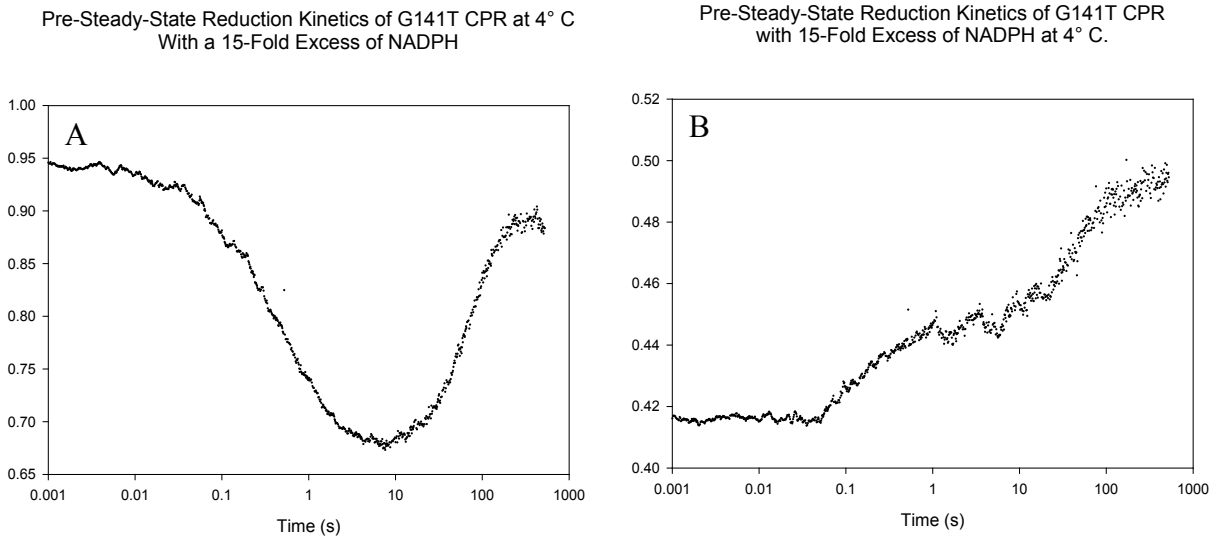

Figure 31: Pre-steady-state reduction kinetics of G141T CPR with a 15-fold excess of NADPH. **(A)** Absorbance changes at 455 nm could be fit by a triple exponential equation with $k_1 = 2.7\ s^{-1}$ and $k_2 = 0.3\ s^{-1}$, $k_3 = 0.013\ s^{-1}$. The first two rates describe the decrease in absorbance while the third rate describes the increase in absorbance. **(B)** Absorbance changes at 581 nm could also be fit by a double exponential equation with $k_1 = 3.6\ s^{-1}$ and $k_2 = 0.04\ s^{-1}$. Both experiments were conducted at 4° C in 100 mM potassium phosphate pH 7.0.

The pre-steady state kinetics for the reduction G141T CPR at 25° C by a stoichiometric amount of NADPH were then measured. This time, three rates were observed at 581 nm (figure 32). The first two rates (69 s^{-1} and 2.1 s^{-1}) correspond with an increase in absorbance at 581 nm, thus they monitor the formation of the semiquinone state. Since NADPH is an obligate 2 electron donor and the only way to form the semiquinone state in CPR is to go from FAD HQ – FMN OX to FAD SQ – FMN SQ, we have no explanation for why two rates are observed corresponding to an increase in semiquinone formation. Even though this experiment was performed with a stoichiometric amount of NADPH rather than a 15-fold excess, which creates pseudo first order conditions, the first observed rate for the stoichiometric NADPH (69 s^{-1}) matched well with the 15-fold excess NADPH data (51 s^{-1}). This indicates that the reductase is saturated with reduced pyridine nucleotide at a very rapid rate, much faster than hydride transfer to the FAD [45]. The G141T CPR data differs from previously published results for wild type CPR, which show that the reduction of wild type CPR by a stoichiometric amount of NADPH is essentially monophasic with a rate of 20 s^{-1} (figure 33) [42]. The single phase observed for wild type CPR corresponds with the formation of the disemiquinoid species as do the first two phases in G141T CPR, while the third phase observed for G141T CPR corresponds with the reduction of the disemiquinoid species. Although the transition from the disemiquinoid species to FAD OX – FMN HQ was very slow, the fact that it did eventually occur in G141T CPR and not wild type CPR is easy to rationalize given the inversion of the relative midpoint potentials of the FMN cofactor in the G141T mutant.

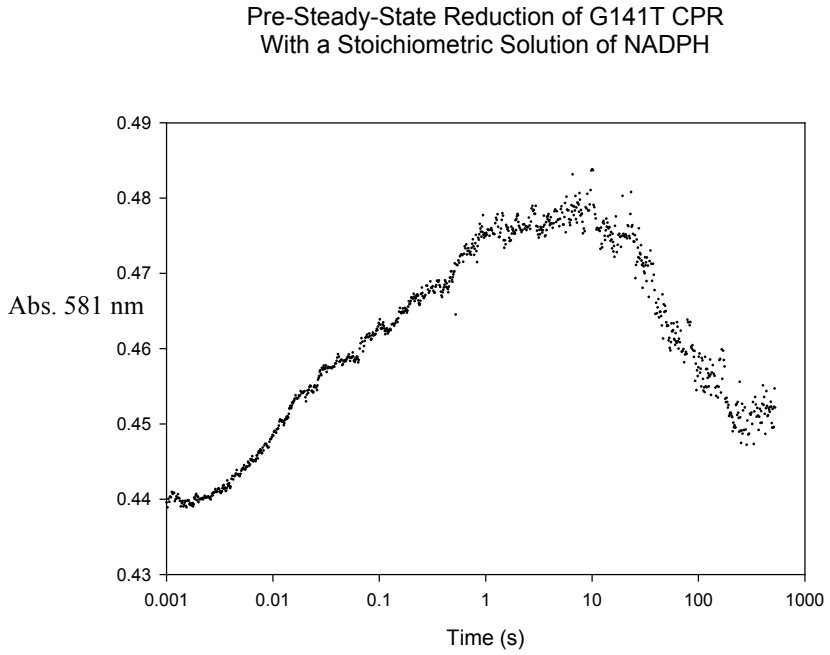

Figure 32: Pre-steady-state reduction kinetics of rat G141T CPR by a stoichiometric amount of NADPH. Abosrbance changes monitored at 581 nm on a logarithmic time scale. The data was fitted with a triple exponential equation with $k_1 = 69\ s^{-1}$, $k_2 = 2.1\ s^{-1}$, $k_3 = 0.014\ s^{-1}$. Time scale is extended to show the eventual decrease in absorbance corresponding with the transition from FAD SQ – FMN SQ to FAD OX – FMN HQ. Reaction was performed at 25° C in 100 mM potassium phosphate, pH 7.0.

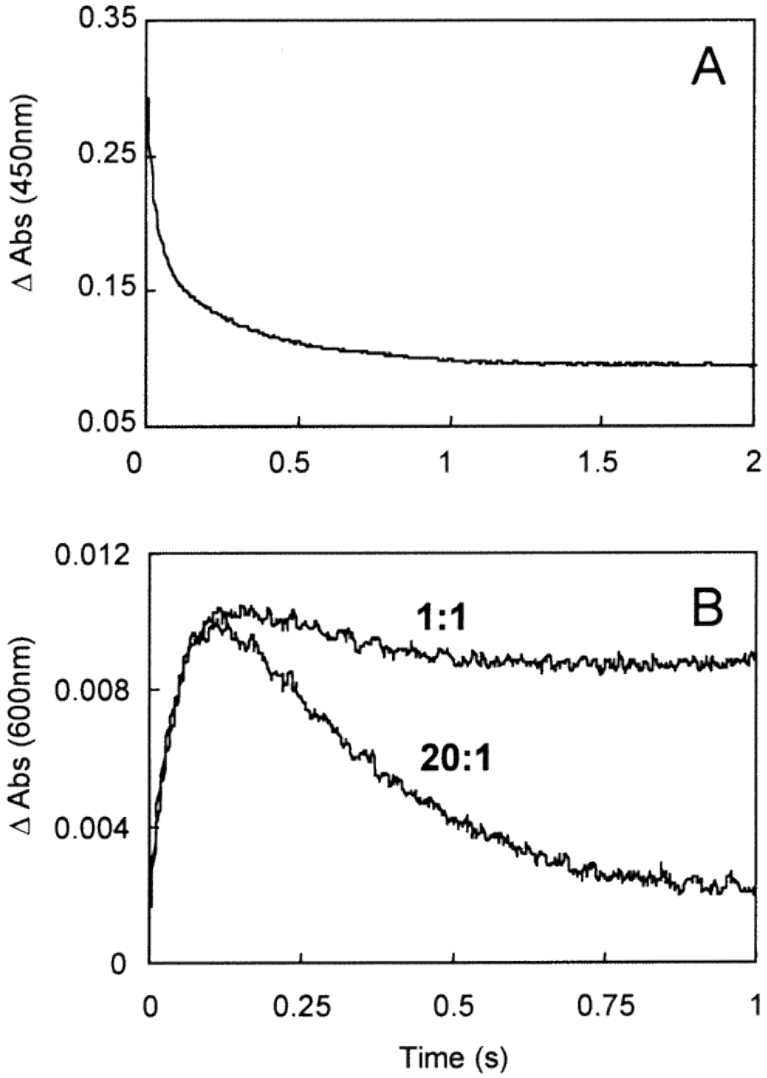

Figure 33: Pre-steady-state reduction kinetics of human wild type CPR by NADPH, observed on a linear time scale. Ratios indicate relative concentrations of CPR and NADPH. **(A)** Absorbance changes monitored at 450 nm to observe reduction of the oxidized state of the flavin cofactor. Human, wild type CPR was mixed against a 20-fold excess of NADPH. The data could be fit by a double exponential equation with $k_1 = 20\ s^{-1}$ and $k_2 = 3.5\ s^{-1}$. **(B)** Absorbance changes monitored at 600 nm to observe formation and reduction of the semiquinone state of the flavin cofactor. For the transient shown with a 20:1 ratio of NADPH/CPR, the data was fitted with a double exponential equation yielding values for K_1 and k_2 of 20 and 3.5 s^{-1}, respectively. For the transients with a 1:1 ratio of NADPH/CPR the data was fitted with a single exponential equation with $k_1 = 20\ s^{-1}$. Reactions performed at 25° C in 50 mM potassium phosphate buffer, pH 7.0. [CPR] 10 uM, [NADPH] 200 uM. Wild type data from reference 42.

FBD Single Turnover Assay: With all transitions in G141T CPR and FBD faster than wild type, but the steady-state turnover data suggesting that G141T CPR is less catalytically efficient than wild type CPR, a series of experiments were performed to measure the kinetics of electron transfer from FBD to cytochrome c (table 5). The rate of electron transfer from FBD to the oxidant potassium ferricyanide had already been measured, however, potassium ferricyanide is a non-physiological chemical oxidant and may interact with the FBD in a different manner than cytochrome c. In the first experiment, sodium dithionite was titrated into a solution of wild type FBD until the FMN cofactor was fully reduced. Care was taken so that excess sodium dithionite was not added. The solution was transferred anerobically to the stopped flow instrument where it was rapidly mixed with a 7-fold excess of cytochrome c with absorbance changes monitored at 550 nm to follow the reduction of cytochrome c (figure 34a). The resulting data had a low signal to noise ratio, but was fit with a double exponential equation 5b with the first phase tracing an increase in absorbance at 550 nm and the second phase tracing a decrease in absorbance at 550 nm. An increase in absorbance at 550 nm corresponds with the reduction of cytochrome c, so the only way for the absorbance at 550 nm to decrease would be for cytochrome c to become oxidized. Unless there was contamination of free oxygen in the cytochrome c solution, we currently have no explanation for these results. Focusing on the first phase, which traces the reduction of cytochrome c, the rate of reduction is significantly slower (0.018 s^{-1}) than the steady state turnover data (rate limiting step of 65 s^{-1}), and the reduction of potassium ferricyanide (8.3 s^{-1}).

Kinetics for Electron Transfer from Wild Type FBD to Cytochrome c

Transition	[Cyt c]	K_1 (s^{-1})	K_2 (s^{-1})
HQ-OX	7x	0.018 +/- 0.01	0.0025 +/- 0.0019
HQ-OX	1 to 1	0.005 +/- 0.007	
SQ-OX	7x	0.032 +/- 0.006	0.0037 +/- 0.0041
SQ-OX	1 to 1	0.0049 +/- 0.001	

Table 5: Single turnover assays for wild type FBD. The FMN cofactor was pre-reduced with sodium dithionite to either the hydroquinone state or the semiquinone state. With the flavin cofactor already reduced, the FBD was mixed against either a solution that contained either a 7-fold excess or equimolar concentration of cytochrome c.

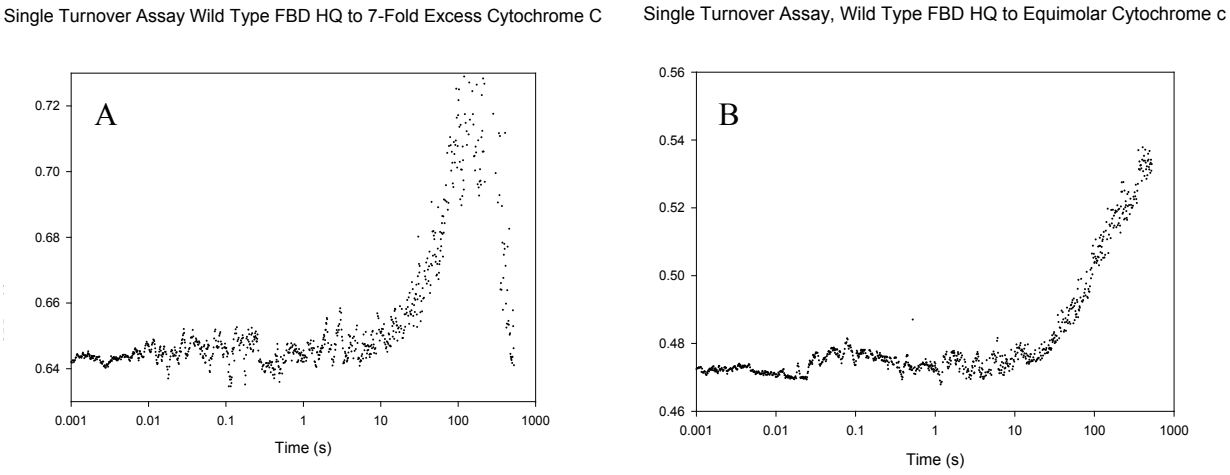

Figure 34: Single turnover assay of wild type FBD with the FMN cofactor in the hydroquinone state. The flavin cofactor was pre-reduced to the hydroquinone state by sodium dithionite. Absorbance changes were monitored at 550 nm to observe reduction of cytochrome c. **(A)** FBD was mixed against a 7-fold excess of cytochrome c. The data could be fit by a double exponential equation with $k_1 = 0.018\ s^{-1}$ and $k_2 = 0.0025\ s^{-1}$. **(B)** FBD was mixed against an equimolar solution of cytochrome c. The data could be fit by a single exponential equation with $k_1 = 0.005\ s^{-1}$. Reactions were performed at 25° C in 100 mM potassium phosphate, pH 7.0.

The experiment was then repeated except this time an equimolar concentration of cytochrome c was mixed with fully reduced FBD (figure 34b). The data from this experiment was fit with a single exponential equation 5a. The rate for this reaction was measured at 0.005 s^{-1}, which is about 3.5 times slower than the rate for experiments with a seven-fold excess of cytochrome c. This discrepancy in rates can be attributed to concentration effects since a seven-fold excess of cytochrome c creates pseudo first order conditions while an equimolar concentration of cytochrome c does not. These results add support to our hypothesis that cytochrome c interacts with the FBD in a different manner than the chemical oxidant potassium ferricyanide. The significantly slower rate of electron transfer to cytochrome c, compared to steady state turnover data, raises new questions. Does cytochrome c need to also interact with the FAD-binding domain in order for efficient electron transfer to occur? Does the FAD-binding domain exert an influence on the FBD which affects electron transfer to cytochrome c? What effect does the redox state of the FMN cofactor have on the FBD's ability to transfer electrons to cytochrome c?

To answer the third question, another experiment was performed wherein wild type FBD was titrated with sodium dithionite until maximal semiquinone formation was achieved. The solution was then transferred anaerobically to the stopped-flow instrument where it was rapidly mixed with a seven-fold excess of cytochrome c (figure 35a). As with the previous experiment where the FMN cofactor of wild type FBD was pre-reduced to the hydroquinone form, the data could be fit with a double exponential equation 5b. As previously described, only one phase was expected. We have no explanation for the second phase, which corresponds with a decrease in absorbance at 550 nm.

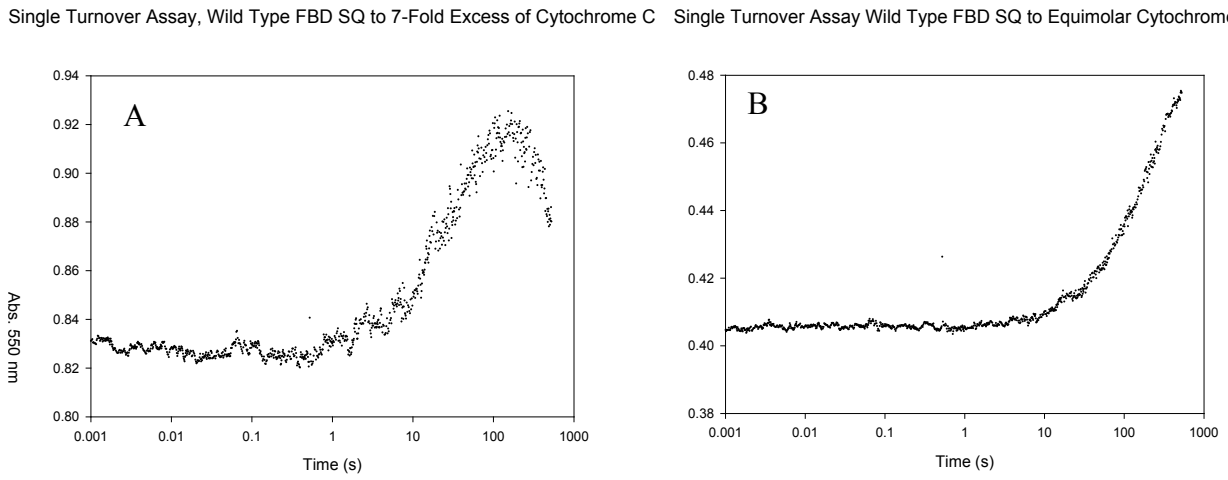

Figure 35: Single turnover assay of wild type FBD with the FMN cofactor in the semiquinone state. The flavin cofactor was pre-reduced to the semiquinone state by sodium dithionite. Absorbance changes were monitored at 550 nm to observe reduction of cytochrome c. **(A)** FBD was mixed against a 7-fold excess of cytochrome c. The data could be fit by a double exponential equation with $k_1 = 0.032\ s^{-1}$ and $k_2 = 0.0037\ s^{-1}$. **(B)** FBD was mixed against an equimolar solution of cytochrome c. The data could be fit by a single exponential equation with $k_1 = 0.0074\ s^{-1}$. Reactions were performed at 25° C in 100 mM potassium phosphate, pH 7.0.

Focusing on the first phase of the reaction, the rate of reduction of cytochrome c by the FMN semiquinone is 0.032 s^{-1}, which is similar to the rate of reduction by the FMN hydroquinone (0.018 s^{-1}). The experiment was repeated except this time an equimolar concentration of cytochrome c was used (figure 35b). The data conformed well with the oxidation of fully reduced, wild type FBD with an equimolar solution of cytochrome c (figure 34b). As with the previous experiment, this data could be fit by a single exponential equation 5a with a rate of 0.005 s^{-1}. Again, this rate is slower than the seven-fold excess cytochrome c experiments. These results indicate that, for the reaction of wild type FBD with cytochrome c, the redox state of the flavin cofactor has a minimal effect on the rate of electron transfer. However, the results obtained in this experiment directly contradict the work of Grunau et al, which show that rapid mixing of one electron reduced human FBD with cytochrome c should give a rate of approximately 3.6 s^{-1} [32]. We cannot account for this discrepancy in the rates of reduction of cytochrome c. Given the unexplained phases encountered with the 7-fold excess of cytochrome c and our inability to replicate literature results, we believe that there may be a technical error with these experiments. As such, these results are given little weight in determining the conclusion.

CPR Single Turnover Assay: Given that the rate of electron transfer from the FBD to cytochrome c was too slow to be physiologically relevant, the rate of electron transfer from CPR to cytochrome c was measured via single turnover assays. Several different approaches were attempted to measure this rate. In the first approach, G141T CPR was pre-reduced with excess NADPH, but due to the equilibration reaction previously described, the four-electron reduced state was not formed. The pre-reduced CPR was

then mixed with a 10-fold excess of cytochrome c. No absorbance changes were observed at 550 nm, indicating that G141T CPR was incapable of reducing cytochrome c (figure 36a), which is consistent with previous experiments on wild type house fly CPR [63]. When the observation period was extended out to over one minute, a decrease in absorbance at 550 nm was observed (figure 36 b). The decrease in absorbance was also observed in the FBD single turnover experiments (figures 34a, 35a) and is most likely due to an experimental artifact such as light scattering or cytochrome c complex formation. The inability of G141T CPR to donate electrons to cytochrome c after incubation with NADPH is likely due to the "third phase" equilibration reaction described above where it is proposed that air-stable inactive FMN is kinetically stabilized upon conformational drifting [32, 45].

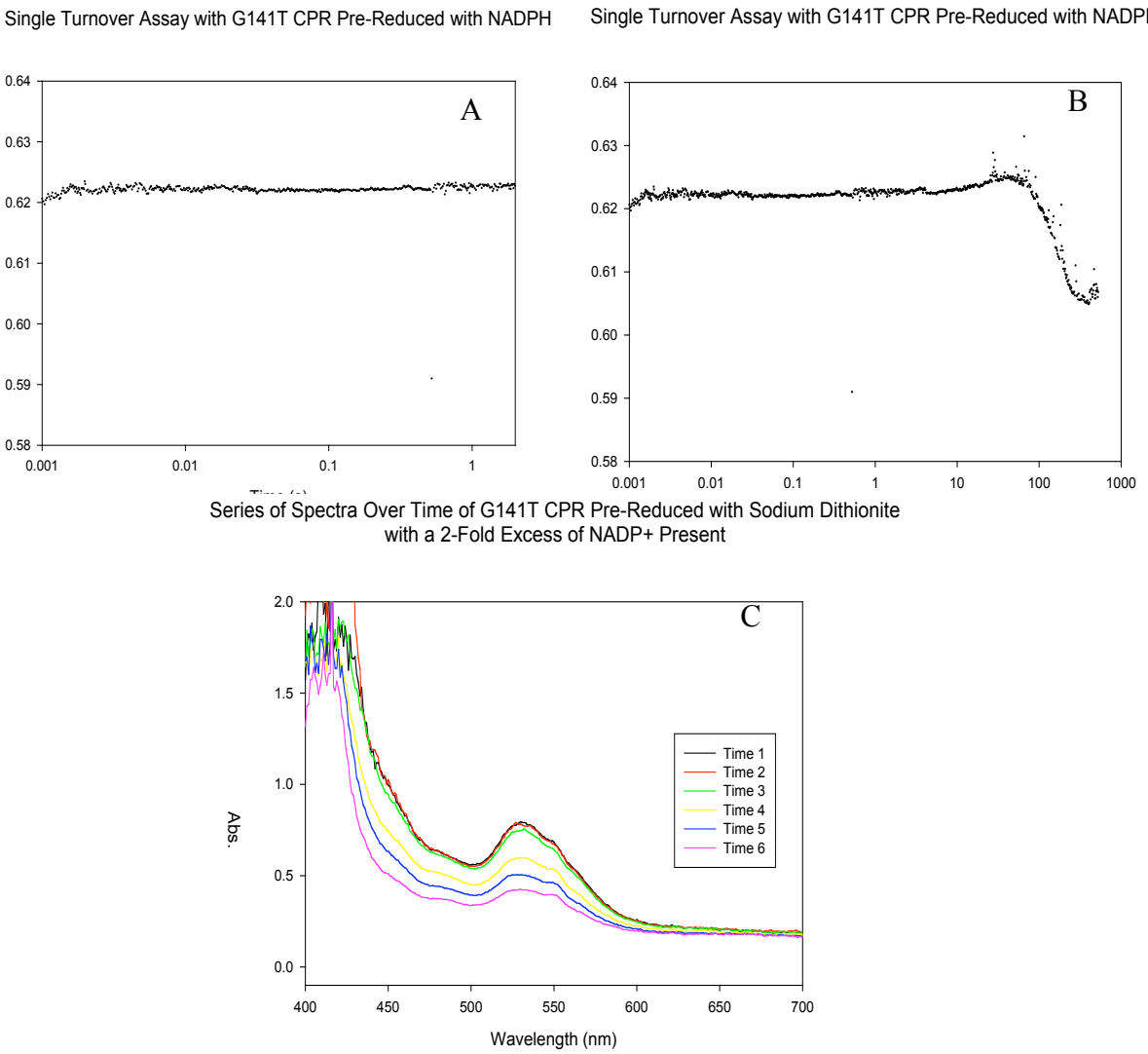

Figure 36: Single turnover assay with G141T CPR pre-reduced in the presence of $NADP^+$. **(A)** G141T CPR was pre-reduced with more than two equivalents of NADPH so that full reduction of the flavin cofactors should have been achieved. The reduced CPR was mixed against a 10-fold excess of cytochrome c and absorbance changes were monitored at 550 nm to observe reduction of cytochrome c. Over a physiologically relevant time frame, no absorbance changes were observed. **(B)** When the time frame is extended out past 5 minutes, a decrease in absorbance is observed at 550 nm. **(C)** G141T CPR was mixed with a 2-fold excess of $NADP^+$ and the system was fully reduced by sodium dithionite. The reduced G141T CPR was mixed against a 10-fold excess of cytochrome c and a series of spectra were taken in the 2 minutes following the mixing of the two proteins. A clear decrease in absorbance at all wavelengths is observed as the observation period is extended. But, a more important observation is that no reduced cytochrome c is observed, meaning that reduction didn't take place in the dead time of the stopped-flow. All experiments were performed at 25° C in 100 mM potassium phosphate buffer, pH 7.0.

Previous experiments by Grunua et al. indicate that interaction between NADPH/$NADP^+$ and CPR is necessary for the FMN binding domain to overcome its constrained state and efficiently interact with cytochrome c [32]. To further explore this phenomenon, G141T CPR was mixed with an equimolar solution of $NADP^+$ and then CPR was reduced with sodium dithionite until maximal semiquinone formation was achieved. The hope was that without NADPH in the solution, the slow equilibration reaction between NADPH/$NADP^+$ and the flavin cofactors could not occur and G141T CPR would be able to donate electrons to cytochrome c so that the single turnover assay could be performed. However, the literature states that the FAD binding domain of CPR is structurally similar to the flavoenzyme ferredoxin-$NADP^+$ reductase (FNR) [15-19]. Additionally both fully reduced, isolated FMN binding domain of human CPR [42] and fully reduced CPR from pig liver [62] have been shown to reduce $NADP^+$ to NADPH. Since there was no data in the literature regarding rat CPR and, of course, the G141T mutant, we proceeded with the experiments. As was suggested by the literature, although sodium dithionite is incapable of reducing $NADP^+$ directly, $NADP^+$ was reduced to NADPH via the FAD hydroquinone and CPR was made catalytically incompetent by the slow equilibration reaction (figure 36c).

Since neither of the two previously described methods allowed G141T CPR to transfer electrons to cytochrome c, a third assay was attempted. In this set up one equivalent of NADPH is combined with varying solutions of cytochrome c. This NADPH/cytochrome c solution is then mixed against G141T CPR in the stopped flow instrument. G141T CPR had a Kmax of 7.9 s^{-1} and a Kd of 103 uM while wild type CPR had a Kmax of 4.55 s^{-1} and a Kd of 88 uM (figure 37) (table 6). The wild type Kmax

does not compare well with previously reported values of 14 s^{-1}, and the Kd obtained does not match the literature value of 37 uM [32]. It should be noted that experiments performed by Grunau et al used 100 mM BES, pH 7.0 while measurements conducted in this laboratory were in 100 mM potassium phosphate, pH 7.0. Since BES is a zwitterion, the ionic strength of the buffer is 39 mM while the potassium phosphate buffer has an ionic strength of 225 mM, which could account for the difference in Kd [64]. Based on pre-steady-state reduction kinetics, it is not surprising that G141T CPR exhibits a Kmax that is nearly twice as high as wild type CPR.

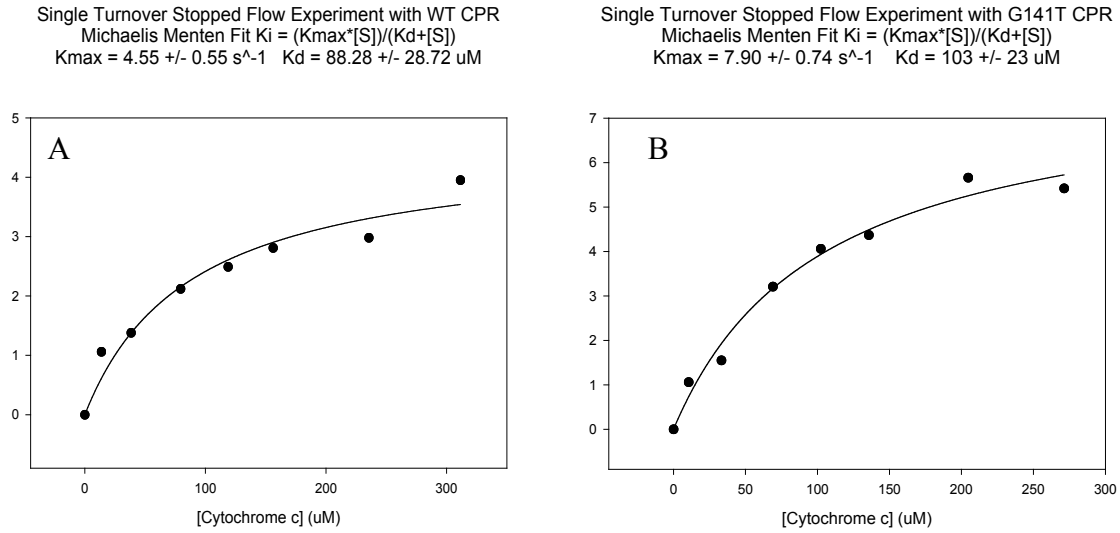

Figure 37: Single turnover stopped flow experiment on CPR. **(A)** Wild type CPR had a Kmax of 4.55 +/- 0.55 s^{-1} and a Kd of 88 +/- 29 uM. **(B)** G141T CPR had a Kmax of 7.90 +/- 0.74 s^{-1} and a Kd of 103 +/- 23 uM. All data was fit using the Michaelis Menten equation (equation 6). Reactions were performed at 25° C in 100 mM potassium phosphate, pH 7.0. A solution of 10 uM CPR was mixed against a solution with 10 uM NADPH and cytochrome c concentrations ranging from 10.5-271 uM.

Single Turnover Summary

Sample	Kmax (s^{-1})	Kd (uM)
WT CPR	4.55 +/- 0.55	88 +/- 29
G141T CPR	7.90 +/- 0.74	103 +/- 23
WT CPR Literature*	14	37

Table 6: Summary of single turnover stopped flow experiments. Wild type and G141T CPR were performed in 100 mM potassium phosphate, pH 7.0 which has an ionic strength of 225 mM. Literature value comes from reference 32. Literature reactions were performed in 100 mM BES, pH 7.0, which has an ionic strength of 39 mM. All reactions were performed with a 10 uM solution of CPR in syringe A mixed against syringe B which contained 10 uM NADPH and cytochrome c concentrations ranging from 10.5 - 271 uM.

Discussion

This study has explored how protein-cofactor interactions modulate the redox properties of the bound cofactor flavin mononucleotide (FMN) by focusing on a conserved glycine residue (glycine-141) that is thought to form a hydrogen bond to the N5H of the reduced flavin through its backbone carbonyl group. Previous studies on this conserved glycine residue in the *D. vulgaris* and *C. beijerinckii* flavodoxins have demonstrated that this hydrogen bonding interaction helps to stabilize the semiquinone state of the FMN cofactor and that insertion of a β-branched amino acid such as valine or threonine can significantly interrupt this interaction and change the redox properties of the bound flavin cofactor. This study has extended the results of the flavodoxin studies to their mammalian homologue, the FMN domain of CPR, and in so doing has confirmed that the conserved glycine residue in the FMN binding loop of CPR plays a crucial role in modulating the flavin redox properties.

The G141T mutation did, in fact, significantly destabilized the semiquinone state as is evidenced by its reduced formation during reductive titrations of both CPR and FBD. However, the extent of the semiquinone destabilization was significantly larger than expected. For *C. beijerinckii*, the glycine to threonine mutation caused the OX/SQ midpoint potential to shift from -92 mV to -270 mV and the SQ/HQ midpoint potential to shift from -399 mV to -320 mV, a shift of -178 mV and +79 mV respectively [47]. In CPR the OX/SQ couple shifted from -43 mV to -250 mV and the SQ/HQ midpoint potential shifted from -280 mV to -219 mV, a shift of -207 mV and +60 mV respectively (figure 38). The changes in midpoint potential for CPR were so large that it actually switched the relative stabilities of the SQ and HQ state, making the HQ more

thermodynamically stable than the SQ for the G141T mutant (Figure 20). None of the glycine mutants in the *C. beijerinckii* flavodoxin resulted in an inversion of relative stabilities of the redox states. The glycine to valine mutant in the *D. vulgaris* flavodoxin resulted in a decrease in the OX/SQ midpoint potential of 190 mV and an increase in the SQ/HQ midpoint potential of 141 mV [46]. Combined, these changes also resulted in an inversion of the relative stabilities of the redox states of the FMN cofactor. However, the FMN binding loop in *D. vulgaris* flavodoxin is significantly larger than the FMN binding loop in CPR and analysis of the crystal structures show that mutation of the glycine residue significantly alters the contacts between the flavin cofactor and the surrounding protein, suggesting that comparisons between CPR and *C. beijerinckii* are more insightful. Thus, mutation of the conserved glycine residue in the FMN binding loop of CPR to a β-branched amino acid results in changes to the midpoint potentials, particularly the OX/SQ midpoint potential, of the FMN cofactor that are similar to, but larger than, those observed in the flavodoxins.

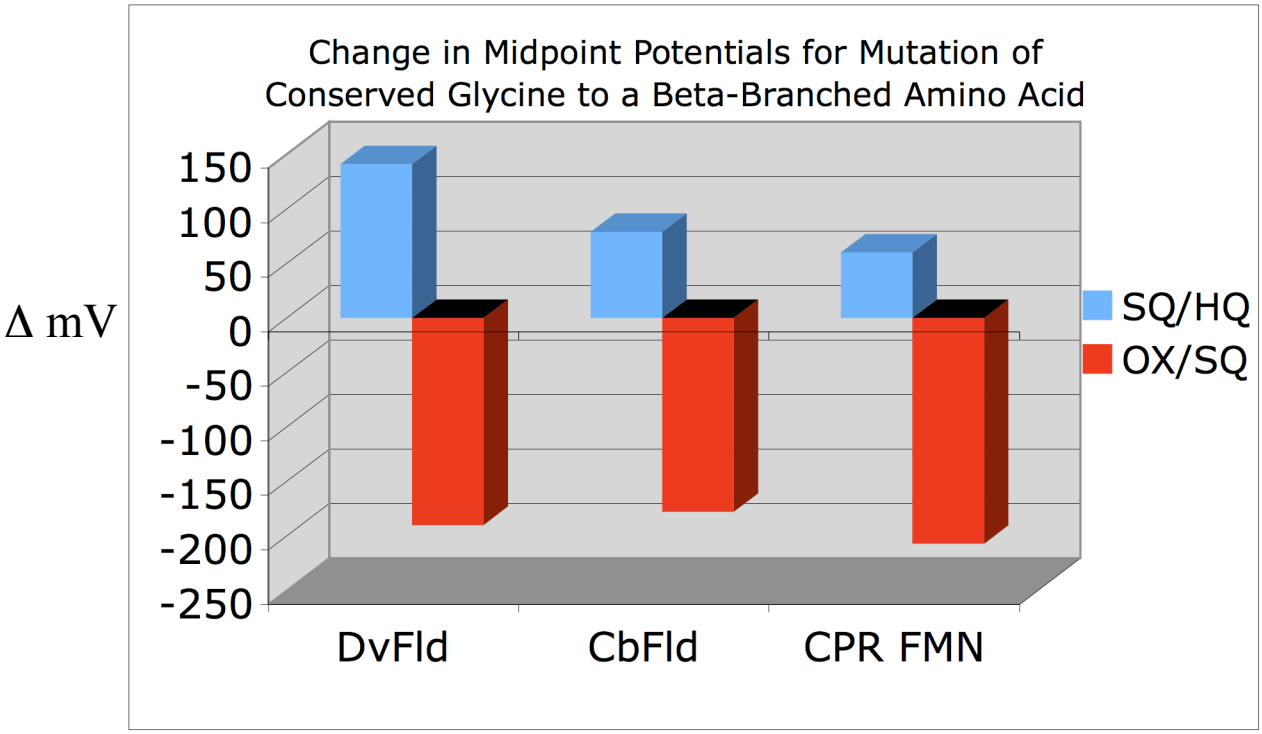

Figure 38: Change in the OX/SQ and SQ/HQ midpoint potentials upon mutation of the conserved glycine residue in the FMN binding loop to a *beta*-branched amino acid. For *D. vulgaris* flavodoxin, glycine was mutated to valine [46], while for *C. beijerinckii* [47] and CPR glycine was mutated to threonine.

How is this accomplished at the molecular level? X-ray crystallography has provided direct structural evidence for a redox-associated conformational change involving a rearrangement of the loop containing this glycine residue in the flavodoxins. This change results in the "flipping" of the carbonyl group of the glycine, which points away from the FMN in the oxidized state, so that it can serve as a hydrogen bond acceptor to the N5H of the FMN cofactor in the reduced states. This newly formed hydrogen bond serves to thermodynamically stabilize the neutral SQ state in these proteins [47]. Based on the similar destabilization of the neutral FMN SQ in the G141T CPR mutant, it is tempting and also reasonable to propose that a conformational change analogous to the one found in *C. beijerinckii* flavodoxin occurs in CPR and that this change is crucial in establishing the redox properties and contributes to the overall electron transfer mechanism in this reductase.

Interestingly, the crystal structure of rat CPR shows the backbone carbonyl of the conserved glycine, residue 141, is already pointed directly at the N5H of oxidized flavodoxin in the *trans* O-up conformation (the phi-psi angles are 77, -110), suggesting that loop flipping may not be necessary for stabilizing the reduced flavin cofactor (figure 15). Residue 141 exists in a region of Ramachandran space normally only occupied by glycine, thus it is plausible that the G141T mutation will cause a conformational change in the FMN binding loop with the oxidized flavin to move threonine 141 into an allowed region of Ramachandran space, equivalent to the cis O-down conformation in *C. beijerinckii*. This would make loop flipping relevant for stabilization of the reduced flavin cofactor, much in the same manner as for the *C. beijerinckii* flavodoxin. However, without crystal structures of the mutant and reduced forms of the enzyme, such propositions are purely speculative (figure 39).

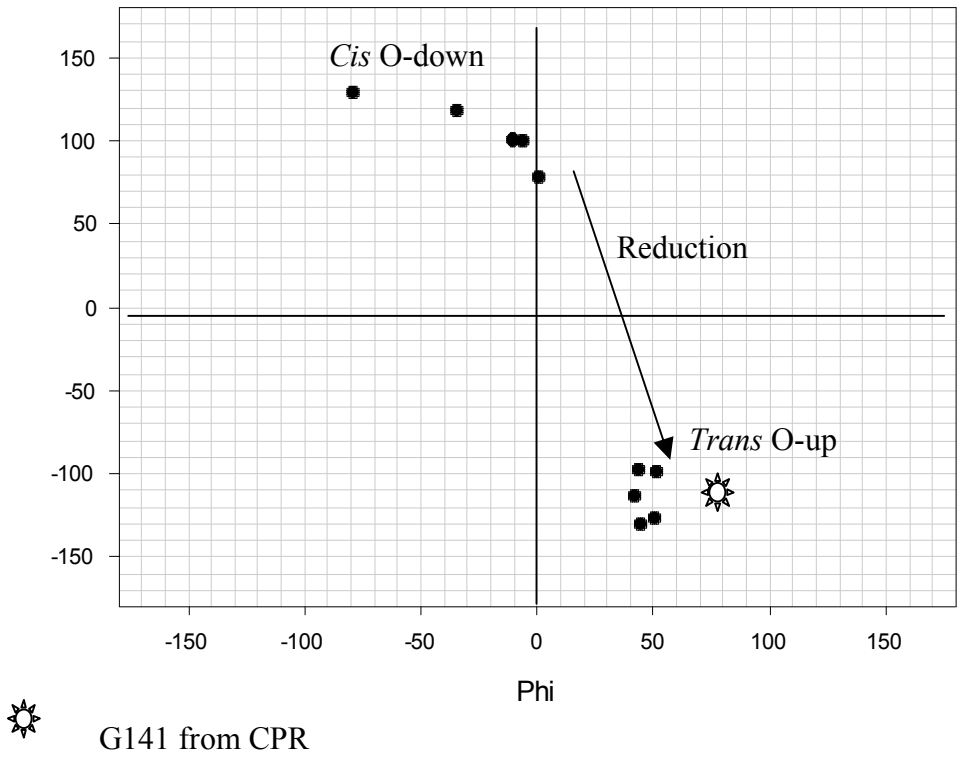

Figure 39: Ramachandran plot of the conserved glycine residue (G57) in the FMN binding loop of wild type and G57T mutant *C. beijerinckii* flavodoxin at various redox states. The position of the conserved glycine residue (G141) in the FMN binding loop of CPR is marked with a star.

The rather surprising inversion of the relative stabilities of the flavin led us to study the electron-transferring activities and mechanistic implications of the G141T mutation. The G141T point mutation decreased the steady-state turnover rate of CPR by 30%. The G141T mutation was designed with the intention of disrupting a hydrogen bonding interaction between the N5H of the reduced flavin and the main chain carbonyl of residue 141, not completely eliminating it. While the glycine replacement did alter substantially the midpoint potential of the OX/SQ couple, these changes were not expected to eliminate or greatly reduce the steady-state turnover activity of CPR because the potentials are still low enough to reduce cytochrome c. So, as was expected, the glycine to threonine replacement did not inactivate the enzyme or even change the activity by orders of magnitude. However, we believe that the results are significant in that this single amino acid replacement did influence the overall cytochrome c reductase activity. It is also important to note, that the electron transfer mechanism is complex, involving multiple steps. It is a well established observation in enzymology that mutations can significantly alter the reaction rate on one step of the enzymatic mechanism without having a substantial impact on the overall steady-state turnover rate if that step is not rate-limiting overall. Thus, that we saw any effect on the activity of the G141T CPR is intriguing.

The focus of the research turned to providing more direct evidence for the effect of the mutation on electron transfer involving the FMN domain using pre-steady state experimental approaches. The mutation was observed to affect the rates of electron transfer involving non-physiological chemical reductant (sodium dithionite) and oxidant (potassium ferricyanide). Stopped-flow kinetic studies with the chemical reductant

sodium dithionite demonstrated that the SQ-HQ transition in G141T FBD occurs 10 times faster than in wild type FBD (6.6 s^{-1} compared to 0.55 s^{-1}). Not only was the reduction of G141T FBD faster than wild type, but so was the oxidation with the chemical oxidant potassium ferricyanide. Stopped flow kinetic studies where fully reduced FBD was mixed against a 20-fold excess of potassium ferricyanide showed that G141T FBD was oxidized with a rate of approximately 26 s^{-1} compared to a rate of approximately 7 s^{-1} for wild type FBD. While these rates clearly demonstrate that the G141T mutation affects electron transfer rates, the use of chemical reductants/oxidants precludes direct comparison of these results to the steady-state turnover data.

Pre-steady state approaches were also applied in the study of electron transfer to cytochrome c, an established experimental surrogate "physiological" electron acceptor for cytochrome P450s. While several experimental challenges were encountered, many of which are inherent to the CPR enzyme itself, some important preliminary observations were made. One of the main arguments for the FMN SQ serving as the primary electron donor to cytochrome c is that wild type CPR is incapable of forming FMN HQ, either as the FAD HQ - FMN HQ or the FAD OX – FMN HQ species in a physiologically relevant manner. Mixing wild-type CPR with a 20-fold excess of NADPH leads to the formation of first the disemiquinoide species and then the fully reduced species with rates of 20 s^{-1} and 3.5 s^{-1} respectively [42]. However, steady-state-turnover experiments to cytochrome c demonstrate a turnover rate of 65 s^{-1}, demonstrating a disconnect between the pre-steady-state kinetics and steady-state-turnover data [54]. Additionally, mixing wild type CPR with an equimolar solution of NADPH in a stopped-flow spectrophotometer leads to the formation of the disemiquinoide species rather than the FAD OX – FMN HQ. This

data led Murataliev et al. argue that the FMN HQ is kinetically incompetent and therefore the FMN SQ is the primary electron donor to cytochrome P450s [63].

Surprisingly, the G141T mutant actually increased the rates of electron transfer for all measurable steps. Reduction of G141T CPR by a 15-fold excess of NADPH led to the formation of the disemiquinoide species and then the fully reduced species with rates of 51 s^{-1} and 9.5 s^{-1} respectively, compared to rates of 20 $s^{-1}$and 3.5 s^{-1} for wild type CPR. The increased rates of electron transfer do not correspond with the steady-state turnover data if the FMN SQ is serving as the primary electron donor in G141T CPR. However, if the FMN HQ serves as the primary electron donor for G141T CPR, then the rate-limiting step would be 9.5 s^{-1} compared to 20 s^{-1} for wild type CPR (figure 40). This corresponds closely with the steady-state turnover data wherein G141T CPR was less than 70% as efficient as wild type CPR.

WT CPR

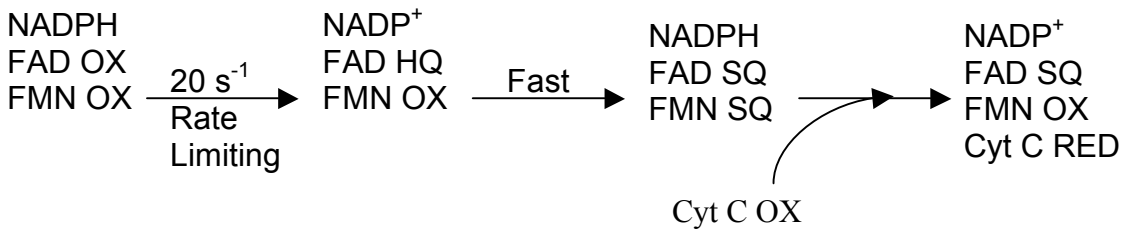

G141T CPR

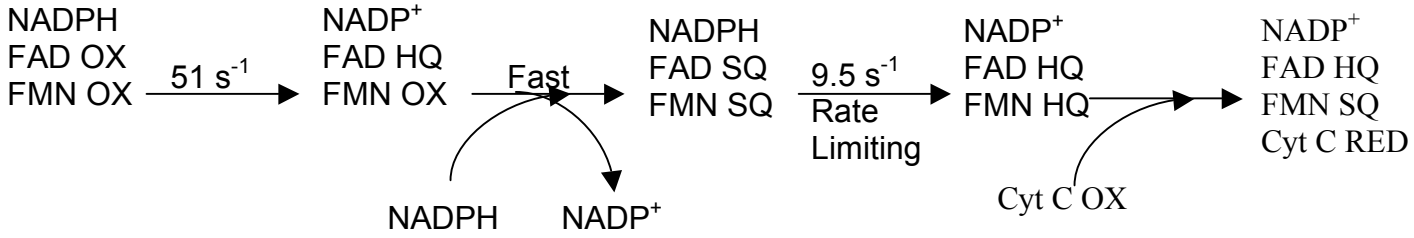

Figure 40: A proposed mechanism of electron transfer for the G141T CPR. The rate-limiting step for wild type CPR is the transfer of the hydride ion from NADPH to the FAD cofactor, which has a rate of 20 s^{-1}. The rate-limiting step for G141T CPR is the transition from the disemiquinoide species to the FMN HQ, which has a rate of 9.5 s^{-1}. Hence, in wild type, the FMN SQ donates an electron to cytochrome c, while in G141T CPR, the FMN HQ donates an electron to cytochrome c.

This conclusion would be more substantially supported by the direct measurement of the electron transfer rate from the FAD OX – FMN HQ redox species to cytochrome c in the stopped flow spectrophotometer. Unfortunately, our ability to directly measure the rates of electron transfer from the FMN HQ in both wild type and G141T CPR has been largely precluded because of issues inherent to the enzyme itself. For example, for the wild-type CPR, the four-electron-reduced reductase takes up to 8 hours of incubation under anaerobic conditions in the presence of NADPH and the NADPH regenerating system to form [41]. This is most likely due to an equilibration reaction of CPR and NADPH wherein the air-stable inactive FMN is kinetically stabilized upon conformation drifting [32, 45]. Similar to wild type CPR, G141T CPR was incapable of forming the four-electron-reduced reductase, but since this observation is the result of kinetic stabilization of the inactive, air-stable semiquinone rather than the midpoint potentials of the flavins themselves, this result is not terribly surprising. Our attempts to measure the rate of cytochrome c reduction by G141T CPR which had been fully reduced chemically by sodium dithionite in the presence of $NADP^+$ were compromised because of the ability of the reduced reductase to partially reduce $NADP^+$ to NADPH by analogy to ferredoxin-$NADP^+$ reductase, its homologue. Even then, no discernable reduction of cytochrome c was observed. The rates of electron transfer to cytochrome c from the G141T FBD (the isolated FMN-binding domain itself) fully reduced by dithionite was experimentally more tractable, but the transfer rates were observed to be very slow, well outside the steady-state turnover rates. We were able to obtain electron transfer rates by single-turnover experiments when the oxidized CPR (wild type and mutant) were rapidly mixed with oxidized cytochrome c containing varying concentrations of NADPH. Electron transfer

to cytochrome c was observed with a Kmax of 7.9 s^{-1} determined for the G141T CPR and Kmax of 4.55 s^{-1} obtained for wild type CPR under similar conditions. The relative rates, while different by about two-fold, are inconsistent with the steady-state-turnover data, however, where the steady-state rate for the mutant is slower than wild type.

While frustrating, these results are consistent with the general observations in the field regarding the interrelationships of pyridine nucleotide binding, the potential influence of the FAD-binding domain on the electron transfer steps involving the FMN-binding domain, and the nature of the formation of the electron-transfer complex with cytochrome c itself. For example, Grunua *et al.* indicate that interaction between NADPH/$NADP^+$ and CPR is necessary for the FMN binding domain to overcome its constrained state and efficiently interact with cytochrome c [32]. Through the use of isothermal titration calorimetry studies, Grunua *et al*. demonstrated that for the isolated FBD to interact with cytochrome c, the FMN cofactor must be reduced to the semiquinone state by sodium dithionite. However, when the FMN cofactor of the intact reductase is reduced by sodium dithionite to the semiquinone state, there is no interaction between CPR and cytochrome c. Isothermal titration calorimetry studies also demonstrated that the number of accessible conformational substates for the FBD increase upon binding of $NADP^+$ or 2',5' ADP. These results led Grunua *et al*. to propose that NADPH binding causes a conformational change between the two domains, allowing the FBD to overcome a kinetically unproductive conformation [32].

In conclusion, my original goals to demonstrate that glycine 141 in rat CPR plays a critical role in stabilizing the reduced forms of the FMN cofactor and to assess the effects of this residue on the electron transfer properties of CPR were reached

successfully. It was conclusively demonstrated that glycine residue in CPR contributes to the redox properties of the FMN cofactor in CPR in a similar manner to the conserved glycine residues in the FMN binding loops of the *D. vulgaris* and *C. beijerinckii* flavodoxins. Like the flavodoxin, the glycine to threonine replacement substantially reduces the stability of the neutral FMN SQ species thereby lowering the midpoint potential for the OX/SQ couple.

Because the neutral FMN SQ has been proposed to be the direct electron donor to the cytochrome during catalysis, the glycine to threonine replacement was expected to alter the activity of the reductase. In fact, although the effect was relatively small, a lower rate of cytochrome c reduction was observed during steady-state turnover. The stopped-flow pre-steady state kinetic studies demonstrated that the glycine-141 to threonine replacement affected the rate of all measurable electron transfer steps; however, the rates were higher than for wild type. Although further experimental proof is needed, perhaps most importantly, the evidence suggests that the G141T mutation may well have changed the mechanism of electron transfer in CPR from the FMN SQ serving as the primary electron donor to cytochrome c to the FMN HQ serving as the primary electron donor, although in a catalytically less efficient manner. Thus, glycine-141 has been conserved in the FMN binding loop to maintain catalytic efficiency and to preserve the mechanism of electron transfer.

References

1. Nelson, D. R., Zeldin, D. C., Hoffman, S. M., Maltais, L. J., Wain, H. M., and Nebert, D. W. (2004) Comparison of cytochrome P450 (CYP) genes from the mouse and human genomes, including nomenclature recommendations for genes, pseudogenes and alternative-splice variants. *Pharmacogenetics. 14*, 1-18.

2. Porter, T. D., Kasper, C. B., (1985) Coding nucleotide sequence of rat NADPH-cytochrome P-450 oxidoreductase cDNA and identification of flavin-binding domains. *Proc. Natl. Acad. Sci. U. S. A. 82*, 973-977.

3. Estabrook, R. W., Franklin, M. R., Cohen, B., Shigamatzu, A., Hilderbrandt, A. G. (1971) Biochemical and genetic factors influencing drug metabolism. Influence of hepatic microsomal mixed function oxidation reactions on cellular metabolic control. *Metabolism. 20*, 187-199.

4. Shephard, E. A., Phillips, I. R., Bayney, R. M., Pike, S. F., Rabin, B. R. (1983) Quantification of NADPH: cytochrome P-450 reductase in liver microsomes by a specific radioimmunoassay technique. *Biochem. J. 211*, 333-340.

5. Guengerich, F. P. (2001) Common and uncommon cytochrome P450 reactions related to metabolism and chemical toxicity. *Chem. Res. Toxicol. 14*, 612-650.

6. Guengerich, F. P. (2000) Pharmacogenomics of cytochrome P450 and other enzymes involved in the biotransformation of xenobiotics. *Drug Dev. Res. 49*, 4-16.

7. Nuwaysir, E. F., Bittner, M., Trent, J., Barrett, J. C., and Afshari, C. A. (1999) Microarrays and toxicology: the advent of toxicogenomics. *Mol. Carcinogen. 24*, 153-159

8. Guengerich, F. P. (1997) Cytochrome P450 enzymes. In *Biotransformation, Vl. 3, Comprehensive Toxicology* (Guengerich, F. P., Ed.) pp 37-68, Elsevier Science, Oxford.

9. Guengerich, F. P. (1995) Human cytochrome P450 enzymes. In *Cytochrome P450: Structure, Mechanism, and Biochemistry* (Ortiz de Montellano, P. R., Ed.) 2nd ed., pp 473-535, Plenum Press, New York.

10. Wrighton, S. A., and Stevens, J. C. (1992) The human hepatic cytochromes P450 involved in drug metabolism. *Crit. Rev. Toxicol. 22*, 1-21.

11. Anandatheerthavarada, H. K., Addya, S., Mullick, J., and Avadhani, N. G. (1998) Interaction of adrenodoxin with P4501A1 and its truncated form P450MT2 through different domains: differential modulation of enzyme activities. *Biochemistry. 37*, 1150-1160.

12. Hildebrandt, A., and Estabrook, R. W. (1971) Evidence for the participation of cytochrome b_5 in hepatic microsomal mixed-function oxidation reactions. *Arch. Biochem. Biophys. 143*, 66-79.

13. Noshiro, M., Ullrich, V., and Omura, T. (1981) Cytochrome b_5 as electron donor for oxy-cytochrome P-450. *Eur. J. Biochem. 116*, 521-526.

14. Gutierrez, A., Grunau, A., Paine, M., Munro, A. W., Wolf, C. R., Roberts, G. C. K., and Scrutton, N. S. (2003) Electron transfer in human cytochrome P450 reductase. *Biochem. Soc. Trans. 31*, 497-501.

15. Wang, M., Roberts, D. L., Paschke, R., Shea, T. M., Masters B. S., and Kim, J. J. (1997) Three-dimensional structure of NADPH-cytochrome P450 reductase: prototype for FMN- and FAD-containing enzymes. *Proc. Natl. Acad. Sci. U.S.A. 94*, 8411-8416.

16. Porter, T. D. and Kasper, C. B. (1986) NADPH-cytochrome P-450 oxidoreductase: flavin mononucleotide and flavin adenine dinucleotide domains evolved from different flavoproteins. *Biochemistry. 25*, 1682-1687.

17. Porter, T. D. (1991) An unusual yet strongly conserved flavoprotein reductase in bacteria and mammals. *Trends Biochem. Sci. 16*, 154-158.

18. Ostrowski, J., Barber, M. J., Rueger, D. C., Miller, B. E., Siegel, L. M., and Kredich, N. M. (1989) Characterization of the flavoprotein moieties of NADPH-sulfite reductase from *Salmonella typhimurium* and *Escherichia coli*. Physiochemical and catalytic properties, amino acid sequence deduced from DNA sequence of cysJ, and comparison with NADPH-cytochrome P-450 reductase. *J. Biol. Chem. 264*, 15796-15808.

19. Karplus, P. A., Daniels, M. J., and Herriott, J. R. (1991) Atomic structure of ferredoxin-NADP+ reductase: prototype for a structurally novel flavoenzyme family. *Science. 251*, 60-66.

20. Narhi, L. O. and Fulco, A. J. (1986) Characterization of a catalytically self-sufficient cytochrome P-450 monooxygenase induced by barbiturates in *Bacillus megaterium. J. Biol. Chem. 261*, 7160-7169.

21. Narhi, L. O. and Fulco, A. J. (1982) Phenobarbital induction of a soluble cytochrome P-450-dependent fatty acid monooxygenase in *Bacillus megaterium. J. Biol. Chem. 257*, 2147-2150.

22. Noble, M. A. Miles, C. S., Chapman, S. K., Lysek, D. A., MacKay, A. C., Reid, G. A., Hanzlik, R. P., and Munro, A. W. (1999) Roles of key active-site residues in flavocytochrome P450 BM3. *Biochem. J. 339*, 371-379.

23. Munro A. W. Daff, S., Coggins, J. R., Lindsay, J. G., and Chapman, S. K. (1996) Probing electron transfer in flavocytochrome P-450 BM3 and its component domains. *Eur. J. Biochem. 239*, 403-409.

24. Sevrioukova, I. F. Li, H., Zhang, H., Peterson, J. A., and Poulos T. L. (1999) Structure of a cytochrome P450-redox partner electron-transfer complex. *Proc. Natl. Acad. Sci. U. S. A. 96*, 1863-1868.

25. Gruez, A., Pignol, D., Zeghouf, M., Coves, J., Fontecave, M., Ferrer, J. L., and Fontecilla-Camps, J. C. (2000) Four crystal structures of the 60 kDa flavoprotein monomer of the sulfite reductase indicate a disordered flavodoxin-like module. *J. Mol. Biol. 299*, 199-212.

26. Zhang, J., Martasek, P., Paschke, R., Shea, T., Masters, B. S., and Kim, J. J. (2001) Crystal structure of the FAD/NADPH-binding domain of rat neuronal nitric-oxide synthase. Comparisons with NADPH-cytochrome P450 oxidoreductase. *J. Biol. Chem. 276*, 37506-37513.

27. Ingelman, M., Bianchi, V., and Eklund, H. (1997) The three-dimensional structure of flavodoxin reductase from *Escherichia coli* at 1.7 Å resolution. *J. Mol. Biol. 268*, 147-157.

28. Hubbard, P. A., Shen, A. L, Paschke, R., Kasper, C. B., and Kim, J. J. P. (2001) NADPH-cytochrome P450 oxidoreductase. Structural basis for hydride and electron transfer. *J. Biol. Chem. 276*, 29163-29170.

29. Smith, G. C., Tew, D. G., and Wolf, C. R. (1994) Dissection of NADPH-cytochrome P450 oxidoreductase into distinct functional domains. *Proc. Natl. Acad. Sci. U. S. A. 91*, 8710-8714.

30. Hodgson, A. V. and Strobel, H. W. (1996) Characterization of the FAD binding domain of cytochrome P450 reductase. *Arch. Biochem. Biophys. 325*, 99-106.

31. Munro, A. W., Noble, M. A., Robledo, L., Daff, S. N., and Chapman, S. K. (2001) Determination of the Redox Properties of Human NADPH-Cytochrome P450 Reductase. *Biochemistry*, *40*, 1956-1963.

32. Grunau, A., Paine, M. J., Ladbury, J. E., and Gutierrez, A. (2006) Global Effects of the Energetics of Coenzyme Binding: NADPH Controls the Protein Interaction Properties of Human Cytochrome P450 Reductase. *Biochemistry. 45*, 1421-1434.

33. Tamburini, P. P., MacFarquhar, S., Schenkman, J. B. (1986) Evidence of binary complex formations between cytochrome P-450, cytochrome b5, and NADPH-cytochrome P-450 reductase of hepatic microsomes. *Biochem. Biophys. Res. Commun. 134*, 519-526.

34. Nadler, S. G. and Strobel, H. W. (1988) Role of electrostatic interactions in the reaction of NADPH-cytochrome P-450 reductase with cytochromes P-450. *Arch. Biochem. Biophys. 261*, 418-429.

35. Nisimoto, Y. and Otsuka-Murakami, H. (1988) Cytochrome b5, cytochrome c, and cytochrome P-450 interactions with NADPH-cytochrome P-450 reductase in phospholipids vesicles. *Biochemistry. 27*, 5869-5876.

36. Murataliev, M. B., Feyereisen, R., Walker, F. A. (2004) Electron transfer by diflavin reductases. *Biochim. Biophys. Acta. 1698*, 1-26.

37. Muller, F., Hemmerich, P., Ehrenberg, A. (1969) On the molecular and sub-molecular structure of flavin free radicals and their properties, in: H. Kamin (Ed.), Flavin and Flavoproteins, Univ. Park Press, Baltimore, pp. 107-122.

38. Massey, V., Palmer, G. (1966) On the existence of spectrally distinct classes of flavoprotein semiquinones. A new method for the quantitative production of flavoprotein semiquinones. *Biochemistry. 5*, 3181-3189.

39. Muller, F., Brustlein, M., Hemmerich, P., Massey, V., Walker, W. H. (1972) Light-absorption studies on neutral flavin radicals. *Eur. J. Biochem. 25*, 573-580.

40. Mayhew, S. G. and Ludwig, M. L. (1975) in *The Enzymes* (Boyer, P., Ed.) 3rd ed., Vol. 12, pp 57-109, Academic Press, New York.

41. Vermilion, J. L. and Coon, M. J. (1978) Purified liver microsomal NADPH-cytochrome P-450 reductase. Spectral characterization of oxidation-reduction states. *J. Biol. Chem. 253*, 2694-2704.

42. Gutierrez, A., Lian, L., Wolf, C. R., Scrutton, N. S., and Roberts, G. C. K. (2001) Stopped-Flow Kinetic Studies of Flavin Reduction in Human Cytochrome P450 Reductase and Its Component Domains. *Biochemistry. 40*, 1964-1975.

43. Shen, A. L, Christensen, M. J., and Kasper, C. B. (1991) NADPH-cytochrome P-450 oxidoreductase. The role of cysteine 566 in catalysis and cofactor binding. *J. Biol. Chem. 266*, 19976-19980.

44. Sem, D. S. and Kasper, C. B. (1993) Interaction with arginine 597 of NADPH-cytochrome P-450 oxidoreductase is a primary source of uniform binding energy used to discriminate between NADPH and NADH. *Biochemistry. 32*, 11548-11558.

45. Oprian, D. D., and Coon, M. J. (1982) Oxidation-Reduction States of FMN and FAD in NADPH-Cytochrome P-450 Reductase by NADPH. *J. Biol. Chem. 257*, 8935-8944.

46. O'Farrell, P. A., Walsh, M. A., McCarthy, A. A., Higgins, T. M., Voordouw, G., Mayhey, S. G. (1998) Modulation of the Redox Potentials of the FMN in *Desulfovibrio vulgaris* Flavodoxin: Thermodynamic Properties and Crystal Structures of Glycine-61 Mutants. *Biochemistry. 37*, 8405-8416.

47. Ludwig, M. L., Pattridge, K. A., Metzger, A. L., Dixon, M. M., Eren, M., Feng, Y., and Swenson, R. P. (1997) Control of Oxidation-Reduction Potentials in Flavodoxin from *Clostridium beijerinckii*: The Role of Conformation Changes. *Biochemistry 36*, 1259-1280.

48. Smith, J. A., and Pease, L. G. (1980). Reverse turns in peptides and proteins. *CRC Crit. Rev. Biochem. 8*, 315-399.

49. Wilmot, C. M., and Thornton, J. M. (1988) Analysis and prediction of different types of beta-turn in protein. *J. Mol. Biol. 203*, 221-232.

50. Chen, D., and Swenson, R. P. (1994) Cloning, sequence analysis, and expression of the genes encoding the two subunits of the methylotrophic bacterium W3A1 electron transfer flavoprotein. *J. Biol. Chem. 269*, 32120-30.

51. Rock, D., Rock, D., and Jones, J.P. (2001) Inexpensive purification of P450 reductase and other proteins using 2',5'-adenosine diphosphate agarose affinity columns. *Protein Expr. Purif. 22*, 82-83.

52. Krey, G. D., Vanin, E. F., and Swenson, R. P. (1988) Cloning, Nucleotide Sequence, and Expression of the Flavodoxin Gene from *Desulfovibrio vulgaris* (Hildenborough). *J. Biol. Chem. 263*, 15436-15443.

53. Klein, M. L. and Fulco, A. T. (1993) Critical residues involved in FMN binding and catalytic activity of cytochrome P450 BM-3. *J. Biol. Chem. 268*, 7553-7561.

54. Shen, A. L., Sem, D. S., and Kasper, C. B. (1999) Mechanistic Studies on the Reductive Half-reaction of NADPH-Cytochrome P450 Oxidoreductase. *J. Biol. Chem. 274*, 5391-5398.

55. Massey, V. (1959) The microestimation of succinate and the extinction coefficient of cytochrome c. *Biochim. Biophs. Acta. 34*, 255-256.

56. Schellenberg, K. A. and Hellerman (1959) Oxidation of reduced diphosphopyridine nucleotide. *J. Biol. Chem. 231*, 547-556.

57. Clark, W. M (1960) *Oxidation-Reduction Potentials of Organic Systems*. The Williams and Wilkins Company.

58. Zhao, Q., Modi, S., Smith, G., Paine, M., McDonagh, P. D., Wolf, C. R., Tew, D., Lian, L., Roberts, G. C. K., and Driessen, H. P. C. (1997) Crystal structure of the FMN-binding domain of human cytochrome P450 reductase at 1.93 resolution. *Protein Sci. 8*, 298-306.

59. Draper, R. D. and Ingraham, L. L. (1968) A potentiometic study of the flavin semiquinone equilibrium. *Arch. Biochem. Biophys. 125*, 802-808.

60. Oster, T., Boddupalli, S.S., and Peterson, J.A. (1991) Expression, purification, and properties of the flavoprotein domain of cytochrome P-450BM-3. Evidence for the importance of the amino-terminal region for FMN binding. *J. Biol. Chem*. *266*, 22718-22725.

61. Sevrioukova, I., Shaffer, C., Ballou, D.P., and Peterson, J.A. (1996) Equilibrium and transient state spectrophotometric studies of the mechanism of reduction of the flavoprotein domain of P450BM-3. *Biochemistry. 35*, 7058-7068.

62. Yasukochi, Y., Peterson, J., and Masters B. S. S. (1979) NADPH-Cytochrome c (P450) Reductase: Spectrophotometric and stopped flow kinetic studies on the formation of reduced flavoprotein intermediates. *J. Biol. Chem. 254*, 7097-7104.

63. Murataliev, M. B., and Feyereisen, R. (1999) Mechanism of cytochrome P450 reductase from the housefly: Evidence for an FMN semiquinone as electron donor. *FEBS Lett. 453*, 201-204.

64. Phillips, A. H. and Langdon, R. G. (1962) Hepatic triphosphopyridine nucleotide-cytochrome c reductase: isolation, characterization, and kinetic mechanism. *J. Biol. Chem. 237*, 2652-2660.